AE-07

Universal Joint and Driveshaft Design Manual

SAE International™

American Axle v. Neapco - IPR2025-00091
PET_AAM_1012-0001

Universal Joint and Driveshaft Design Manual

Advances in Engineering Series No.7

Published by:
The Society of Automotive Engineers, Inc.
400 Commonwealth Drive
Warrendale, PA 15096

American Axle v. Neapco - IPR2025-00091
PET_AAM_1012-0002

Illustrators
Gilbert B. Arnold
Vincent Platek

Designer
Raymond Sevin

Second Printing
Paperback 1991

Copyright © 1979 Society of Automotive Engineers, Inc.

ISBN 0-89883-007-9
Library of Congress Number: 79-63005

All rights reserved. Printed in the United States of America.

Permission to photocopy for internal or personal use, or the internal or personal use of specific clients, is granted by SAE for libraries and other users registered with the Copyright Clearance Center (CCC), provided that the base fee of $.50 per page is paid directly to CCC, 27 Congress St., Salem, MA 01970. Special requests should be addressed to the SAE Publications Group.

0-89833-0007-9/79 $.50.

American Axle v. Neapco - IPR2025-00091
PET_AAM_1012-0003

PREFACE AND ACKNOWLEDGMENT

The universal joint, which is a mechanism for transmitting torque or rotary motion through an angle, has been produced in many different design concepts. The origin of the universal joint can be traced to the Thirteenth Century. Since that time, the universal joint, because of its unique kinematic characteristics, has been studied by engineers, scientists, and mathematicians. Their combined efforts have resulted in the publication of many theoretical and practical analyses and in the development and application of many useful devices that are classified as universal joints. Considerable progress has been made in design innovations, analytical procedures, and manufacturing techniques.

The SAE *Universal Joint and Driveshaft Design Manual*, was developed to present information on the latest technologies practiced in the power transmission field, along with related references. Another purpose of the design manual is to present explanations of the various subject matter that will fulfill the varied needs of engineers, designers, students, and others associated with drivetrain engineering and related activities.

Design guidelines and technology, from applicable dynamic and kinematic disciplines, are described and explained in detail for a wide range of pertinent topics. These guidelines aid in the establishment of new designs, improvements in existing designs, or solving specific problems. These design guidelines are necessary for the analysis and evaluation of a universal joint, other driveshaft components, or a complete driveshaft for a specific application. All information or data described has been obtained from actual laboratory tests and substantiated by successful field applications. Design and application practices which have been successfully used are described in detail.

The following is a brief description of the subjects covered by the SAE *Universal Joint and Driveshaft Design Manual*.

- All types of power transmitting mechanisms classified as universal joints, which are either of the constant velocity or the nonconstant velocity types, are discussed. The description of their concept, kinematic characteristics, functional capabilities, and design procedures are presented in detail in an easy-to-understand format.
- The most commonly used driveshaft arrangements that couple universal joints to other driveshaft and drivetrain components are explained, including functional characteristics and detailed design procedures for the various components and attachment methods.
- All types of applications requiring the transmission of power from the power source to a driven member are described, including operating requirements and design parameters for many specific applications.
- Drivetrain disturbances, their sources of excitation, and the various methods of controlling them are presented.
- Analytical procedures necessary for design analysis, evaluation, and application of universal joints, driveshaft components, and complete driveshaft assemblies are shown for the first time in one publication.
- The evaluation of universal joints, driveshaft components, and complete driveshaft assemblies by laboratory and vehicle testing is described.
- Pertinent references are listed at the end of chapters, sections, appendices, and in the Bibliography, which substantiate the material presented and provide the opportunity to obtain more detailed information on a particular subject.

Recognition and appreciation is expressed to the members of the Driveshaft Subcommittee of the SAE Transmission and Drivetrain Technical Committee and to the many other SAE members who have contributed their time, knowledge, and talents to this publication.

Special recognition is extended to Mr. E. R. Wagner, P.E., Secretary of the Driveshaft Subcommittee of the SAE Transmission and Drivetrain Technical Committee, whose contributions and organizational skills are self-explanatory.

Our gratitude and appreciation is expressed to the members of the SAE Editorial and Publication Subcommittee of the SAE Transmission and Drivetrain Technical Committee, and especially the Committee Chairman, Mr. E. L. Clary, P.E., for the efficient manner in which the many manuscripts for this publication were reviewed.

American Axle v. Neapco - IPR2025-00091
PET_AAM_1012-0004

Past and present members of the SAE Driveshaft Subcommittee responsible for the technical content of this publication are:

C. E. Cooney, Chairman—Mechanics Division, Borg-Warner Corp.
E. R. Wagner, P.E., Secretary—Saginaw Steering Gear Division, GMC
A. H. Berker—Ford Motor Co.
D. W. Holzinger—Spicer Universal Joint Division, Dana Corp.
F. C. Nagele—Rockwell International
E. T. Hendzel—Ford Motor Co.
R. W. Powers—Oldsmobile Division, GMC
F. H. Abar—Ford Motor Co.
G. N. McCulloch—Ford Motor Co.
T. S. Trojanowski, P.E.—Hayes Dana, Ltd.
L. W. Szymanski—Lift Parts Mfg., Inc.
E. E. Sowers—Spicer Universal Joint Division, Dana Corp.
J. Koinis—Detroit Universal Division, Chrysler Corp.
J. M. Lyons—Mack Trucks, Inc.
N. W. Webster—Neapco, Inc.
F. F. Miller—Spicer Universal Joint Division, Dana Corp.
J. H. Dodge—Oldsmobile Division, GMC
R. A. MacDonald—Chevrolet Motor Division, GMC
C. M. Zeigler—Neapco, Inc.

Members of the Editorial Review and Publication Subcommittee of the SAE Transmission and Drivetrain Technical Committee are:

E. L. Clary, P.E., Chairman—Buick Motor Division, GMC
P. D. Cruise, P.E.—Axle Division, Clark Equipment Co.
D. J. Drayton—Buick Motor Division, GMC
M. G. Gabriel—Ford Motor Co.
R. W. Halberg—Warner Gear Division, Borg-Warner Corp.
N. Hull—International Harvester Co.
E. L. Jones—Chrysler Corp.
D. A. Kulczyk—The Torrington Co.
J. E. Mahoney—General Motors Technical Center
O. E. Phelps—Spicer Universal Joint Division, Dana Corp.
T. F. Ristau—Saginaw Steering Gear Division, GMC
G. R. Smith—General Motors Technical Center
E. R. Wagner, P.E.—Saginaw Steering Gear Division, GMC
K. L. Westercamp—Saginaw Steering Gear Division, GMC

Charles E. Cooney, Jr.
Chairman
Driveshaft Subcommittee
SAE Transmission and
Drivetrain Technical Committee

American Axle v. Neapco - IPR2025-00091
PET_AAM_1012-0005

Table of Contents

CHAPTER 1
Driveline and Driveshaft Arrangements and Constructions 3

CHAPTER 2
Basic Driveline Requirements 13
Section 2.1– Driveline Functions 15
Section 2.2– Application Parameters and Established Practices 17
Section 2.3– Design Torque Considerations 23
Section 2.4– Vehicle Driveline Analysis 25
Section 2.5– Duty Cycle Determination 31

CHAPTER 3
Universal Joints – Introduction 35
Section 3.1– Nonconstant Velocity Universal Joints
Section 3.1.1– Cardan or Hooke Universal Joint 39
Section 3.1.2– Ball and Trunnion Universal Joint 77
Section 3.1.3– Roller and Trunnion Universal Joint 85
Section 3.1.4– Sliding Block and Trunnion Universal Joint 89
Section 3.1.5– Rubber Couplings 93

Section 3.2– Constant Velocity Universal Joints
Section 3.2.1– Basic Requirements for Constant Velocity (CV) Universal Joints 99
Section 3.2.2– Double Cardan Universal Joint 103
Section 3.2.3– Double Cardan Universal Joint (Trunnion Pin Type) 119
Section 3.2.4– Double Cardan Universal Joint (Twin Ball and Centering Plate Type) 123
Section 3.2.5– Tracta Universal Joint 127
Section 3.2.6– Tripot Universal Joint (End Motion Type) 131
Section 3.2.7– Tripot Universal Joint (Fixed Center Type) 141
Section 3.2.8– Rzeppa Universal Joint 145
Section 3.2.9– Ball Spline Rzeppa Universal Joint 151
Section 3.2.10– Weiss Universal Joint (End Motion Type) 155
Section 3.2.11– Weiss Universal Joint (Fixed Center Type) 159
Section 3.2.12– Cross Groove Universal Joint 163
Section 3.2.13– Double Offset Universal Joint (End Motion Type) 167
Section 3.2.14– Double Offset Universal Joint (Fixed Center Type) 171

American Axle v. Neapco - IPR2025-00091
PET_AAM_1012-0006

CHAPTER 4
Tubing 177

CHAPTER 5
Splines and Axial Motion Devices 185

CHAPTER 6
Shaft Support Bearings 201

CHAPTER 7
Driveshaft Attachment Methods 209

CHAPTER 8
Balancing 215

CHAPTER 9
Vibration Control 223
Section 9.1– Basic Vibration–Fundamentals and Terminology 225
Section 9.2– Description of Drivetrain Disturbances 227
Section 9.3– Control of Drivetrain Disturbances 231
Section 9.4– Designing of Vibration Control Devices
Section 9.4.1– Rubber Element Tubes 239
Section 9.4.2– Torsional Dampers 259
Section 9.4.3– Liners 263

CHAPTER 10
Critical Speed 267

CHAPTER 11
Test Procedures 279

CHAPTER 12
Accessory Drives 287

CHAPTER 13
Agricultural Implement Driveshafts 293

CHAPTER 14
Axle Driveshafts 311

CHAPTER 15
Nomenclature and Terminology 323

American Axle v. Neapco - IPR2025-00091
PET_AAM_1012-0007

APPENDICES 335
Appendix A – Hertz Contact Stress, Stress and Strength Gradients Along the Load Axis, Allowable Compressive Stress and Determination of Carburized Case Depth 337
Appendix B – Basic Load-Speed-Life-Stress Relationships and Equations for Universal Joints with Rolling Elements 379
Appendix C – Needle Roller Bearing Computation Procedure 381
Appendix D – Stress Concentration Factors 383
Appendix E – Typical Drivetrain Component Efficiencies 391
Appendix F – Torsional Rigidity (Spring Rate) 393
Appendix G – Joint Angle Capabilities of End Motion Universal Joints 395
Appendix H – Bending Moment (Secondary Couple) Analysis of Ball Type Constant Velocity Universal Joints 397
Appendix I – Universal Joint Rating Procedure 399
Appendix J – Mass Polar Moment of Inertia 401
Appendix K – Basic Mathematics for Cardan Universal Joint Problems 407
Appendix L – Useful Design Aids 411
Appendix M – Conversion from U.S. Customary to SI (Revised Metric) Units 417
Appendix N – Torque Required to Accelerate Power Train Systems 421
Appendix O – Basic Cardan Universal Joint Computation Procedures 425

BIBLIOGRAPHY 429

INDEX 435

American Axle v. Neapco - IPR2025-00091
PET_AAM_1012-0008

Driveline and Driveshaft Arrangements & Constructions

Chapter 1

American Axle v. Neapco - IPR2025-00091
PET_AAM_1012-0009

Chapter 1
Driveline and Driveshaft Arrangements and Constructions

E. R. Wagner, P.E. — Saginaw Steering Gear Div., GMC

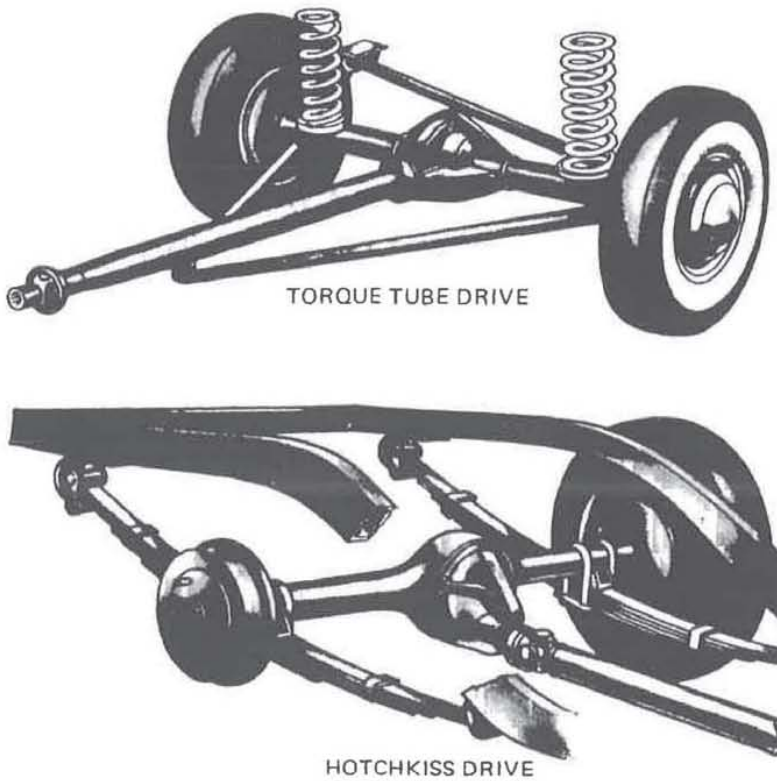


Fig. 1 — Basic drivelines

Introduction

In the classic layout of a typical automotive vehicle, the power source, or engine, has been at the front and the drive at the rear. A connecting shaft, or driveline, is required to transmit the power from the engine and transmission to the differential or final drive unit. Basically, the driveline acts as a torsional elastic member in a typical vehicle drivetrain and in its simplest form is a torsional spring connecting two masses of relatively large rotating inertias. In a more practical sense, the driveline is an assembly of one or more universal jointed solid or tubular driveshafts. It provides for axial movement and transmits torque and rotational motion at a fixed or varying angular relationship from one shaft to another.

For example, when the differential is part of the flexibly mounted or unsprung live, rigid axle, the driveline obviously must provide for axial length changes and require universal joints to accommodate the relative angular movement. Even when the differential is frame-mounted, flexibility in the structure as well as assembly tolerances generally do not allow the elimination of universal joints and provisions for axial movement. Also, this latter drivetrain layout requires universal jointed axle driveshafts or halfshafts connecting the sprung differential with the unsprung wheels. In addition, these universal jointed axle driveshafts are required on vehicles having the power source and driving wheels located at the same end, such as front-located engine with front drive, or rear-located engine with rear drive.

Basic Vehicle Driveline Types

The two basic types of main drivelines used in automotive applications have been the torque tube drive and the Hotchkiss drive (open driveline) constructions shown in Fig. 1. Typical driveshafts used in these torque tube and open drivelines are illustrated in Fig. 2.

The torque tube drive, now nearly obsolete, was once commonly used in passenger cars. In addition to transmitting driving

American Axle v. Neapco - IPR2025-00091
PET_AAM_1012-0011

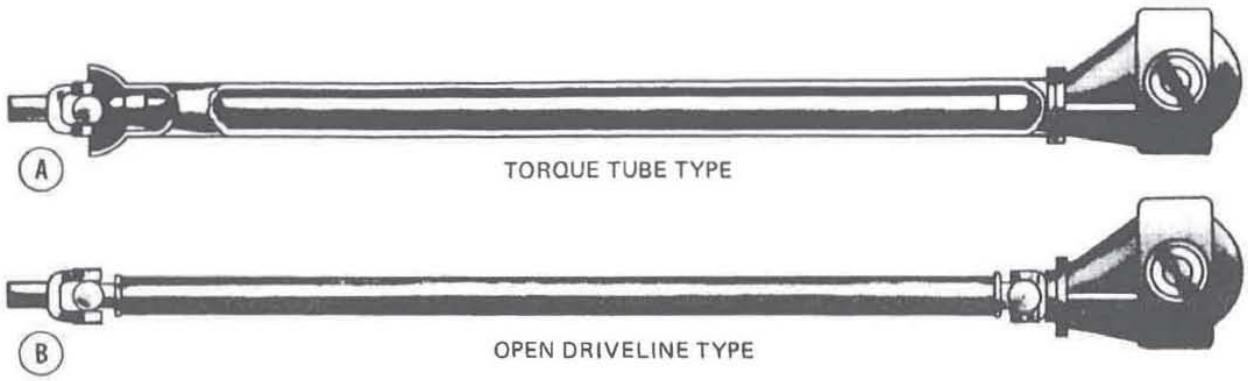


Fig. 2 — Driveshaft types

torque from the engine and transmission to the live rigid rear axle differential, the torque tube drive also had to resist torque reaction and transmit driving and braking thrust forces from the wheels to the vehicle, through the torque ball located on its forward end. This torque ball contained an enclosed universal joint. There have also been modified torque tube drive constructions used with live axles which differed somewhat from the conventional design in functional and force transmitting characteristics or abilities. In addition, there have been some torque tube driveshaft configurations used wherein the rear differential has been frame mounted and with no universal joints incorporated in the driveshaft. Among the major disadvantages of the torque tube drive have been high cost, adding to unsprung weight when used with a live axle and the hollow tube acting as an amplifier, resulting in the transmission of undesirable driveline noises and disturbances. In addition, repair or servicing costs, if needed, tend to be high.

The open driveline design, having two or more universal joints, is presently the most common means of transmitting power from the engine and transmission to the axle final drive unit. With this construction, only driveline torque is transmitted through the driveshaft. The driving and braking thrust forces from the wheels and the axle torque reaction forces are transmitted to the vehicle through the suspension components. The only thrust forces imposed on the driveshaft are due to suspension motions, powerplant movements, and wind-up or wind-down of the rear axle carrier nose, especially under conditions of high torque application. Among the major advantages of the open driveline are: low cost, ease of manufacture, reduced vehicle weight, and ease of installation and servicing. Also, the open driveshaft allows the flexibility to design a satisfactory driveline arrangement to meet widely varying vehicle installation requirements.

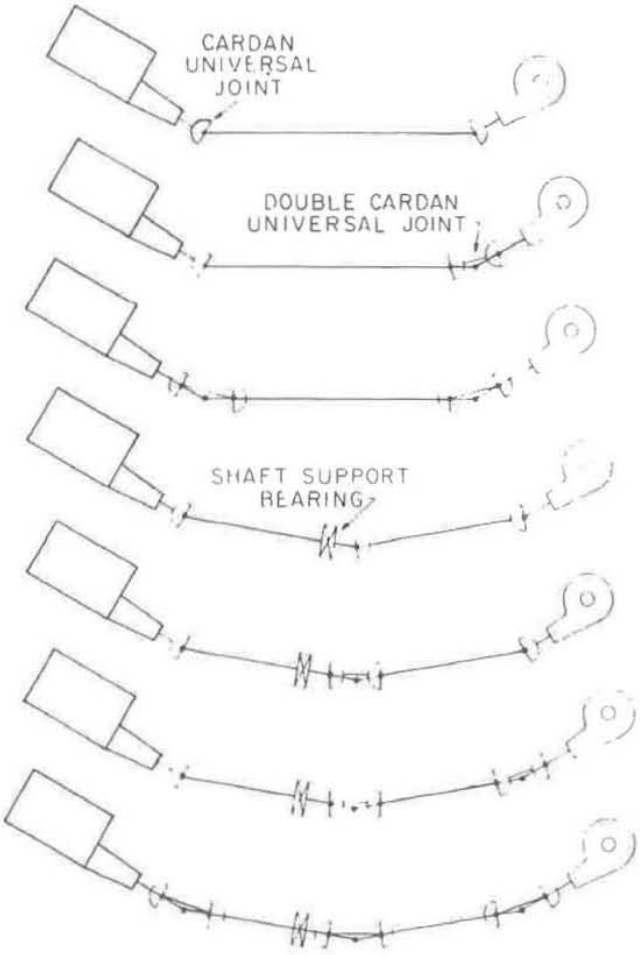


Fig. 3 — Typical passenger car driveline arrangements

Driveline Arrangements

Because of widely varying application requirements, drivelines can be designed in numerous arrangements. Generally, drivelines are designed in two-joint or multijoint shaft arrangements. Fig. 3 illustrates typical passenger car driveshaft arrangements where two or three universal joints are usually used in the main driveline.

The use of trucks with more than one driving axle in military applications led to a commonly used system of designating drivetrain configurations for these and other on-highway and off-highway vehicles. Thus, a 4 x 2 truck is a four-wheel truck with two-wheel drive, and a 4 x 4 truck is a four-wheel truck with four-wheel drive. There are also 6 x 2, 6 x 4, and 6 x 6 trucks

American Axle v. Neapco - IPR2025-00091
PET_AAM_1012-0012

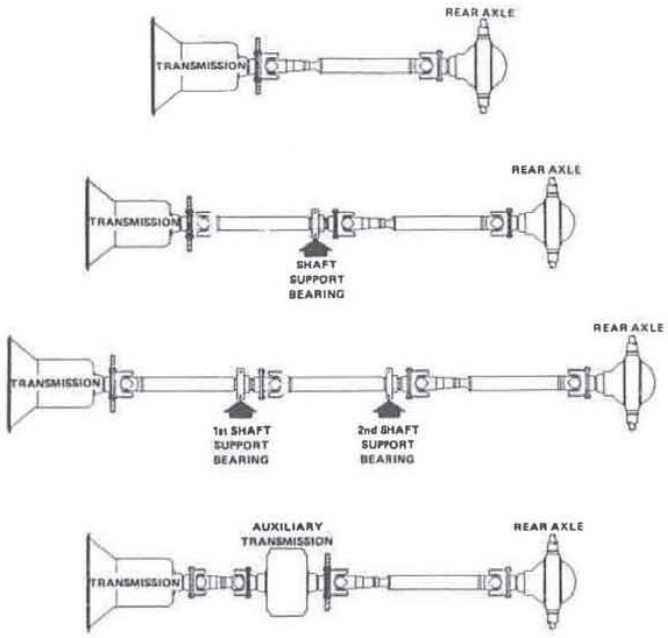


Fig. 4 — Typical 4 x 2 and 6 x 2 truck driveline arrangements

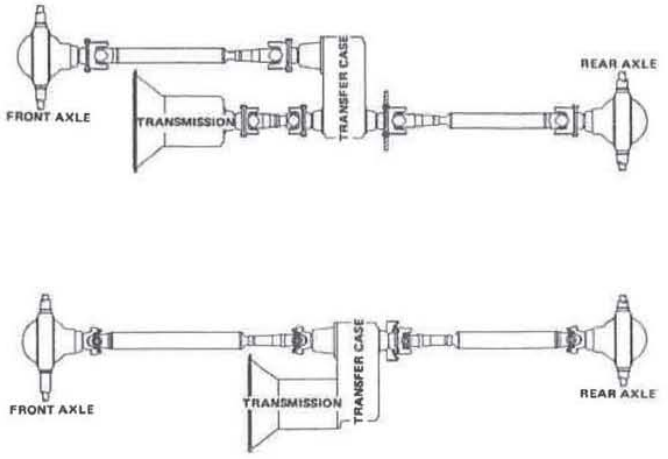


Fig. 5 — Typical 4 x 4 truck driveline arrangements

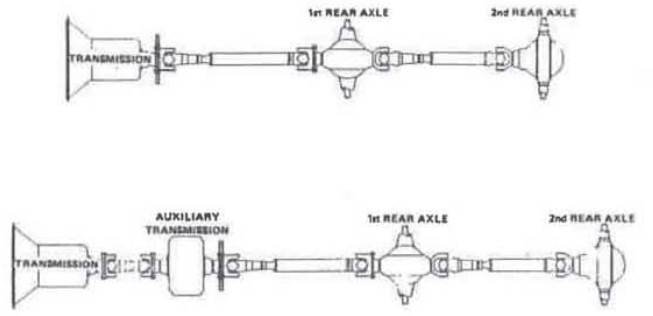


Fig. 6 — Typical 6 x 4 truck driveline arrangements

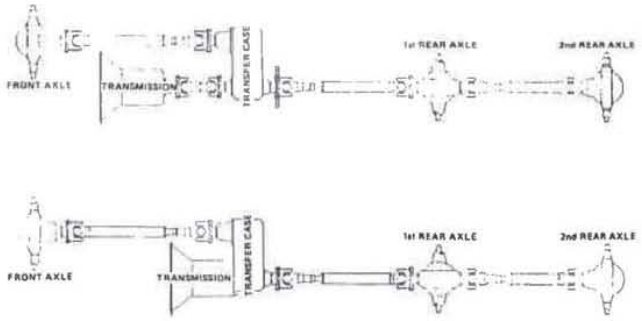


Fig. 7 — Typical 6 x 6 truck driveline arrangements

which are six-wheelers with drive on two, four, and six wheels respectively. Figs. 4, 5, 6, and 7 show typical main driveline arrangements for these various types of vehicles.

In addition to main driveline arrangements, certain vehicles also incorporate universal jointed axle driveshafts or halfshafts in the drivetrain system. Fig. 8 illustrates a typical 4 x 4 vehicle with front and rear live rigid axles, where a universal joint is thus required at each front steerable wheel. Fig. 9 shows a typical 6 x 6 vehicle with independent suspension at all wheels. Also, vehicles which have the powerplant and driving wheels located at the same end, such as front engine with front drive or rear engine with rear drive, require universal jointed axle driveshafts. Fig. 10 illustrates the driveline arrangement of a typical small front wheel drive passenger car. Also shown in this illustration is a typical universal jointed steering shaft generally required for such a vehicle.

Agricultural implements incorporate various driveline arrangements between the tractor's power take-off drive system and the implement. Fig. 11 shows a typical two-joint shaft arrangement with the tractor and implement in various relative angular relationships to each other.

Various driveline arrangements are also used in railway, marine, industrial, and stationary drive applications. Fig. 12 illustrates a typical Diesel locomotive driveline arrangement and Fig. 13 shows a typical cargo pump drive system.

Driveline Constructions

Depending on the widely varying application requirements, driveline constructions can assume numerous design configurations in order to accommodate the necessary relative angular and axial movements. In the chapter on *Universal Joints,* numerous joint constructions are described. Depending on their design characteristics, some of these joints may be used in a wide variety of applications where angular motion only is required, while other joints have limited application. Besides providing angular movement, some joints also accommodate axial stroke simultaneously. In addition, various types of driveline splines and axial motion mechanisms are described in the chapter on *Splines and Axial Motion Devices.*

In typical passenger car and truck applications, the two-joint driveshaft incorporating Cardan universal joints represents the

American Axle v. Neapco - IPR2025-00091
PET_AAM_1012-0013

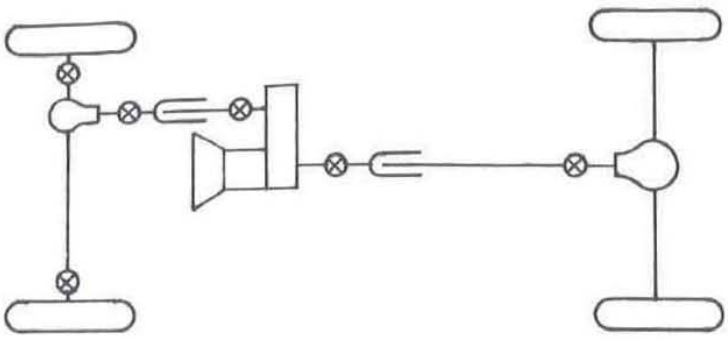


Fig. 8 — Typical driveline arrangement of 4 x 4 vehicle with front and rear live, rigid axles

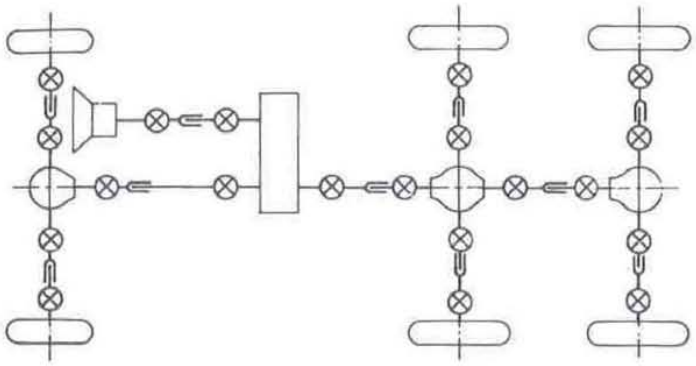


Fig. 9 — Typical driveline arrangement of 6 x 6 vehicle with independent suspension at all wheels

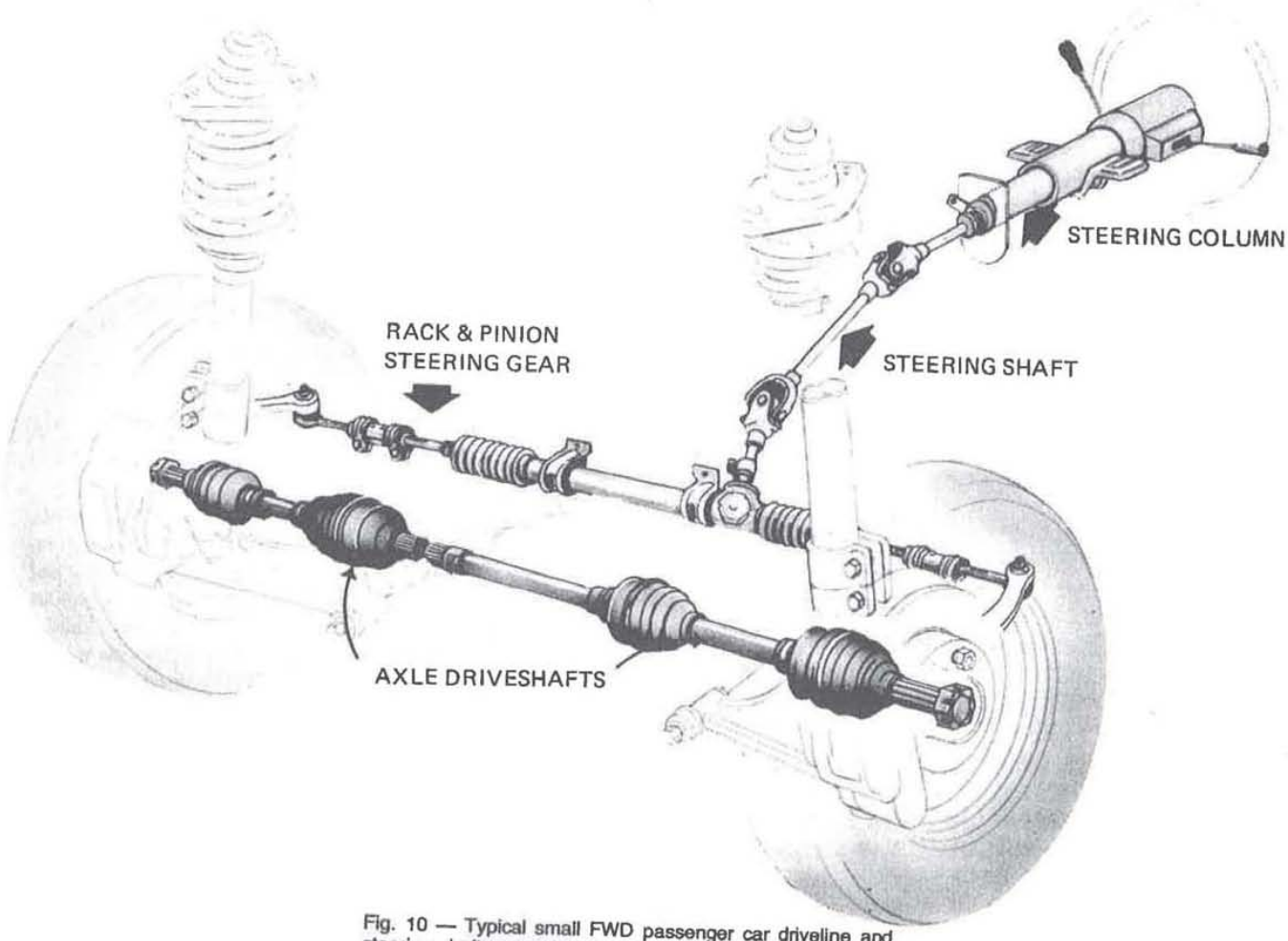


Fig. 10 — Typical small FWD passenger car driveline and steering shaft arrangements

American Axle v. Neapco - IPR2025-00091
PET_AAM_1012-0014

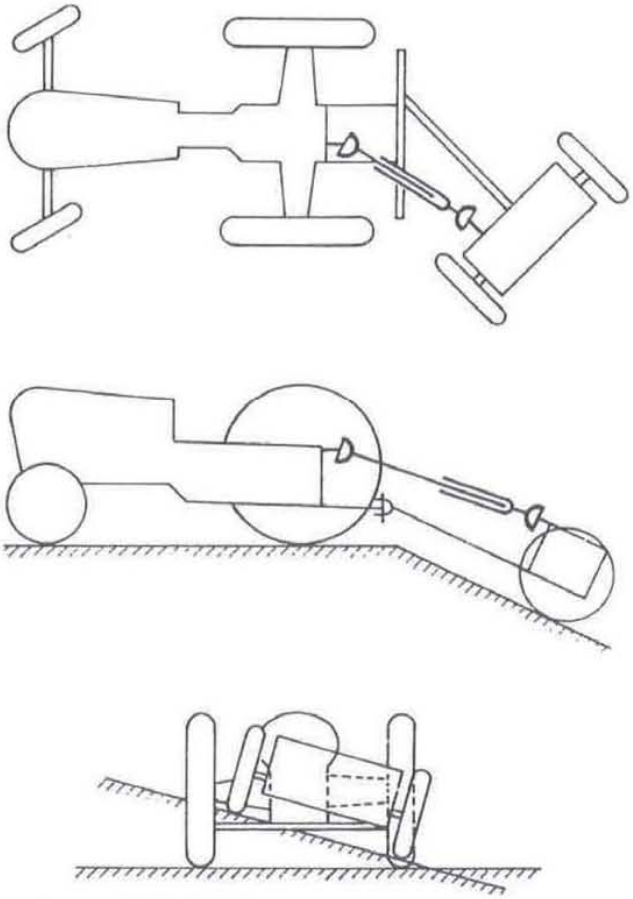


Fig. 11 — Typical driveline arrangement between tractor and agricultural implement showing required relative movement

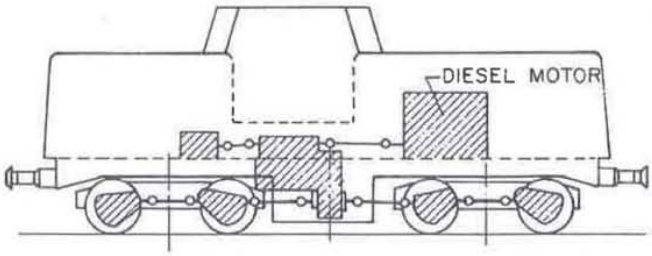


Fig. 12 — Typical driveline arrangement of Diesel locomotive

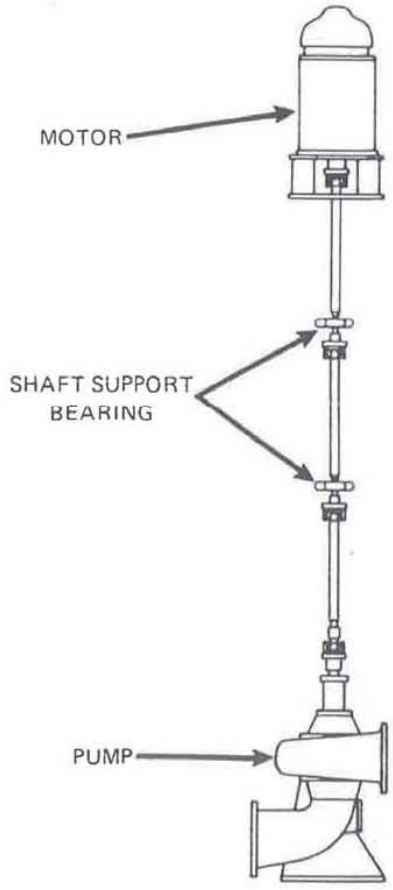


Fig. 13 — Typical cargo pump drive system

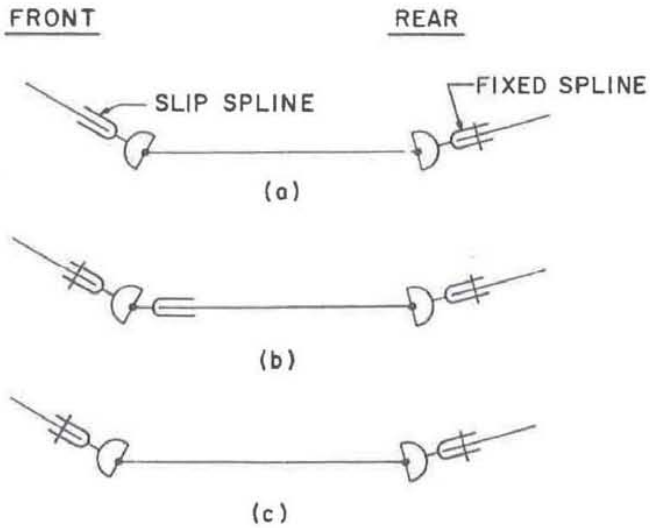


Fig. 14 — Two-joint driveshaft constructions

most commonly used driveline construction. This construction is generally referred to as either a two-joint outboard slip or a two-joint inboard slip driveshaft, depending on the location of the slip spline or other axial motion device. The two-joint outboard slip driveshaft is a driveshaft or part of a driveline with a universal joint at each end. Axial movement is provided outboard of joint centers. This type of shaft, illustrated schematically in Fig. 14(a), is commonly used in passenger car applications. The two-joint inboard slip driveshaft is a driveshaft or part of a driveline with a universal joint at each end. Axial movement is provided inboard of joint centers. This type of shaft, shown schematically in Fig. 14(b), is usually used in truck applications. A two-joint driveshaft construction without provision for axial or telescopic motion, illustrated schematically in Fig. 14(c), is also used in certain limited applications as a structural member to resist thrust forces in addition to transmitting torque.

Fig. 15 shows a two-joint outboard slip driveshaft with various typical Cardan joint yoke, bearing, bearing retainer, and tube

American Axle v. Neapco - IPR2025-00091
PET_AAM_1012-0015

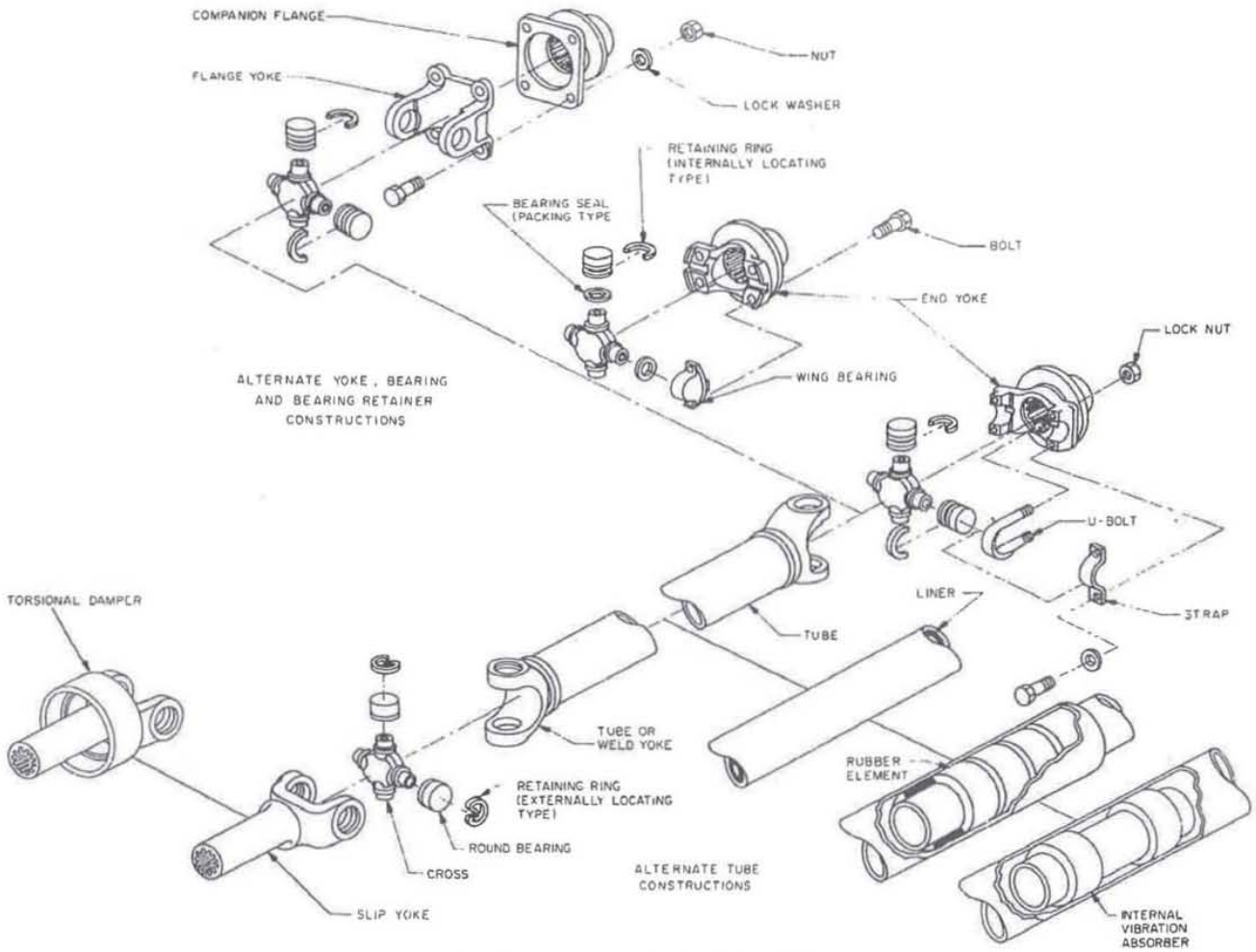


Fig. 15 — Two-joint outboard slip driveshaft

constructions. Additional yoke, bearing, and bearing retainer constructions are described in the section on the Cardan joint. Fig. 16 illustrates a typical two-joint inboard slip driveshaft construction.

Three-joint drivelines, which are are used in some passenger cars, are more often required in truck applications. A shaft support bearing at an intermediate position must be used in these two-piece driveline arrangements. Various support bearing designs are shown in the chapter on *Shaft Support Bearings*. Fig. 17 illustrates schematically two common types of shaft constructions used in truck drivelines. The front section of these shaft constructions is referred to as a single joint coupling shaft. It is the coupling member or members of a multiple joint driveline which consists of a universal joint, tube, shaft support bearing, and a slip or fixed spline shaft. In a multiple joint driveline, when more than one support bearing is necessary, these coupling shafts can be connected in series as required. In Fig. 17(a), a slip spline shaft is shown at the support bearing. Hence, the rear section must be of the two-joint outboard slip driveshaft construction in order to accommodate the axial travel required by rear axle movements. In Fig. 17(b), an interference or permanent fit (fixed) spline shaft is

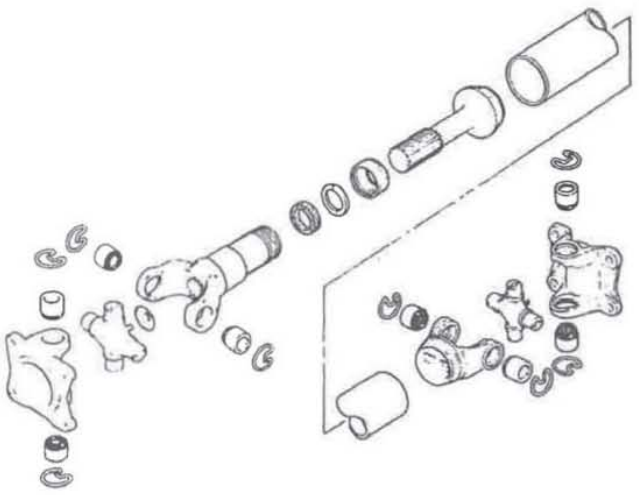


Fig. 16 — Two-joint inboard slip driveshaft

American Axle v. Neapco - IPR2025-00091
PET_AAM_1012-0016

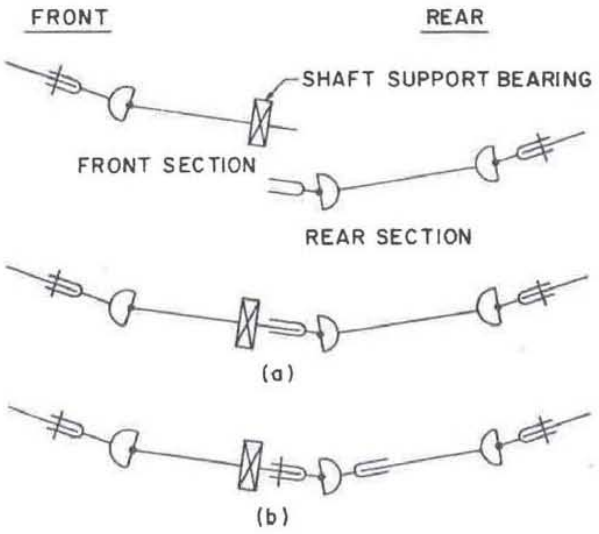


Fig. 17 — Three-joint driveshaft constructions

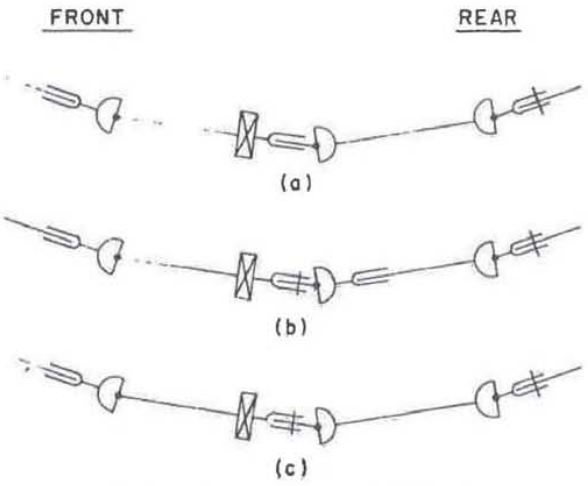


Fig. 18 — Three-joint driveshaft constructions

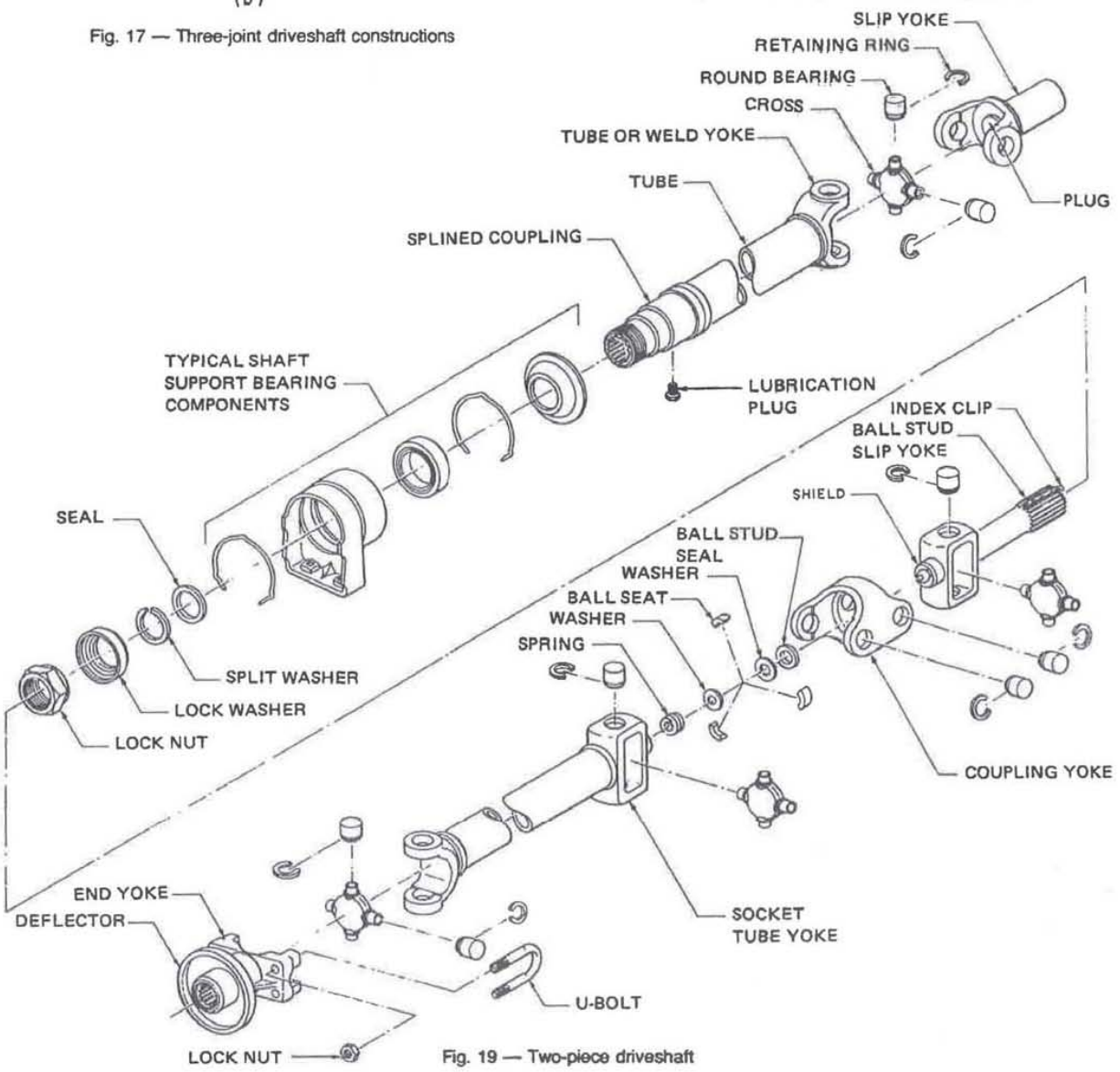


Fig. 19 — Two-piece driveshaft

American Axle v. Neapco - IPR2025-00091
PET_AAM_1012-0017



Fig. 20 — Agricultural implement PTO driveshaft

illustrated at the support bearing. Therefore, the rear section must be of the two-joint inboard slip driveshaft construction in order to accommodate the required axial stroke. In both of these shaft constructions, an interference or permanent fit spline is shown at the front or transmission end, as well as at the rear end.

It is possible to employ both of these shaft constructions with a slip spline at the front instead, as shown schematically in Fig. 18 (a) and (b). This design concept, most often found in passenger cars, can reduce the driveline cost and readily accommodate vehicle build tolerances. Fig. 19 illustrates such a typical two-piece passenger car driveshaft featuring a Cardan, double Cardan, and Cardan joint in series. Since a slip spline is employed at the support bearing, the rear section of the driveline must be of the two-joint outboard slip driveshaft construction as shown schematically in Fig. 18(a).

When a passenger car is equipped with independent rear suspension, the main driveline is not required to accommodate axial travel due to rear wheel movements. Hence, when a two-piece driveshaft is necessary in such a vehicle, a slip spline is required only to provide build tolerances. A shaft construction with a slip spline at the front, as illustrated schematically in Fig. 18(c), has been used.

In agricultural implement applications, a typical two-joint inboard slip driveshaft construction, such as shown in Fig. 20, has been commonly used. This telescoping power take-off driveshaft incorporates a quick-disconnect yoke design for ease of attachment to the tractor's power take-off drive system and a safety shield. The chapter on *Agricultural Implement Driveshafts* describes other typical driveshaft constructions being used.

Axle driveshaft constructions of various designs have been used depending on the vehicle application requirements and are described in the chapter on *Axle Driveshafts*. Fig. 21 illustrates a typical axle driveshaft with a Cardan joint which is used at the front steerable wheel of a live, rigid axle for a light-duty truck. The universal joint is positioned inside the commonly used open steering knuckle construction. Axle driveshafts which are employed with independent wheel suspensions, in general, require universal joints other than the common Cardan joint. Fig. 22 shows a typical axle driveshaft or halfshaft with constant velocity joints for a front drive passenger car. The chapter on *Universal Joints* describes various joint designs which may be used for axle driveshafts depending on the application requirements.

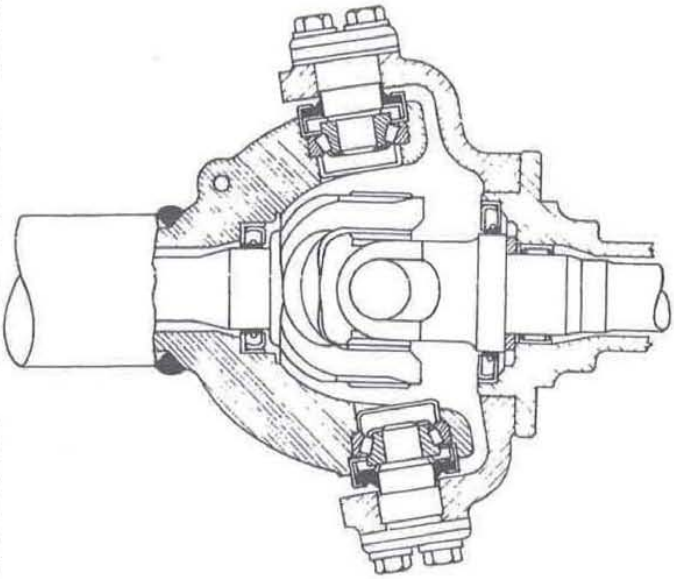


Fig. 21 — Light-duty truck axle driveshaft with Cardan joint for front live, rigid axle

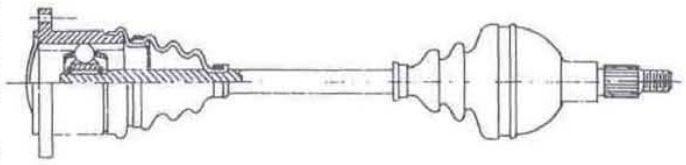


Fig. 22 — FWD passenger car axle driveshaft with constant velocity joints

American Axle v. Neapco - IPR2025-00091
PET_AAM_1012-0018

Basic Driveline Requirements

Chapter 2

American Axle v. Neapco - IPR2025-00091
PET_AAM_1012-0019

Section 2.1—Driveline Functions 15
Section 2.2—Application Parameters and Established Practices 17
Section 2.3—Design Torque Considerations 23
Section 2.4—Vehicle Driveline Analysis 25
Section 2.5—Duty Cycle Determination 31

Basic Driveline Requirements

American Axle v. Neapco - IPR2025-00091
PET_AAM_1012-0021

Section 2.1
Driveline Functions

D. W. Holzinger — Spicer Universal Joint Div., Dana Corp.

The driveline or driveshaft in an application must perform certain basic functions which vary in importance from one application to another. The four basic functions which the driveline must fulfill are:

Torque

The primary purpose of the driveshaft in an application is to transmit torque through an angle between the power source and the driven member.

Rotation

The driveshaft must be capable of rotating through a speed range as required by a given application.

Angles

The universal joints used in a driveshaft must be capable of operating at fixed or varying angles of the intersecting shaft rotational axes.

Length Changes

Most driveshaft installations require some means of compensating for or effecting shaft length changes. In a typical two-joint driveshaft, these length changes or axial movements may occur as follows:

1. Between the universal joint centers.
2. At one or both ends outside of the universal joint centers.
3. Within one or both universal joints which have end motion capabilities.

Since the driveline is essentially a rotating power transmission element in a drive system, it depends upon the driving and driven members for its support. The dynamic characteristics of these supports can substantially influence the driveline in operating smoothly, while performing its required functions. These functions determine the dynamic operating characteristics of the driveline and their effects on the application's overall system. It is important to evaluate these functions and to consider their effects in the selection of a driveline for a given application.

In summary, the four basic functions that the driveline is expected to satisfy are torque, rotation, angles, and length changes. In conjunction with these basic functions, the means of support for the driveline provide an important contribution in the successful performance of these functions.

References

1. P. J. Mazziotti, *Dynamic Characteristics of Truck Driveline Systems*, SAE Paper SP-262, 1964.

American Axle v. Neapco - IPR2025-00091
PET_AAM_1012-0023

Section 2.2
Application Parameters and Established Practices

D. W. Holzinger — Spicer Universal Joint Div., Dana Corp.
R. W. Powers — Oldsmobile Div., GMC
J. M. Lyons — Mack Trucks, Inc.

Introduction

The design of a driveline or driveshaft requires consideration of the basic functions which it is expected to perform in conjunction with the specific application parameters of the intended application. The driveline's basic functions are described in the previous section on *Driveline Functions*.

In correlating the driveshaft's functions with the required application parameters, design limits relative to torque capacity, performance, and life expectancy or durability, must be established. These limits may be of the evolutionary type, such as those which have been obtained through experience and successful performance in applications, or by evaluation of the design parameters with the use of a computerized mathematical model. It is good practice to substantiate the results of the mathematical analysis with physical test procedures such as laboratory and field tests. Once established, these limits and test data can serve as useful design guidelines or practices and together with the application's requirements, a satisfactory driveline can be designed for the intended application.

The following application parameters and established practices apply, in particular, to vehicle main or longitudinal drivelines, while those requirements related specifically to accessory drives, agricultural implement driveshafts, and axle driveshafts are discussed in the chapters pertaining to those shaft constructions. Also, the following established practices can apply to numerous other drive system possibilities when properly altered or modified for a specific application.

Durability

The driveline in an application must be capable of functioning satisfactorily for the intended life expectancy when subjected to all the operating requirements for which it is designed. Each driveshaft design has an operating capability which is basically the durability or life of the driveshaft assembly.

Based on a comprehensive knowledge and understanding of all the parameters pertaining to an application, it is possible to design a driveshaft for the application. The complete driveshaft should have the torsional strength characteristics to transmit the torque without premature fatigue failure. The driveshaft universal joints must have a bearing design that is capable of transmitting the torque and speed through the required joint angles and under the environmental conditions encountered. The slip splines or other axial motion means employed must be capable of accommodating the required length change and be designed with adequate wear life and lubricant retention to withstand the combined effects of torque, axial motion, and environmental conditions. The driveshaft design dimensions must be proportioned so as to minimize the effects of the dynamic forces and have adequate stiffness or a large enough diameter to operate safely at the maximum operating speed.

The durability of a driveshaft or the final substantiation that the design will meet the intended requirement is most effectively established by actual vehicle tests. These tests can be used to determine the effects of torque, speed, joint angles, length changes, environment, vibration, and manufacturing limits on the life and suitability of the design for the application.

Torque Capacity

The driveline in an application must be capable of transmitting the maximum torque developed by the drivetrain. In a typical application, the drivetrain may be subjected to various torsional loading modes during its service life. These torque loads can be applied steadily under static or rotating conditions or the drivetrain may be subjected to intermittent shock or impact type torsional loads which, depending on the source or origin of these loads, can be considerably higher than the maximum computed steady load.

For example, the torque requirements for a typical passenger car driveshaft are selected on the basis of the vehicle's weight, the normal continuous operating torque, and the maximum short duration torques resulting from normal vehicle usage. Also, the passenger car's weight as well as the design and functional characteristics of the entire power train and drivetrain system determine the maximum levels of various shock torques which may be achieved in a vehicle. The driveshaft must be capable of safely transmitting these maximum torques which can be developed by various abusive loading modes as described in the following section on *Design Torque Considerations*.

The continuous operating torque is representative of that torque which the driveshaft is required to transmit for the greatest percentage of time during the vehicle's life expectancy. This torque is dependent on the transmission output torque required to propel the car at normal highway cruising speeds.

The maximum short duration torque is the greater of either the engine torque multiplied by the torque converter stall and transmission low gear ratios, or the wheel slip torque. In most cases, the passenger car is tractive limited and, therefore, the maximum short duration torque will be controlled by wheel slip. This condition is generally true for the larger cars where engine size and

American Axle v. Neapco - IPR2025-00091
PET_AAM_1012-0025

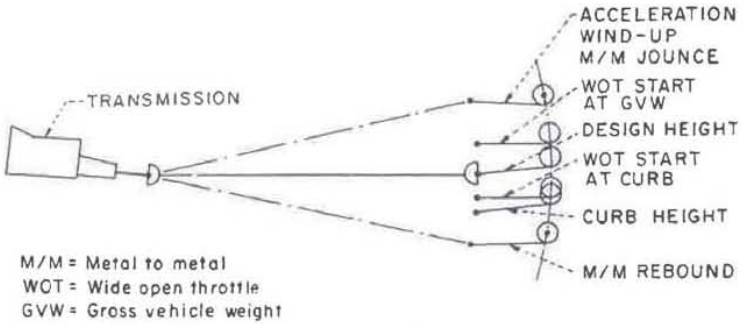


Fig. 1 — Typical passenger car rear axle movements affecting driveline geometry

transmission gear ratios are in excess of that required for normal performance. It is always prudent to compare both the maximum engine delivered and wheel slip torques. This mathematical procedure is shown in the *Vehicle Driveline Analysis* section of this chapter for various typical vehicles.

The various torsional loading modes described for passenger cars also apply, in general, to truck drivelines. The loading severity on the driveshaft, however, can vary greatly depending on the usage of the specific vehicle. In passenger car and light-duty truck applications, the lower gears are not as widely used as in medium and heavy-duty trucks. In off-highway vehicles, the percentage of the total operating time which is spent in the lower gears is still greater. Since the maximum torque operating time in these vehicles is much longer by comparison, and the lower gear torques are used considerably more, additional information about the application's operating characteristics must be known in order to predict universal joint life. For these vehicle applications, a load or duty cycle must be established in order to determine a total life expectancy. This procedure is shown in the *Duty Cycle Determination* section of this chapter.

Rotational Speed

Depending on the application, the driveline may be required to rotate through a relatively large speed range, which can vary from zero to the engine's maximum speed. In addition, higher speeds can result from engine "overspeeds" and/or gear unit overdrive ratios. Consequently, the driveshaft must be capable of performing safely for sustained periods of time at the peak operating speed of the drivetrain for which it is intended.

This speed capability requires that the critical speed of the driveshaft must be higher than the maximum design rotational speed of the drivetrain. To avoid operation in the critical speed range, the accepted practice for typical passenger car and light-duty truck applications has been to design the driveshaft and powerplant (engine and transmission) so that the peak operating speed encountered is equal to or less than 85% of the driveshaft's true critical speed. For medium and heavy-duty truck applications, the peak operating speed of the driveshaft should be equal to or less than 75% of the shaft's critical speed.

These critical speed design practices or guidelines can limit the maximum permissible installed length of the driveline as well as the minimum tube diameter and the maximum tube wall thickness. Therefore, if the required shaft length and the available underbody clearance space do not permit the use of a commonly used one piece driveshaft, a two piece or multipiece driveline must be employed to meet the critical speed and clearance requirements. The subject of critical speed is discussed in detail in the chapter on *Critical Speed*.

Universal Joint Angles

The universal joints of the driveline must be capable of operating through the required range of angles at varying torque loads and operating speeds without causing objectionable disturbances. The true universal joint angles of the driveline can be established by means of a layout or by a computer analysis procedure at the normal and extreme operating conditions.

Fig. 1 illustrates schematically the rear axle movements of a typical passenger car which affect its driveline geometry. By means of a layout computation or computer analysis procedure, it is possible to determine the location of the universal joint centers, true joint angles and shaft length changes, or axial movement of the driveshaft for all positions of rear wheel and axle carrier nose movement. In addition, from this study, the operating envelope of the driveshaft can be determined and, therefore, disclose the necessary underbody clearances that must be provided. The determination of the maximum varying joint angles resulting from the given application's requirements is extremely important in the design of a universal joint. Interference of joint components at the extreme instantaneous angle condition can result in joint failure.

The permissible magnitude of the continuous or normal design operating angles of the driveline's universal joints, as well as the relative values of these angles when they are not equal, requires particular consideration in determining the optimum driveline geometry. Depending on the application parameters, both constant and nonconstant velocity type of joints have limitations on the continuous operating angles due to their specific design and functional characteristics, as described in the chapter on *Universal Joints*.

For example, the Cardan joint is commonly used in automotive vehicle drivelines, as shown schematically in Fig. 1; and, because of its nonuniform motion characteristics, the maximum size of the

American Axle v. Neapco - IPR2025-00091
PET_AAM_1012-0026

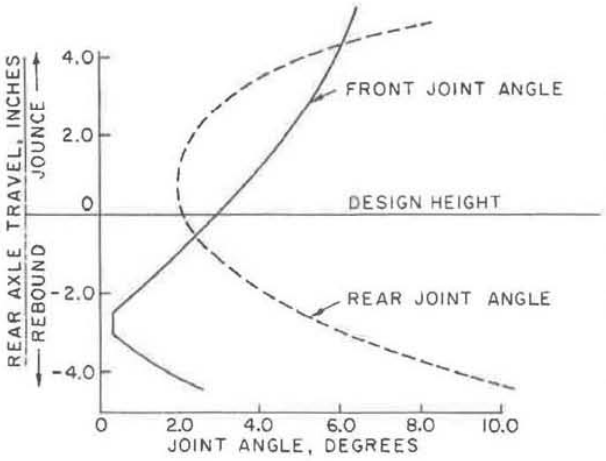


Fig. 2 — Front and rear joint angles

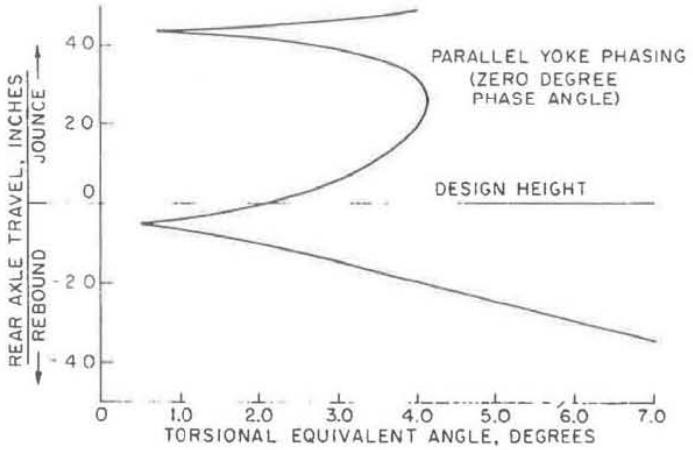


Fig. 3 — Torsional equivalent angles

true joint angles at a normal continuous operating condition must be limited. This limit is necessary in order to control certain inherent objectionable disturbances. These disturbances are generally related to torsional, inertia, and secondary couple excitations which are produced by the Cardan joint's nonconstant velocity motion characteristics reacting on the driveshaft and its supporting members. These excitations and their effects are described in detail in the section on the *Cardan or Hooke Universal Joint* and also briefly in the chapter on *Vibration Control*.

For the entire range of rear axle movements illustrated in Fig. 1, the front and rear joint angles for a typical passenger car one piece driveshaft are shown in Fig. 2, while Fig. 3 illustrates the torsional equivalent angles. Although they are not shown, it is also possible to determine by layout computations or computer analysis other driveline kinematic characteristics such as inertia equivalent angles and secondary couple forces as required. By studying Figs. 2 and 3, it is apparent that the selection of joint angles and resulting kinematic characteristics for the design position represent an optimum compromise in a driveshaft application where widely varying operating angles may be possible. Generally acceptable limits for the various excitations which are explained in detail in the section on the *Cardan or Hooke Universal Joint* are described briefly as follows:

Torsional Excitation Limits

The amplitude of torsional oscillation produced by the Cardan joints, which can be accepted without causing excessive disturbance, depends upon the operating speed of the driveshaft and the characteristics of supporting structures and other units in the drivetrain. Experience has shown that if this form of excitation is maintained under approximately 400 rad/s² maximum angular acceleration in any continuous operating position and speed, the driveshaft, in general, will perform satisfactorily in passenger car and most truck installations. In some other applications, this torsional excitation level may be increased and still provide satisfactory performance.

Inertia Excitation Limits

This excitation is produced by the oscillating torque loads resulting from the driveshaft inertia being accelerated through nonuniform motion. Automotive vehicle installations are extremely sensitive to this type of excitation and to the disturbance it creates. For typical passenger car and light-duty truck two-joint driveshafts, which are quite long and have a relatively large shaft inertia, the acceptable excitation level must be kept under a maximum angular acceleration of approximately 1000 rad/s² in any continuous operating position. When the shaft inertia is relatively small, as is often the case in many multipiece truck drivelines, the maximum angular acceleration can be increased to 2000 rad/s². In some other applications, this inertia excitation level may be increased further without causing excessive disturbance.

For the numerous driveshaft applications where the accepted maximum acceleration level is 1000 rad/s², Table 1 may be used as an application guide for determining permissible operating joint angles. In this table, the angles and speeds are continuous conditions for a one piece, two-joint driveshaft with equal joint angles.

Table I — Allowable Operating Joint Angles

Driveshaft Speed, rpm	Maximum Operating Angle, Deg
5000	3° 30′
4500	3° 50′
4000	4° 20′
3500	5° 00′
3000	5° 45′
2500	6° 55′
2000	8° 40′
1500	11° 30′

Secondary Couple Excitation Limits

This excitation is caused by the Cardan joints transmitting torque at an angle. The secondary couples react about the shaft's supporting members and are equivalent to a static force plus an

American Axle v. Neapco - IPR2025-00091
PET_AAM_1012-0027

oscillating force with a frequency of two cycles per revolution. The magnitude of the excitation depends on the transmitted torque, joint angle size, supporting bearing spans, and phase relationships of the joint yokes.

The shaft support bearing used at an intermediate location in a typical automotive vehicle three-joint, two piece driveshaft is quite sensitive to this excitation because it usually has a well defined resonant frequency. The secondary couple forces will excite the support bearing at a shaft rotating speed equivalent to one half of the resonant frequency due to the fact that the oscillating force occurs twice per revolution of the shaft.

Experience in vehicle driveline installations having shaft support bearings has shown that the dynamic or rotating couple force should be maintained under a certain maximum value in order to prevent an objectionable shudder type of vibration. In Table 2 are shown the limits on the oscillating force, which have been found to be generally acceptable at maximum transmitted torque occurring during low speed accelerating conditions of the vehicles indicated. As previously indicated, these rotating couple forces act twice per driveshaft revolution on the shaft support bearing.

Table 2 — Maximum Dynamic Couple Forces

Installation	Maximum Dynamic (Rotating) Couple Force, lb
Passenger Cars	8
Light-Duty Trucks	15
Medium-Duty Trucks	25
Heavy-Duty Trucks	75

Length Changes

Driveline length changes or axial movements are required during varying operating and loading conditions in an application, as well as for those length changes necessary to facilitate assembly and disassembly. Additional length changes are also necessary to accommodate vehicle build tolerances and to compensate for the effects of temperature change.

More specifically, the driveshaft length changes during operation of a typical automotive vehicle are due to the extremes of suspension travel as shown in Fig. 1, ranging from full jounce to full rebound positions, as well as rear axle carrier nose windup and winddown. In addition, flexibility in the structure such as frame twist and compliance or deflection of the engine and transmission rubber mounts at the front and suspension rubber bushings at the rear, affect these length changes. All of these variations in shaft length must be studied in order to determine the required total axial motion or slip capability of the driveshaft. These length variations can be determined by means of a drivetrain layout or by its computerized equivalent.

In order to most accurately determine the changes in length, the dynamic operating conditions of the drivetrain can also be simulated with a computer program. High torque loads, when applied to the drivetrain, cause the various drivetrain members to shift to new positions from their initial static locations. The dynamic operating position of the drivetrain is necessary in order to predict the true driveline geometry (true joint angles and length) for a particular dynamic condition.

Typical driveshaft constructions which provide for length changes are described in the chapter on *Driveline and Driveshaft Arrangements and Constructions*. Conventional sliding or slip splines are generally used to accommodate these length changes. When end movement is required during high torsional load applications on the driveline, the resulting axial thrust forces produced by the slip spline may be excessive depending on its design and are, therefore, undesirable. The chapter on *Splines and Axial Motion Devices* describes splined mechanisms and end motion type universal joints suitable for various applications, as well as means of reducing these high thrust loads, which can be detrimental not only to the driveshaft itself but also to the supporting bearing structures of the other drivetrain members.

Clearances

The driveline in an application must be provided with adequate clearances during varying operating and loading conditions. In a typical passenger car application, for example, operating clearances must be provided for such underbody components as the floor pan, exhaust system, brake control cables, or any other obstructions which could be placed within the operating envelope of the driveshaft. This envelope is determined by the rear suspension travel and axle differential carrier nose windup and winddown, as well as the swing diameter of the universal joints, tube and driveshaft mounted vibration control devices. The actual tolerances on clearances of such components as the exhaust system is mainly dependent on available space. It is always desirable to keep the exhaust system as far away as possible because of its high temperatures. The floor pan, however, is usually designed so that the driveline tunnel in the passenger compartment can be made as low as possible for maximum utilization of the interior space for passengers.

The critical speed for the driveshaft required in a given application depends on the peak operating speed of the drivetrain. This critical speed requirement can restrict or limit the permissible maximum installed length of the driveshaft as well as the minimum tube diameter and the maximum tube wall thickness. As previously explained for a typical passenger car driveline shown in Fig. 1, the driveshaft must operate within an envelope and this envelope should provide adequate underbody clearances.

In order to solve underbody clearance problems in a typical vehicle, it is often possible to reduce this tube diameter along certain portions of the shaft length where a minimum effect on critical speed occurs. This procedure is possible when the tube size possesses excess torsional strength and was chosen only for critical speed considerations. Since the effect on critical speed is a minimum at or near the ends, the usual practice in passenger car driveline design is to reduce or swage one or both ends of the tube as required to provide the necessary clearance while still satisfying the torque and rotational speed requirements of the application.

If the required shaft length and the available underbody clearance space do not permit the use of a commonly used one piece driveshaft, a two piece driveline may be employed to meet the critical speed and operating clearance requirements. In addition to

American Axle v. Neapco - IPR2025-00091
PET_AAM_1012-0028

the various underbody clearances, the passenger car driveline must also be provided with adequate ground or road clearance which a typical on-highway vehicle may require during normal service.

In many truck applications, multipiece driveshafts are extensively used. The front section or sections of these shaft constructions are called single joint coupling shafts, which operate in relatively fixed positions. The rear section is either a two-joint outboard slip or a two-joint inboard slip driveshaft design. When only one single joint coupling shaft is employed, its front end is attached to the transmission or other drivetrain gear unit, while near its rearmost end it is supported by a shaft support bearing, which is generally attached to a frame cross member. When an additional single joint coupling shaft or shafts are required, they are commonly coupled in series by attaching them to the rear of the preceding coupling shaft. Also, these additional coupling shafts are attached to frame cross members with shaft support bearings. Besides being provided with operating clearances for the typical underbody obstructions as previously described for the passenger car, the front section or sections of multipiece drivelines must have adequate clearances at the truck frame cross members. Usually, in these multipiece drivelines, only the rear two-joint driveshaft section must be designed to accommodate clearances due to suspension and axle movements.

Another clearance problem which must be analyzed, especially with regard to off-highway operation of trucks, is terrain clearance. The variation in the terrain, including obstructions or hazards found on this terrain, may interfere with the driveline in performing its principal functions. Therefore, the driveshaft should be positioned so that it will not interfere with or contact the variations in the terrain. If this is not possible, protection should be provided for in the form of a skid plate or shield.

In the case of an all wheel drive installation such as in a typical four-wheel drive vehicle, the front driveshaft extending from the transfer case to the front differential can present an additional clearance design problem during front suspension and axle movements. This shaft must have sufficient clearance as it passes the transmission and engine to the front axle, and because of its required location in some vehicle applications, the maximum tube diameter may be limited.

A factor which can affect the design parameters of the front driveshaft is whether the four-wheel drive vehicle is capable of full-time or only part-time four-wheel drive operation. If the vehicle is designed with a full-time four-wheel drive system, then both torsional strength and critical speed must be considered in selecting the tube size. However, when the driveshaft's length is relatively short, which is the case in most of these vehicles, the tube size can usually be based primarily on torsional strength and not critical speed to meet the application's requirements. In a part-time four-wheel drive system, the all-wheel driving mode is limited to a relatively low speed range of the vehicle and thus torsional strength and not critical speed is most often the major factor in determining the required tube size.

Environment

The driveline must be capable of operating satisfactorily in extreme or adverse environmental conditions as dictated by the application's requirements. This capability requires that the driveshaft may have to operate for sustained periods of time without functional damage to such vital driveline components as universal joints, splines, and shaft support bearings, as well as breakdown or deterioration of the lubricants used in these components.

These driveline components have seals which are usually of elastomeric or part elastomeric material construction. These vital seals must withstand exposure to adverse or detrimental environmental conditions which can include dust, sand, dirt, mud, and other foreign particles or substances as well as temperature, moisture, humidity, salt spray, and destructive atmospheric elements such as ozone. Of these environmental effects, the levels of vehicle underbody ambient temperatures in the areas of the joints, as well as actual joint temperatures, have been found to be quite important to the life of the driveshaft.

When conventional Cardan or double Cardan joints are utilized in a typical automotive vehicle driveshaft, the highest joint bearing temperatures will commonly occur in those yoke members which are attached directly to the transmission output shaft at the front and to the final drive pinion shaft at the rear. These higher joint bearing temperatures result from additional heat being conducted from the transmission and final drive unit thru the connecting shafts. In general, sustained high speed level road driving does not yield the highest joint ambient or bearing temperatures. Driving in congested city traffic, for example, usually results in higher temperatures. The negotiation of relatively steep grades for an extended period of time will generally develop the highest operating temperatures. Also, certain controlled idle operations can produce higher temperatures than high speed level road driving. In addition, immediately after the engine has been turned off following any sustained vehicle operation, an additional temperature increase may occur for a short period of time. Hence, depending on the application, special seal materials and lubricants may be required in the driveline components if extremely high temperatures or other adverse environmental conditions are encountered.

Design and Manufacturing

The driveline must be designed and manufactured within predetermined specifications so that it can perform its basic functions and meet the various application requirements for its intended life expectancy. Practical limits for satisfactory driveshafts have been established through design and manufacturing experience as well as successful performance in their particular applications.

For example, a driveshaft rotating at high speed must be maintained at a satisfactory level of dynamic balance to prevent vibrational disturbances from reaching objectionable levels. The amount of unbalance which can be tolerated depends upon the sensitivity of the driveshaft's end supports. The need for an additional shaft support bearing in a two piece driveline provides still another mounting to the drive system that can transmit disturbances.

Driveshaft balance is a function of shaft weight and straightness, tube ovality and control of the dimensions that affect clear-

American Axle v. Neapco - IPR2025-00091
PET_AAM_1012-0029

ances. Hence, good design practice and manufacturing quality are important in achieving good dynamic balance. The chapter on *Balancing* describes typical commonly used manufacturing unbalance limits for passenger car and truck driveshafts. The chapter on *Tubing* lists typical straightness and ovality tolerances for various sizes of commonly used tubing.

With regard to the universal joints employed in a driveshaft, limits on optimum clearances within these joints, as well as a specified articulating, rocking, or flexing torque, should not be exceeded, otherwise objectionable vibration may result and universal joint life may be reduced. When the limits on optimum clearances between mating components of the driveshaft slip member are exceeded, objectionable vibrations or noises may also result. Further, when axial thrust forces are excessive during shaft length changes, the effects on the driveshaft itself and on the shaft supporting members may be detrimental.

Attachment

The attachment of a driveline to other drivetrain members in an application can be accomplished in a number of ways as described in the chapter on *Driveshaft Attachment Methods*. These other drivetrain members also serve as the supporting means for the driveline. Since the driveshaft is an integral member of the drivetrain, the characteristics of these supporting members, the method of attaching the driveshaft to these members, and the design of the attachment means have a major influence on the shaft in performing its required functions and in attaining its intended life expectancy.

The attachment means chosen or required must have sufficient strength to withstand the forces which may result from the functional requirements and operating characteristics of the application. Also, the ease of assembly and disassembly, for servicing, should be considered when selecting a particular attachment method. In addition, economic considerations may influence the usage of a certain attachment design instead of an alternate proposal in relatively high volume production, such as for passenger car applications.

A typical passenger car one piece driveshaft, utilizing conventional Cardan or double Cardan joints, is generally attached to the transmission output shaft by means of a slip spline connection incorporated in the front universal joint. At the rear, the driveshaft is usually attached to the final drive pinion gear shaft with an end yoke or with a flange yoke and companion flange using appropriate fasteners of sufficient strength. The size of the fastener must be large enough to retain the driveshaft at maximum torque and it should not prematurely fatique under the effects of the various operating requirements. When a two piece driveline is incorporated in the vehicle, the shaft must also be attached to the vehicle's structure at an intermediate location with a shaft support bearing having a bracket configuration suitable for attachment.

References

1. P. J. Mazziotti, "Universal Joints and Propeller Shafts," *Dana Corporation Bulletin J-1371*, October 15, 1954.
2. R. R. Burkhalter and P. J. Mazziotti, *The Low Silhouette Drive Line*, SAE Paper 691, 1956.
3. M. C. Kaye, *Some Aspects of the Truck Drive Train Vibration Problem*, SAE Paper 402A, 1961.
4. J. A. Kayser, *Drivelines for Heavy Equipment*, SAE Paper 403A, 1961.
5. W. T. Condon, *Application of Universal Joints to Construction and Industrial Machinery*, SAE Paper 403B, 1961.
6. H. R. Pickford, "Hints on How to Reduce Truck Drive Train Vibration" (Written Discussion on SAE Paper 402A), *SAE Journal*, April, 1962, pp. 70-73.
7. P. J. Mazziotti, *Dynamic Characteristics of Truck Driveline Systems*, SAE Paper SP-262, 1964.
8. B. R. Reimer, *Design and Application Considerations for Agricultural PTO Drivelines*, SAE Paper 650680, 1965.
9. C. E. Cooney, *Design and Application of Universal Joints for Off-Highway Vehicles*, SAE Paper 650681, 1965.
10. C. E. Cooney, *Practical Procedures for Designing and Analyzing a Tandem Truck Driveline*, SAE Paper 660413, 1966.
11. C. W. Haines, *Drivelines for High Performance*, SAE Paper 700742, 1970.

American Axle v. Neapco - IPR2025-00091
PET_AAM_1012-0030

Section 2.3
Design Torque Considerations

E. R. Wagner, P.E. — Saginaw Steering Gear Div., GMC

It was stated previously that for any specific application, the maximum applied torque, however developed, must be considered in driveline system or component design. The drivetrain is subjected to various torsional loading modes during typical vehicle testing or actual service. These torque loads can be applied steadily under static or rotating conditions or the drivetrain may be subjected to shock or impact type torsional loads which, depending on the source or origin of these loads, can be considerably higher than the maximum computed steady load. The magnitude and frequency of occurrence of these torsional load pulses during operation will vary considerably with the specific vehicle application and the characteristics of the complete engine, clutch, transmission, and drivetrain system to and including the road wheels. Therefore, in the design of a driveshaft or any of its components for a specific application, a suitable safety factor for these shock or impact effects must be used based on past experience with a similar installation. Also, the actual peak shock loading can be determined readily with an instrumented drive system.

The computation procedures determining the maximum torque developed by the power trains of some typical vehicles is illustrated in the following section on *Vehicle Driveline Analysis*. Also for each vehicle, the maximum driveshaft torque due to tractive effort or wheel slip is computed to show its magnitude relative to engine delivered torque. Although it is not shown, the maximum engine delivered torque in the various drivetrain components can vary due to the different maximum torque multiplication ratios possible in the gear reduction units which may be used in a given application as optional equipment. Also, the maximum tractive effort torque can vary substantially when various tire sizes and axle ratios are employed. Therefore, not only is the level of the maximum transmitted torque affected, but also the normal or continuous operating torque level will vary. In addition, the operating speeds of the driveshafts in the main driveline system and of the axle driveshafts are affected. For example, when a typical rear drive passenger car is being driven on a level highway at constant car speed, the driveshaft will experience a higher road load torque with a lower numerical axle ratio than with a higher numerical axle ratio. However, with regard to rotational speed, the driveshaft will rotate more slowly with the lower axle ratio than with the higher axle ratio when this same vehicle is operating at constant car speed. Thus, the vehicle's entire drive system must be studied with regard to various possible combinations of torque and rotational speed which can affect the driveline component design parameters.

In the computations in the following section on *Vehicle Driveline Analysis*, neither the maximum engine developed torque nor the torque resulting from tractive effort include possible shock or impact effects. Depending on the type of vehicle considered, these shock or abusive loads can be imposed on the driveline by various means either by testing procedures or during actual service. Vehicle manufacturers utilize various typical controlled test procedures to determine these shock peaks with instrumented vehicles. When a manual transmission is employed, for example, a severe shock torque can be developed on a dry paved surface during the commonly called "clutch pop" procedure.

Another common method of inducing severe shock torque in the driveline is with the "rock cycle" procedure, which can be readily accomplished with a typical automatic transmission equipped passenger car. These high torsional load impulses are due to the acceleration of the vehicle's torsional system inertia in a very short period of time.

A high torsional load, but with a less severe shock characteristic than that occurring during "clutch pop" or "rock cycle" testing, can be applied during a typical "stoplight drag" or "jack-rabbit" start condition. This loading condition, which includes some inertia produced torque can occur quite frequently during actual service in typical automobiles and is usually more severe in a manual transmission equipped vehicle. Compared with a typical wide open throttle (WOT) start from engine idle, this loading condition is more severe.

In passenger car applications, vehicle weight, as well as the design and functional characteristics of the entire power train system including the engine, clutch, transmission, various drivetrain components, and the road wheels can affect the intensity of the various described shock effects. Hence, all of these factors must be considered in determining the magnitude of the maximum applied torque which the driveline experiences.

For relatively small size passenger cars with a curb weight of less than approximately 2200 lb, the shock torque due to "clutch pop" and "rock cycle" loading conditions can be from 2 to nearly 2¾ times the maximum theoretical engine delivered torque in the driveline disregarding drivetrain component efficiencies.

Also, for small manual transmission equipped cars, the "stoplight drag" generated torque is usually higher than the maximum theoretical value. In an automatic transmission car, the "stoplight drag" is approximately the same as the maximum theoretical torque. The entire drive system's torsional inertia is the important factor in the small car's ability to develop these high shock torque loadings with a relatively small engine.

For typical passenger cars in the 2200-4400 lb curb weight range, the effect of the inertia produced torque on shock loading generally decreases with increasing vehicle weight. Also, the engine torque usually increases at a faster rate than vehicle weight. In addition, automatic transmissions are more commonly used in this size range of cars. For most automatic and manual transmission equipped vehicles in the upper half of this weight range, the shock torque values produced by "rock cycle" and "clutch pop" test, respectively, are approximately 50% higher than the maximum theoretical engine developed torque in the

American Axle v. Neapco - IPR2025-00091
PET_AAM_1012-0031

driveline.

For typical passenger cars in the over 4400 lb curb weight range where automatic transmissions are standard equipment, the vehicle generally has considerably more engine torque available relative to its weight than a smaller car. The torsional shock loading produced in these size vehicles by "rock cycle" test may be from somewhat less than the maximum theoretical engine delivered torque in the driveline, to slightly above this value. Therefore, in these vehicles, the maximum theoretical engine delivered torque through the automatic transmission (stall torque) is usually the highest torsional load imposed in the driveline.

The previously described torsional loading conditions governing the various size passenger cars will of course likewise apply to axle driveshafts or halfshafts when they are used. These axle driveshafts may be employed in a car with front located engine and transmission, but with the rear differential chassis mounted instead of being part of the common live axle design. The independently sprung rear driving wheels are thus driven by universal jointed halfshafts. These axle driveshafts are also used in front engine-front drive or rear engine-rear drive vehicles. In these vehicle drive system arrangements, the power train has a relatively shorter power flow path than a conventional rear drive vehicle with the engine and transmission located at the front.

When vehicles with axle driveshafts employ inboard or chassis mounted (sprung) brakes rather than the common unsprung (outboard located) brakes, the maximum engine delivered torque through the automatic transmission (stall torque), for example, does not reach these shafts with the brakes applied. Instead, they must resist the full effects of the braking torque including decelerating effects of the wheel rotational inertia. Braking torque as compared to engine delivered stall torque is instantaneous in nature and, depending on the type of brakes used, can have a relatively high shock or impact value and, therefore, must be considered when inboard brakes are employed in the vehicle.

For truck applications, the factors which affect torque in the drivetrain system are similar in many respects to those factors previously described for passenger cars. As in passenger cars, vehicle weight influences the torsional loading characteristics. Trucks are commonly classified according to gross vehicle weight (gvw) categories as follows:

1. Light-Duty Trucks: 4000-10 000 lb (gvw)
2. Medium-Duty Trucks: 10 000-22 000 lb (gvw)
3. Heavy-Duty Trucks: Over 22 000 lb (gvw)

Because of the large variety of drivetrain arrangements possible, especially in medium and heavy-duty trucks, and because of the severity of the operating and environmental conditions encountered in service by these vehicles, additional factors must be considered. Trucks in this size range are often used in on- off-highway operations which can have a considerable effect on the drivetrain torque loads encountered. Also, torsional loading impulses can be affected by the type of engine employed in these on-highway or off-highway vehicles where both gasoline or spark ignition and Diesel engines are utilized. In addition, the Diesel engine may be of the two or four stroke cycle type. These and other various powerplant types can produce torsional excitation in the drivetrain system. The engine firing impulses cause a torsional acceleration with the magnitude depending on the inertia of the flywheel and other rotating components. Also, engine misfiring produces load impulses of a detrimental nature in the drive system. Depending on the specific characteristics of a particular vehicle power train, many other possible sources of nonuniform rotating motion exist which can produce a disturbing force on the rotating system and must therefore be considered in driveline design.

In agricultural implements, the driveline is subjected to widely varying loading conditions during operation. The implements can be severely overloaded, for example, by jamming or clogging of the operating system by the crop or by a foreign object. Hence, the load levels in critical areas of the operating system are generally limited by design with torque overload protection devices to prevent serious equipment damage.

In industrial or other stationary drive systems, load impulses from typical reciprocating machinery such as compressors must be considered in driveshaft design. Other sources producing variable torque load characteristics are nonuniform contact of gears, cams, linkages or other motion transferring devices.

American Axle v. Neapco - IPR2025-00091
PET_AAM_1012-0032

Section 2.4
Vehicle Driveline Analysis

E. R. Wagner, P.E. — Saginaw Steering Gear Div., GMC

For the following typical highway vehicle configurations, basic mathematical analyses are made illustrating the maximum torque delivered from the engine, the maximum wheel slip torque, and the maximum speed in the driveshaft. Also, the maximum acceleration is determined for the rear wheel drive passenger car only.

Rear Wheel Drive Passenger Car

A typical large rear wheel drive passenger car has the following application parameters:

Maximum installed net engine torque	430 lb-ft
Torque converter stall ratio	2.02
Transmission low gear ratio	2.48
Rear axle ratio	2.94
Automatic transmission with torque converter efficiency factor	0.85
Rear axle efficiency factor	0.95
Wheelbase	130 in
Center of gravity (c.g.) height	21.50 in

Static weight distribution (five passengers)

Total	Front	Rear
5573 lb	2724 lb	2849 lb

Tire rolling radius	14.00 in
Coefficient of friction between tire and road	1.00

The maximum driveshaft stall torque is:

$$T = 12T_eR_cR_{lg}\eta_{at}$$

where:

12 = A constant = 12 lb-in/1 lb-ft
T_e = Maximum installed net engine torque, lb-ft
R_c = Torque converter stall ratio
R_{lg} = Transmission low gear ratio
η_{at} = Automatic transmission efficiency factor

$$= 12 \times 430 \times 2.02 \times 2.48 \times 0.85$$
$$T = 21\ 972 \text{ lb-in}$$

Also, the driveshaft torque due to wheel slip at maximum acceleration with a five passenger load is computed. Fig. 1 shows the dynamic forces acting on the car at such a condition.

The distance of the c.g. from the front wheels is:

$$A = \frac{W_{sr}L}{W}$$

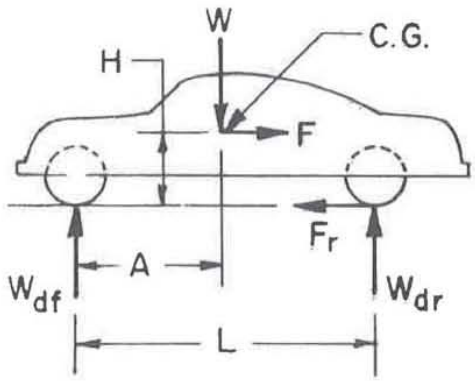


Fig. 1 — Rear wheel drive passenger car at maximum acceleration

where:

W = Total car weight, lb
W_{sr} = Static rear wheel weight, lb
L = Wheelbase, in

$$= \frac{2849 \times 130}{5573}$$
$$A = 66.46 \text{ in}$$

The basic equation for the maximum tractive force at the rear wheels is:

$$F_{r\ max} = \mu\ W_{dr}$$

where:

μ = Coefficient of friction between tire and road
W_{dr} = Dynamic rear wheel weight, lb

The dynamic axle weight at the rear wheels is:

$$W_{dr} = \frac{WA}{L} + \frac{FH}{L}$$

where:

F = Inertia force equals maximum tractive force $F_{r\ max}$, lb
H = Center of gravity height, in

Substituting this expression into the above equation and simplifying, the maximum traction force is:

$$F_{r\ max} = \frac{\mu\ WA}{L - \mu\ H}$$
$$= \frac{1.00 \times 5573 \times 66.46}{130 - 1.00 \times 21.50}$$
$$F_{r\ max} = 3414 \text{ lb}$$

American Axle v. Neapco - IPR2025-00091
PET_AAM_1012-0033

The maximum rear wheel slip torque per wheel is:

$$T = \frac{F_{r\ max}\ r_r}{2}$$

where:

r_r = Tire rolling radius, in

$$= \frac{3414 \times 14.00}{2}$$

$$T = 23\ 898 \text{ lb-in}$$

The maximum driveshaft torque at wheelslip is:

$$T = \frac{F_{r\ max}\ r_r}{\eta_{ra}\ R_{ra}}$$

where:

η_{ra} = Rear axle efficiency factor

R_{ra} = Rear axle ratio

$$= \frac{3414 \times 14.00}{0.95 \times 2.94}$$

$$T = 17\ 113 \text{ lb-in}$$

Assuming a terminal vehicle speed of 120 mph, the maximum driveshaft speed is:

$$N = \frac{168\ R_{ra} V}{r_r}$$

where:

168 = A constant

V = Vehicle speed, mph

$$= \frac{168 \times 2.94 \times 120}{14.00}$$

$$N = 4234 \text{ rpm}$$

In the previous computations, the maximum tractive force at the rear wheels was found to be 3414 lb, and when the coefficient of friction between the tires and road is 1.00, the dynamic rear wheel weight is also 3414 lb. The maximum acceleration corresponding to this dynamic vehicle condition can be determined.

The dynamic front wheel weight is:

$$W_{df} = W - W_{dr}$$

$$= 5573 - 3414$$

$$W_{df} = 2159 \text{ lb}$$

The inertia force at the center of gravity can be found from the following equation of equilibrium:

$$FH + W_{df}A - W_{dr}(L-A) = 0$$

$$F \times 21.50 + 2159 \times 66.46 - 3414 \times (130-66.46) = 0$$

$$21.50\ F = 73\ 438.42$$

$$F = 3416 \text{ lb}$$

As a check, the inertia force as it should, equals the maximum tractive force:

$$F = F_{r\ max}$$

$$3416 \text{ lb} \approx 3414 \text{ lb}$$

The maximum acceleration is:

$$a = \frac{Fg}{W}$$

where:

g = 32.2 ft/s/s

$$= \frac{3416 \times 32.2}{5573}$$

$$a = 19.74 \text{ ft/s/s}$$

Front Wheel Drive Passenger Car

A typical large front wheel drive passenger car with outboard brakes has the following application parameters:

Maximum installed net engine torque	525 lb-ft
Torque converter stall ratio	2.03
Transmission low gear ratio	2.48
Final drive ratio	3.07
Automatic transmission efficiency factor (with torque converter)	0.85
Final drive efficiency factor	0.95
Wheelbase	120 in
Center of gravity height	21.50 in

Static weight distribution (five passengers)

Total	Front	Rear
5650 lb	3390 lb	2260 lb

Tire rolling radius	14.00 in
Coefficient of friction between tire and road	1.00

The maximum stall torque per front half axle driveshaft is:

$$T = \frac{12 T_e R_c R_{lg} R_{fd}\ \eta_{at}\ \eta_{fd}}{2}$$

where:

12 = A constant = 12 lb-in/1 lb-ft

T_e = Maximum installed net engine torque, lb-ft

R_c = Torque converter stall ratio

R_{lg} = Transmission low gear ratio

R_{fd} = Final drive ratio

η_{at} = Automatic transmission efficiency factor

η_{fd} = Final drive efficiency factor

$$= \frac{12 \times 525 \times 2.03 \times 2.48 \times 3.07 \times 0.85 \times 0.95}{2}$$

$$T = 39\ 313 \text{ lb-in}$$

Also, the front half axle driveshaft torque due to wheel slip at maximum acceleration with a five passenger load is computed. Fig. 2 shows the dynamic forces acting on the car at such a condition.

The distance of the c.g. from the rear wheels is:

$$B = \frac{W_{sf} L}{W}$$

American Axle v. Neapco - IPR2025-00091
PET_AAM_1012-0034

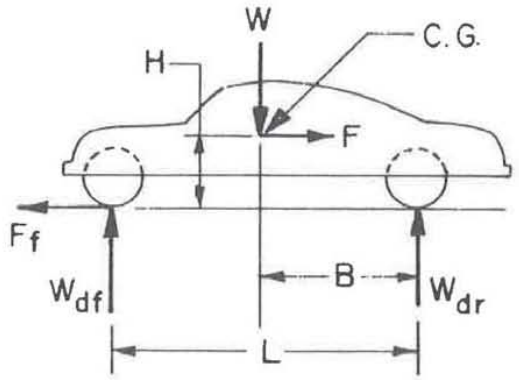


Fig. 2 — Front wheel drive passenger car at maximum acceleration

where:

W = Total car weight, lb
W_{sf} = Static front wheel weight, lb
L = Wheelbase, in

$$= \frac{3390 \times 120}{5650}$$

$$B = 72.00 \text{ in}$$

The basic equation for the maximum tractive force at the front wheels is:

$$F_{f\,max} = \mu W_{df}$$

where:

μ = Coefficient of friction between tire and road
W_{df} = Dynamic front wheel weight, lb
The dynamic axle weight at the front wheels is:

$$W_{df} = \frac{Wb}{L} - \frac{Fh}{L}$$

where:

F = Inertia force equals maximum tractive force $F_{f\,max}$, lb
H = Center of gravity height, in
Substituting this expression into the above equation and simplifying, the maximum traction force is:

$$F_{f\,max} = \frac{\mu WB}{L - \mu H}$$

$$= \frac{1.00 \times 5650 \times 72.00}{120 + 1.00 \times 21.50}$$

$$F_{f\,max} = 2875 \text{ lb}$$

The maximum front wheel slip torque per wheel is:

$$T = \frac{F_{f\,max}\, r_r}{2}$$

where:

r_r = Tire rolling radius, in

$$= \frac{2875 \times 14.00}{2}$$

$$T = 20\,125 \text{ lb-in}$$

Assuming a terminal vehicle speed of 120 mph and equal traction at both wheels, the maximum axle driveshaft speed is:

$$N = \frac{168V}{r_r}$$

where:

168 = A constant
V = Vehicle speed, mph

$$= \frac{168 \times 120}{14.00}$$

$$N = 1440 \text{ rpm}$$

Four-Wheel Drive, Light-Duty Truck

A typical four-wheel drive, light-duty truck has the following application parameters:

Maximum installed net engine torque	256 lb-ft
Transmission low gear ratio	6.55
Transfer case ratios	1.00 and 1.96
Rear axle ratio	6.17
Front axle ratio	6.17
Manual transmission efficiency factor	0.90
Transfer case efficiency factor	0.90
Front and rear axle efficiency factors	0.95
Wheelbase	132 in
Center of gravity height	35.00 in

Static weight distribution (gross vehicle weight)

Total	Front	Rear
9200 lb	4000 lb	5200 lb

Tire rolling radius	18.50 in
Coefficient of friction between tire and road	0.70

This vehicle is capable of being driven either in full time rear wheel drive or in part time four-wheel drive. In rear wheel drive, the maximum torque in the rear driveshaft is:

$$T = 12 T_e R_{lk} \eta_{mt}$$

where:

12 = A constant = 12 lb-in/1 lb-ft
T_e = Maximum installed net engine torque, lb-ft
R_{lk} = Transmission low gear ratio
η_{mt} = Manual transmission efficiency factor

$$= 12 \times 256 \times 6.55 \times 0.90$$

$$T = 18\,109 \text{ lb-in}$$

Also, the driveshaft torque due to wheel slip at maximum acceleration in rear wheel drive with a gvw load is computed. Fig. 3 shows the dynamic forces acting on the truck at such a condition.

The distance of the c.g. from the front wheels is:

$$A = \frac{W_{sr} L}{W}$$

American Axle v. Neapco - IPR2025-00091
PET_AAM_1012-0035

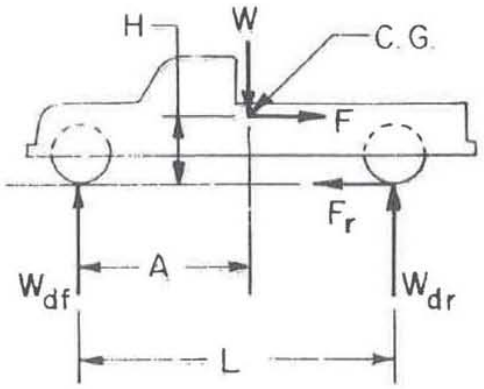


Fig. 3 — Rear wheel drive, light-duty truck at maximum acceleration

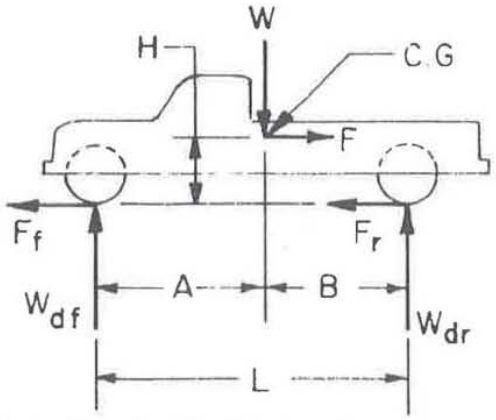


Fig. 4 — Four-wheel drive, light-duty truck at maximum acceleration

where:

W = Total truck weight, lb
W_{sr} = Static rear wheel weight, lb
L = Wheelbase, in

$$= \frac{5200 \times 132}{9200}$$

A = 74.61 in

The maximum tractive force at the rear wheels is:

$$F_{r\ max} = \frac{\mu WA}{L - \mu H}$$

where:

μ = Coefficient of friction between tire and road
H = Center of gravity height, in

$$= \frac{0.70 \times 9200 \times 74.61}{132 - 0.70 \times 35.00}$$

$F_{r\ max}$ = 4470 lb

The maximum rear driveshaft torque at wheel slip is:

$$T = \frac{F_{r\ max}\, r_r}{\eta_{ra} R_{ra}}$$

where:

r_r = Tire rolling radius, in
η_{ra} = Rear axle efficiency factor
R_{ra} = Rear axle ratio

$$= \frac{4470 \times 18.50}{0.95 \times 6.17}$$

T = 14 108 lb-in

Assuming a terminal vehicle speed of 70 mph, the maximum driveshaft speed is:

$$N = \frac{168\ R_{ra} V}{r_r}$$

where:

168 = A constant
V = Vehicle speed, mph

$$= \frac{168 \times 6.17 \times 70}{18.50}$$

N = 3922 rpm

In four-wheel drive, the maximum torque output of the transfer case is:

$$T = 12 T_e R_{lg}\, \eta_{mt} R_{tc}\, \eta_{tc}$$

where:

R_{tc} = Transfer case ratio
η_{tc} = Transfer case efficiency factor

$$= 12 \times 256 \times 6.55 \times 0.90 \times 1.96 \times 0.90$$

T = 31 945 lb-in

Since a conventional transfer case is assumed with a solid connection and no differential with a torque dividing (biasing) device incorporated, this output torque is equally divided between the front and rear driveshafts as follows:

$$T = \frac{31\ 945}{2}$$

T = 15 972 lb-in

However, it may be assumed that under certain instantaneous conditions, all the available torque output from a transfer case without a differential, or a transfer case with a locking differential, can be transmitted through either the front or rear driveshafts.

In the following computations, the driveshaft torques due to front and rear wheel slip are determined. For the four-wheel drive arrangement, full vehicle weight can theoretically be utilized in producing tractive forces. This ideal condition is realized, however, only when tractive forces (and engine torque) are distributed to the axles in the same proportion as are the dynamic weights on the respective axles. A variable torque dividing (biasing) mechanism in the transfer case would be required for this purpose. Fig. 4 shows the dynamic forces acting on the truck during the four-wheel drive condition.

American Axle v. Neapco - IPR2025-00091
PET_AAM_1012-0036

The distance of the c.g. from the rear wheels is:

$$B = L - A$$
$$= 132 - 74.61$$
$$B = 57.39 \text{ in}$$

The basic equation for the maximum tractive force at all four wheels is:

$$F_{4\ max} = \mu W$$

The dynamic axle weight at the front wheels is:

$$W_{df} = \frac{WB}{L} - \frac{FH}{L}$$

Substituting the maximum tractive force expression into this equation results in:

$$W_{4f} = \frac{W}{L}(B - \mu H)$$

The dynamic axle weight at the rear wheels is:

$$W_{dr} = \frac{WA}{L} + \frac{FH}{L}$$

Substituting the maximum tractive force expression into this equation results in:

$$W_{4r} = \frac{W}{L}(A + \mu H)$$

Assuming that the tractive forces are distributed to the axles in the same proportion as are the dynamic axle weights on the respective axles, the following relationship results:

$$\frac{F_{4f}}{F_{4r}} = \frac{W_{4f}}{W_{4r}} = \frac{B - \mu H}{A + \mu H}$$

The tractive force at the front axle is:

$$F_{4f} = W_{4f} = \frac{W}{L}(B - \mu H)$$
$$= \frac{9200}{132}(57.39 - 0.70 \times 35.00)$$
$$F_{4f} = 2292 \text{ lb}$$

The maximum front driveshaft torque at wheel slip is:

$$T = \frac{F_{4f}\, r_r}{\eta_{fa} R_{fa}}$$

where:

η_{fa} = Front axle efficiency factor
R_{fa} = Front axle ratio

$$= \frac{2292 \times 18.50}{0.95 \times 6.17}$$
$$T = 7234 \text{ lb-in}$$

The tractive force at the rear axle is:

$$F_{4r} = W_{4r} = \frac{W}{L}(A + \mu H)$$
$$= \frac{9200}{132}(74.61 + 0.70 \times 35.00)$$
$$F_{4r} = 6908 \text{ lb}$$

The maximum rear driveshaft torque at wheel slip is:

$$T = \frac{F_{4r} r_r}{\eta_{ra} R_{ra}}$$
$$= \frac{6908 \times 18.50}{0.95 \times 6.17}$$
$$T = 21\,803 \text{ lb-in}$$

These computed maximum front and rear driveshaft torques at wheel slip would be possible if a variable torque dividing mechanism were incorporated in the transfer case, and if the tractive forces were distributed to the axles in the same proportion as the dynamic axle weights.

The top speed of the vehicle in four-wheel drive and with the transfer case in low gear is limited by the maximum governed engine speed of 4200 rpm. The maximum vehicle speed is:

$$V = \frac{N r_r}{168\, R_{ra} R_{tc}}$$
$$= \frac{4200 \times 18.50}{168 \times 6.17 \times 1.96}$$
$$V = 38 \text{ mph}$$

The maximum front and rear driveshaft speeds in four-wheel drive are:

$$N = \frac{4200}{1.96}$$
$$N = 2143 \text{ rpm}$$

References

1. J.J. Taborek, "Mechanics of Vehicles," *Machine Design*, 1957.

American Axle v. Neapco - IPR2025-00091
PET_AAM_1012-0037

Section 2.5
Duty Cycle Determination

E. R. Wagner, P.E. — Saginaw Steering Gear Div., GMC

A driveline duty cycle is a graph, chart, or table showing the period of time spent at various combinations of torque, speed, and joint angle for a typical load cycle or operational sequence of a vehicle in a given overall period of time. The duty cycle expresses in engineering terms the performance and durability requirements of the design. The duty cycle can be computed from engineering estimates; however, when possible, this duty cycle should be established from an instrumented vehicle under actual operating conditions. Then realistic laboratory life testing can be conducted with tape-controlled test machines. If elaborate testing equipment is not available, one can establish a duty cycle and determine the life expectancy with a simpler conventional wear test machine and by computation.

First, the load cycle is analyzed and divided into groups of fixed combinations of torque, speed, and joint angle. These groups represent fractions or percentages of the total operating time of the load cycle. Life expectancy values can then be established by laboratory testing for fixed relationships of these variables and expressed graphically.

According to Miner's Theory, which is most commonly used, the total life expectancy for an application due to the cumulative damage effect of operating at various stress levels caused by continuously varying conditions can then be established by summation as follows:

$$L_{Total} = \frac{1}{\sum_{j=1}^{m} \frac{N_j}{L_j}}$$

where:

N_j = Fraction of total time at operating condition j
L_j = Life expectancy at operating condition j
m = Total number of operating conditions

This equation can be expressed in the following commonly used simplified form:

$$\text{Total Life Expectancy} = \frac{1}{\frac{N_1}{L_1} + \frac{N_2}{L_2} + \frac{N_3}{L_3} + \cdots + \frac{N_m}{L_m}}$$

where:

N_1 = Fraction of total time at operating condition 1
L_1 = Life expectancy at operating condition 1, hours

In an illustrative problem for a particular type of universal joint, operating conditions representing three combinations of torque, speed, and joint angle are assumed at the percentages of time shown in Table 1.

TABLE 1 — UNIVERSAL JOINT OPERATING CONDITIONS

Operating Load Condition	Fraction of Time, Percent	Life Expectancy Hours
1	5	400
2	10	1800
3	85	70 000

Also, for each condition shown is the resultant life expectancy which can be determined, for example, from previously established load-life curves or by laboratory testing a given type of universal joint. With the previous equation, it is possible to determine the total life expectancy as follows:

$$\text{Total Life Expectancy} = \frac{1}{\frac{0.05}{400} + \frac{0.10}{1800} + \frac{0.85}{70000}}$$

Total Life Expectancy = 5190 h

Among other cumulative damage theories proposed for evaluating fatigue life, the Corten-Dolan theory has also been used. It should be indicated that the duty cycle, regardless of how determined, is at best the most realistic approximation of the intended usage of the design because, neither the designer nor the manufacturer has full control over the final usage. Hence, if possible, the evaluation of a driveline is best accomplished under actual operating conditions of an application.

References

1. J.A. Kayser, *Drivelines for Heavy Equipment*, SAE Paper 403A, 1961.
2. W.T. Condon, *Application of Universal Joints to Construction and Industrial Machinery*, SAE Paper 403B, 1961.
3. *Universal Joint Layout and Selection Data Book*, Rockwell Standard, 1964.
4. B. R. Reimer, *Design and Application Considerations for Agricultural P.T.O. Drivelines*, SAE Paper 650680, 1965.
5. C.E. Cooney, *Design and Application of Universal Joints for Off-Highway Vehicles*, SAE Paper 650681, 1965.
6. *The Birfield Joint, An Angular Contact Constant Velocity Universal Joint*, Hardy Spicer Ltd., 1967.
7. A.F. Madayag, *Metal Fatigue: Theory and Design*, New York: John Wiley and Sons, Inc., 1969.

American Axle v. Neapco - IPR2025-00091
PET_AAM_1012-0039

Universal Joints

Chapter 3

American Axle v. Neapco - IPR2025-00091
PET_AAM_1012-0041

Chapter 3
Universal Joints
Introduction

E. R. Wagner, P.E. — Saginaw Steering Gear Div., GMC

A universal joint is a mechanical device which can transmit torque and/or rotational motion from one shaft to another at fixed or varying angles of intersection of the shaft axes. There are many types of universal joints and they can be classified according to their basic design characteristics.

Generally, the initial interest in any universal joint is in its motion transmission characteristic, which can be either nonuniform or uniform. A nonuniform motion or nonconstant velocity universal joint transmits motion with varying ratios of instantaneous angular velocity between output or driven, and input or driving members, when operating at joint angles greater than zero. The average angular velocity ratio is unity. A uniform motion or constant velocity universal joint transmits motion with an angular velocity ratio of unity between output and input members.

In addition, a third category of universal joints is the near constant velocity universal joint which transmits motion with an angular velocity ratio of unity when operated at the design joint angle and at zero. When operated at other angles, the angular velocity ratio is near unity. Since the deviations from unity are small compared to the deviations for nonconstant velocity universal joints, the near constant velocity universal joints are generally included in the same category as the constant velocity universal joints.

Universal joints are also classified with regard to their supporting capabilities. A self-supporting universal joint is supported by internal means and hence requires location at only one shaft, which can be either the driving or the driven member of the joint. On the other hand, a non-self-supporting universal joint requires external supporting means at both driving and driven shaft members in order to maintain the proper alignment of joint components.

Universal joints are categorized further either as a fixed center or as an end motion type. A fixed center universal joint maintains the joint center at a fixed location and can resist axial thrust forces. An end motion universal joint permits relative axial movement between input and output members and, therefore, has a variable joint center location.

Another characteristic of universal joints is their operating joint angle capability. Universal joints are referred to as either high or low angle types. A high angle universal joint is generally of the fixed center type, while a low angle universal joint is usually of the end motion type.

In addition, universal joints can be described with regard to directional capabilities of power transmission. Most universal joints are bi-directional and therefore transmit torque from either joint member to the other, with equal efficiency, capacity, and various other functional characteristics.

In the following sections, functional and design characteristics are discussed in varying detail for the different universal joint types. In addition, various rubber couplings, used to a limited extent in some European driveline and axle driveshaft applications, are shown and described briefly.

American Axle v. Neapco - IPR2025-00091
PET_AAM_1012-0043

Section 3.1—Nonconstant Velocity Universal Joints
Section 3.1.1— Cardan or Hooke Universal Joint 39
Section 3.1.2— Ball and Trunnion Universal Joint 77
Section 3.1.3— Roller and Trunnion Universal Joint 85
Section 3.1.4— Sliding Block and Trunnion Universal Joint 89
Section 3.1.5— Rubber Couplings 93

Universal Joints

American Axle v. Neapco - IPR2025-00091
PET_AAM_1012-0045

Section 3.1.1
Cardan or Hooke Universal Joint

E. R. Wagner, P.E. — Saginaw Steering Gear Div., GMC
C. E. Cooney — Mechanics Div., Borg Warner Corp.

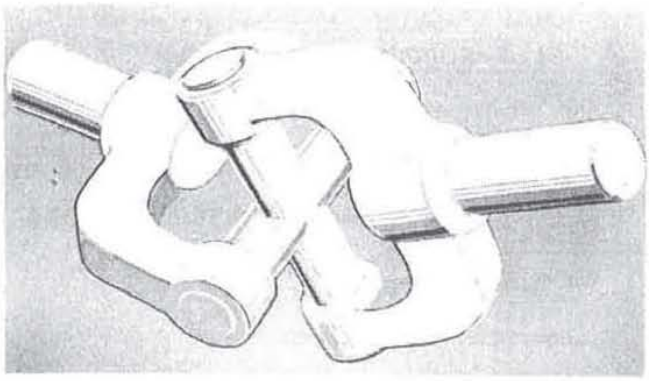


Fig. 1 — Cardan or Hooke universal joint

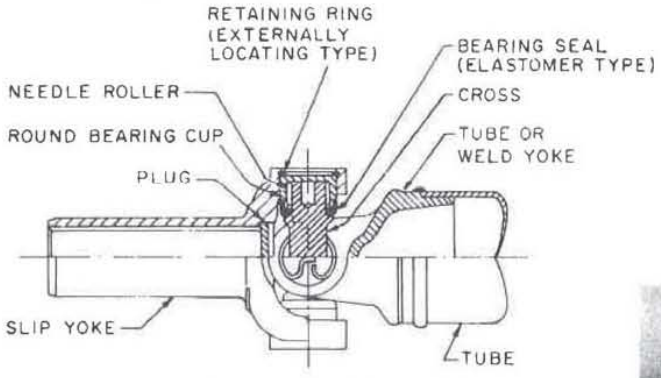


Fig. 2 — Cardan universal joint

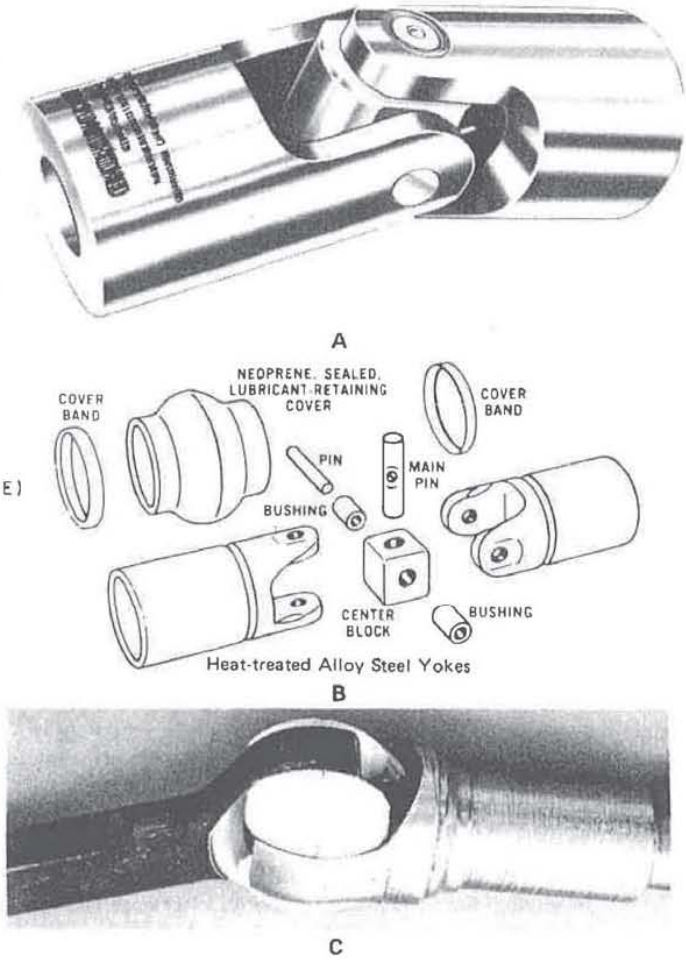


Fig. 3 — Various other Cardan type joint constructions

Introduction

The universal joint, commonly referred to as either the Cardan or Hooke universal joint, is an extremely old device. The first known description of this mechanism can be found in a manuscript by Villard Honnecourt, a thirteenth century architect. Later, Geronimo Cardano, an Italian mathematician who lived in the sixteenth century, utilized a mechanism to suspend a ship's compass which maintained its horizontal position independent of the ship's movements. This was later known as the Cardan suspension. In the seventeenth century, the British scientist Robert Hooke was granted a patent on the universal joint. He discovered the nonuniform motion characteristics of this joint and found that these undesirable characteristics could be eliminated by correct phasing of two joints operating in series at identical joint angles.

The Cardan or Hooke universal joint shown in Fig. 1, is a nonconstant velocity universal joint which consists of two yokes drivably connected by a cross through four bearings. A kinematic study of this joint reveals the presence of unusual motions and forces when it operates at an angle. These characteristics impose certain limitations on its applications which are discussed in the following section on *Kinematics*. Fig. 2 shows a typical automotive design of this joint while Fig. 3 illustrates some other Cardan type joint designs which have similar operating characteristics. Fig. 3(a) and (b) show pin and block type constructions, and Fig. 3(c) illustrates a grooved spherical ball construction. These and other possible intermediate member constructions perform the same function as the cross in the conventional type of Cardan joint.

Through the years, the Cardan joint has found the most widespread usage of any type of universal joint in the passenger car, truck, and various other on-and off-highway vehicle driveline,

American Axle v. Neapco - IPR2025-00091
PET_AAM_1012-0047

axle driveshaft, power take-off, and steering shaft systems. Other applications have been in aircraft, railway, marine, agricultural, industrial, and stationary drive system installations. As shown schematically in Fig. 4(a), it has been most generally used as a self-supporting joint, but it has also been used as a non-self-supporting joint illustrated in Fig. 4(b). The principal usage of the self-supporting joint has been in conventional, open-type driveline constructions, while the non-self-supporting joint was once widely used in former torque tube drive constructions of passenger cars.

The principal advantages of the Cardan joint are its relatively low cost to manufacture as well as simple and rugged construction, combined with long life and ease of serviceability. In addition to providing the necessary torque capacity in a limited operating space, the joint has the thrust capability to withstand relatively high, externally imposed axial forces which may be produced, for example, by sliding spline when shaft length changes are required during vehicle suspension movements. Further, the joint offers the versatility and flexibility to permit the design of numerous yoke and bearing constructions to meet the functional and durability requirements of a large variety of applications.

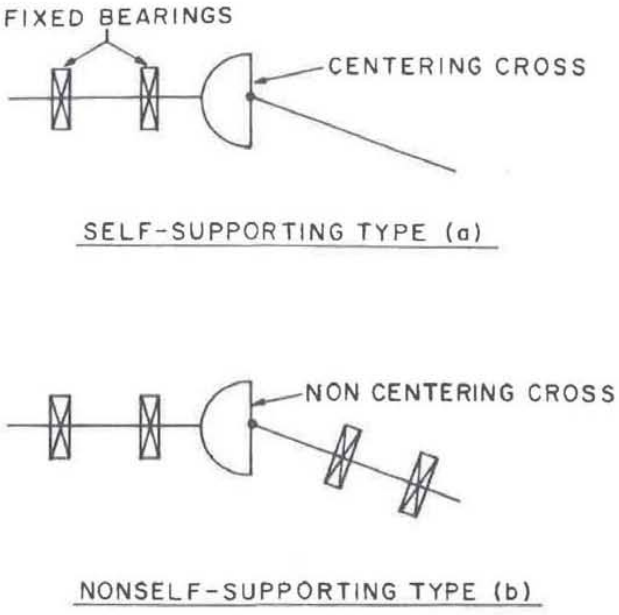


Fig. 4 — Cardan universal joint types

Kinematics

Motion Characteristics

The kinematics of motion of a Cardan joint are quite unusual. Whenever it operates at an angle, nonuniform motion is developed. When the driving yoke of the joint is operating at a uniform rotational velocity, the driven yoke rotates nonuniformly with respect to angular displacement, velocity, and acceleration. This motion has the following characteristics:

1. The average angular displacement and velocity is uniform. That is, if the driving yoke rotates one revolution, the driven yoke also rotates one revolution. However, during this one revolution, the incremental angular displacement and instantaneous angular velocity and acceleration are not transmitted uniformly through the joint.
2. The angular displacement of the driven yoke during one revolution lags and leads the driving yoke twice.
3. Assuming constant input motion of the driving yoke, the driven yoke has a maximum difference of output angular velocity with respect to the driving yoke when the driving yoke lies in the plane described by the joint angle, and also, when the driving yoke is normal or perpendicular to this plane. The driven yoke has the same instantaneous angular velocity as the driving yoke at approximately 45 deg from the joint angle plane for small joint angles.
4. The maximum instantaneous angular acceleration and deceleration of the driven yoke occurs when the angular velocity of the driven yoke is the same as the driving yoke. Also, the maximum acceleration and deceleration coincide with the maximum lag and lead respectively.
5. The incremental angular displacement, velocity, and acceleration increase as the joint angle increases, but at an increasing rate.

Equations of Motion and Force

The equations of motion and force of a Cardan joint have been developed according to the following nomenclature:

ω = Input angular velocity of driving yoke (assumed uniform in the analysis)
ω_1 = Output angular velocity of driven yoke

θ = Joint angle

β = Angle of rotation of driving yoke from position where it is normal or perpendicular to the plane of the joint angle
β_1 = Angle of rotation of driven yoke from position where it is in the plane of the joint angle
T = Input torque on driving yoke (assumed uniform in the analysis)
T_1 = Output torque on driven yoke

C = Secondary couple on driving yoke

C_1 = Secondary couple on driven yoke

α = Input angular acceleration of driving yoke (assumed zero in the analysis)
α_1 = Output angular acceleration of driven yoke

σ = Angle of lag of driven yoke

A = Amplitude of torsional vibration

τ = Angle between driving yoke and cross

American Axle v. Neapco - IPR2025-00091
PET_AAM_1012-0048

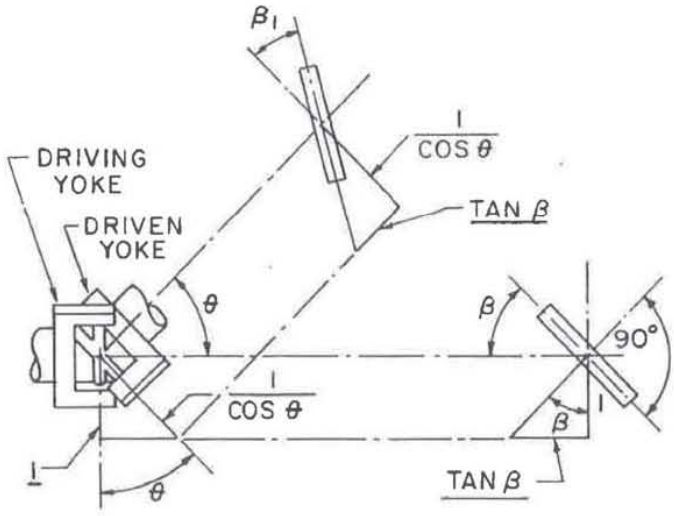


Fig. 5 — Cardan joint angular relationship

μ = Angle between driven yoke and cross

T_o = Torque on cross

v = Linear velocity vector of point on cross trunnion

r = Radius from joint center to point on cross trunnion

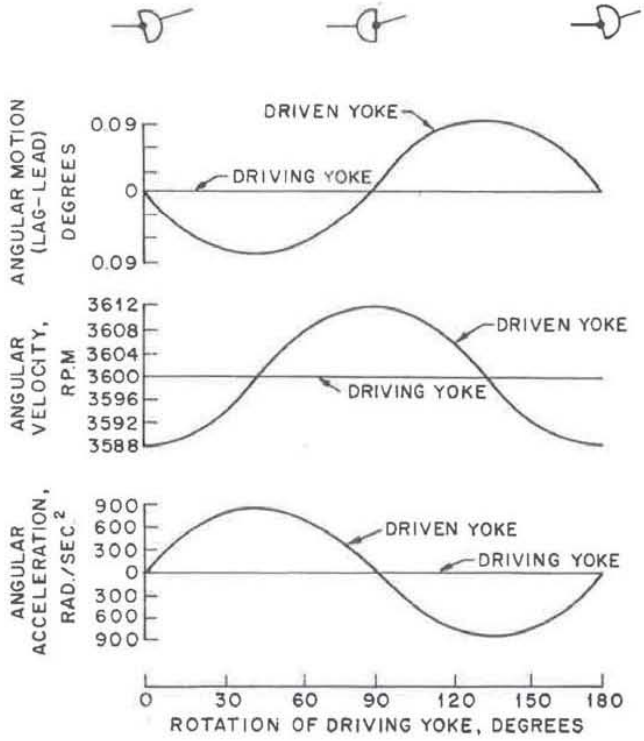


Fig. 6 — Cardan joint motion characteristics at 4°30′ joint angle and 3600 rpm

Fig. 5 shows the basic angular relationship of a Cardan joint operating at an angle. The illustration shows the fundamental relationship between β and β_1 as follows:

$$\tan \beta_1 = \cos \theta \tan \beta$$

By differentiating this expression with respect to time, and simplifying, the output angular velocity can be found as follows:

$$\omega_1 = \frac{\omega \cos \theta}{1 - \sin^2 \beta \sin^2 \theta}$$

The output angular acceleration can be found by differentiating the velocity equation with respect to time and simplifying as follows:

$$\alpha_1 = \frac{2\omega^2 \cos \theta \sin^2 \theta \sin 2\beta}{(1 - \sin^2 \theta \sin^2 \beta)^2}$$

The amplitude of the torsional vibration resulting from a Cardan joint operating at an angle is the maximum difference between β and β_1 as follows:

$$A = \text{Arctan} \left(\frac{1}{\cos \theta}\right)^{1/2} - \text{Arctan} (\cos \theta)^{1/2}$$

These equations satisfy the actual motion, velocity, and acceleration characteristics of a Cardan joint operating at an angle. A much simpler set of equations can be used in solving practical problems when the joint angle is small or less than approximately 10 deg. These approximate equations are:

$$A \approx \tfrac{1}{2} (1 - \cos \theta)$$

where:

A is in rad

or:

$$A \approx \frac{\theta^2}{4}$$

where:

A and θ are in rad

$$\sigma_1 = -A \sin 2\beta$$
$$\omega_1 = \omega - 2A\,\omega \cos 2\beta$$
$$\alpha_1 = 4A\,\omega^2 \sin 2\beta$$
$$\alpha_{1\,(max)} = 4A\,\omega^2$$

These motion characteristics are illustrated in Fig. 6 for a Cardan joint operating at a 4°30′ joint angle and at 3600 rpm. This figure shows that the motion characteristics vary twice during each revolution of the shaft when the joint operates at an angle. A simplified derivation of the Cardan joint's nonconstant velocity

American Axle v. Neapco - IPR2025-00091
PET_AAM_1012-0049

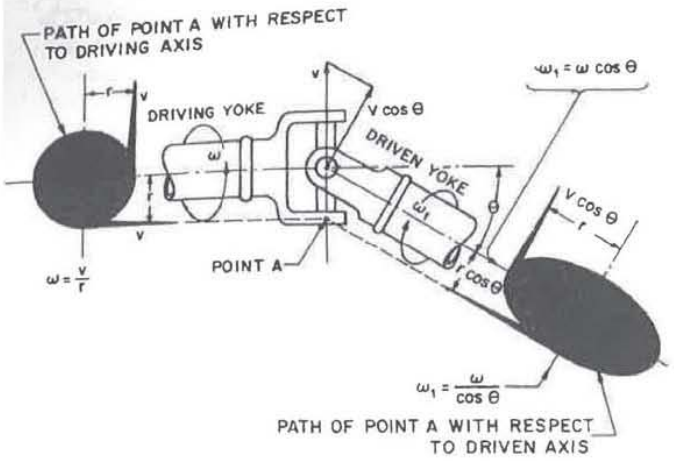


Fig. 7 — Cardan joint motion characteristics

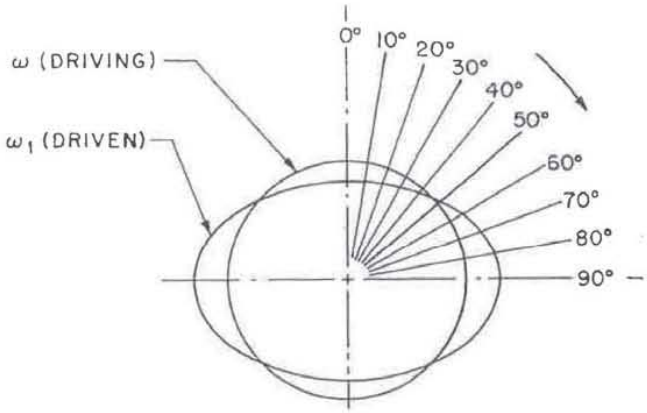


Fig. 8 — Polar diagram for Cardan joint angular velocity

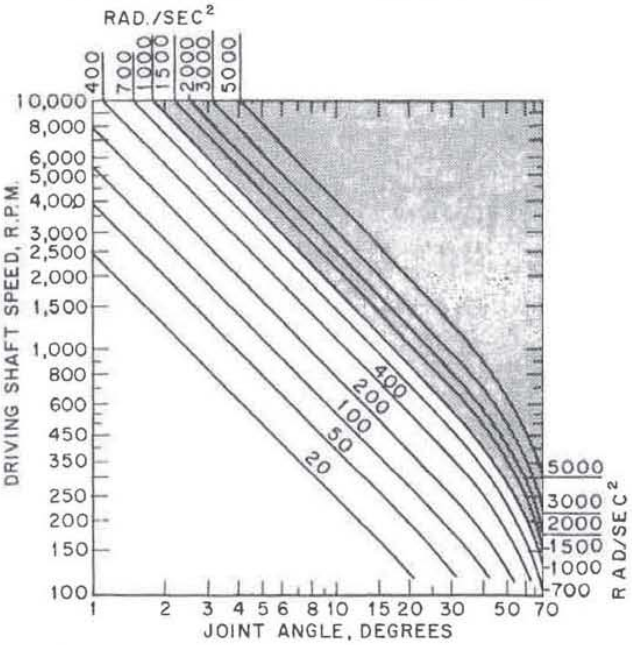


Fig. 9 — Maximum angular acceleration of Cardan joint driven shaft

characteristics is shown in Fig. 7. If it is initially assumed that the joint is operated with no angle between the driving and driven yokes, then the effective length of the lever arms in the intermediate cross member which cause rotation are the same when viewed from either the driving or the driven ends. Therefore, at zero joint angle the output angular velocity is the same as the input angular velocity and thus constant velocity is transmitted. However, when an angle is imposed on the joint, the effective lever arm varies when viewed along the driven yoke rotational axis. Hence, when the input angular velocity of the driving yoke is assumed constant, the output angular velocity of the driven yoke is nonuniform.

To analyze this speed variation, first consider the speed of a point on the cross trunnion, point A, as it appears when viewed along the driving yoke rotational axis. Point A rotates around this axis in a circular path of radius r and at a constant speed which can be represented as a constant length linear velocity vector v. Therefore, the input angular velocity of the driving yoke is:

$$\omega = \frac{v}{r}$$

When viewed along the driven yoke rotational axis, the circular path of point A appears as an ellipse with a major axis radius of r and a minor axis radius of r cos θ. With point A located as shown, its distance from the driven yoke rotational axis is r cos θ and its linear velocity vector around this axis is v. Therefore, the rotational speed of the driven yoke in terms of the input angular velocity is:

$$\omega_1 = \frac{v}{r \cos \theta} = \frac{\omega}{\cos \theta}$$

If the driving yoke is rotated 90 deg from the position shown, the distance from point A to the rotational axis of the driven yoke becomes r and the linear velocity vector around this axis becomes v cos θ. Therefore, at this instant, the rotational speed of the driven yoke in terms of the input angular velocity is:

$$\omega_1 = \frac{v \cos \theta}{r} = \omega \cos \theta$$

Thus, in 90 deg of constant speed rotation of the driving yoke, the instantaneous driven yoke output angular velocity has changed from $\omega/\cos \theta$ to $\omega \cos \theta$. These speeds are the maximum and minimum rotational speeds of the driven yoke. Hence, the output angular velocity varies continually and produces two complete cycles of speed variation for every revolution of the driving yoke.

A polar diagram is shown in Fig. 8 which shows the angular velocity of both the driving and driven yokes for one complete revolution of the Cardan joint. Since the driving yoke is assumed to have a constant angular velocity, its polar diagram is a circle. The diagram for the driven yoke, however, is an ellipse which intersects the circle at four places. This means that there are four instantaneous positions during a single rotation where the angular

American Axle v. Neapco - IPR2025-00091
PET_AAM_1012-0050

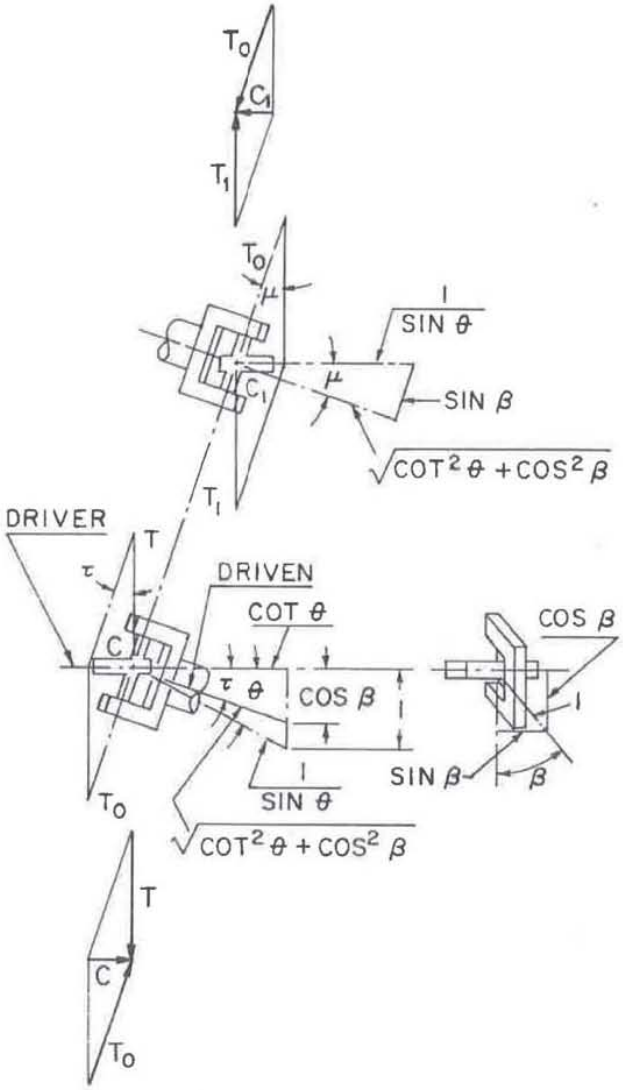


Fig. 10 — Cardan joint force relationships

velocities of both yokes are equal. During the remaining time, the driven yoke rotates either faster for part of the time or slower for part of the time.

Fig. 9 shows the effect of rotational speed and joint angle on maximum angular acceleration. The constant acceleration curves shown in this figure result from the following relationships:

A. Angular acceleration is proportional to angular velocity squared for a given joint angle.
B. Angular acceleration is proportional to joint angle squared for a given angular velocity.
C. If joint angle times angular velocity is constant, then angular acceleration is constant.

Therefore, from these relationships, the following useful approximate equation results:

$$\alpha_{1(max)} = \theta^2\omega^2$$

Another derivation of simplified basic mathematical relationships for the Cardan joint is developed in *Appendix K*. It is also shown in this appendix that the use of these approximate equations would produce a negligible error in computations involving practical joint angle problems.

The force relationships which exist on a Cardan joint transmitting torque at an angle are shown in Fig. 10. This illustration indicates the presence of bending moments acting on both the driving and driven yokes. These bending moments are called secondary couples and are produced whenever torque is transmitted around a corner by a universal joint operating at an angle.

The secondary couple in the plane of the driving yoke is:

$$C = T \tan\theta \cos\beta$$

This equation is a cos wave form with a maximum amplitude of:

$$C_{max} = T \tan\theta \text{ (at 90 deg to the plane of the joint angle)}$$

In the plane of the driven yoke, the secondary couple is:

$$C_1 = T \sin\theta \sin\beta (1 + \tan^2\theta \cos^2\beta)^{1/2}$$

For small joint angles, this equation can be reduced to:

$$C_1 \approx T \sin\theta \sin\beta$$

This equation is a sine wave form with a maximum amplitude of:

$$C_{1\,max} \approx T \sin\theta \text{ (at 90 deg to the plane of the joint angle)}$$

For small joint angles $\tan\theta \approx \sin\theta$ and, therefore, the secondary couples on the driving and driven yokes are approximately equal.

Joint Phasing — (Application Motion and Force Equations)

Torsional Equivalent Angle — In solving practical joint angle problems of Cardan joints, the following motion equation is used to determine the basic relationship:

$$A \approx \frac{\theta^2}{4} \approx K\theta^2$$

where:

K = A constant

θ = Joint angle in rad

This equation merely establishes the basic relationship that the maximum value of torsional amplitude is directly proportional to the joint angle squared.

Parallel Shafts Arrangement — The first two-joint driveshaft system to be analyzed is the *parallel shafts* arrangement as shown in Fig. 11. The joint angles shown are true angles, since the input and output shafts as well as the connecting or intermediate shaft lie in the same plane when seen in the plan view.

American Axle v. Neapco - IPR2025-00091
PET_AAM_1012-0051

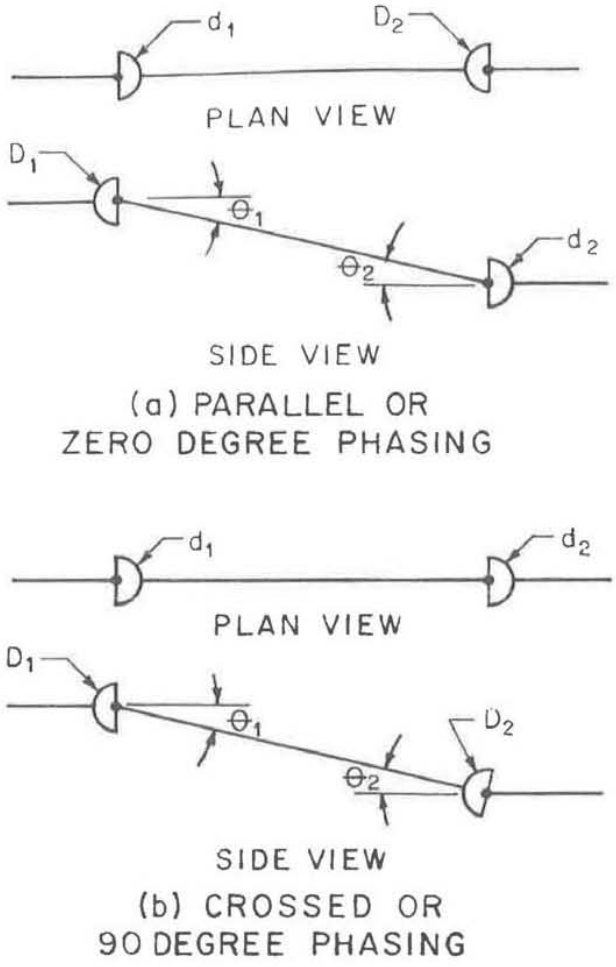


Fig. 11 — Parallel shafts arrangement

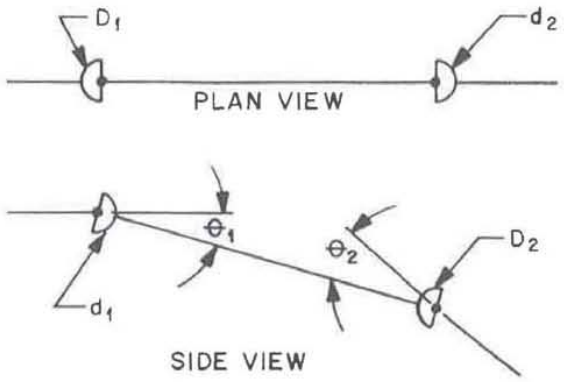


Fig. 12 — Intersecting shafts arrangement

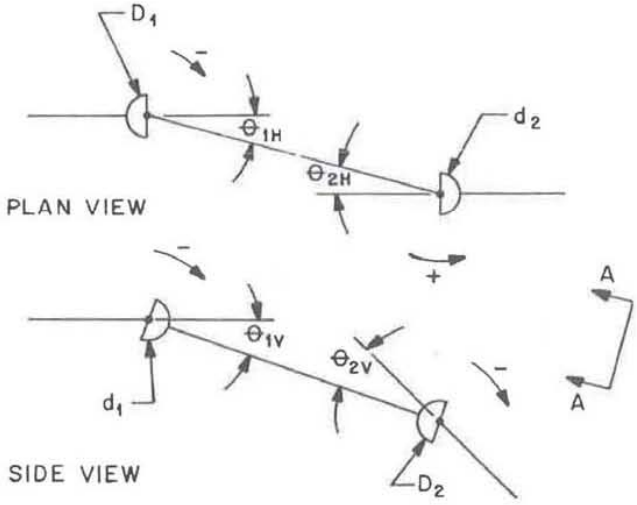


Fig. 13 — General two-joint shaft arrangement

In this arrangement, the input and output shafts as seen in the side view, intersect at infinity when they are parallel or at some point outboard of joint centers for approximately parallel shafts. It should be noted in Fig. 11(a), that the driving yoke D_1 of joint 1 lies in the plane of its joint angle at the same instant that the driving yoke D_2 of joint 2 is normal or perpendicular to the plane of its joint angle. This arrangement is the conventional combination where the inboard yokes d_1 and D_2 of the driveshaft are phased *in line* or *parallel* and can also be expressed as zero degree phase angle. Hence, the *phase angle* is the relative rotational position of the joint yokes on a driveshaft. With this combination, the residual torsional amplitude and joint angle of the system is:

$$A_{res} \approx K\,\theta_{res}^2$$

$$\theta_{res} \approx \sqrt{\theta_1^2 - \theta_2^2}$$

When the joint angles are equal, θ_{res} equals zero and constant velocity is transmitted. Also, there is no significance to the imaginary numbers possible in this equation. Only the arithmetical difference in these values should be used and the negative sign possibility ignored. For small joint angles, the angle in deg or rad may be used.

For example, when $\theta_1 = 5$ deg and $\theta_2 = 4$ deg for the case of unequal joint angles, the residual joint angle is:

$$\theta_{res} = \sqrt{(5)^2 - (4)^2}$$
$$\theta_{res} = 3 \text{ deg}$$

This computation shows that the same torsional amplitude, angular acceleration and other motion characteristics occur overall with the 5 deg and 4 deg joint angle combination as occurs in a single joint operating at a 3 deg joint angle. This single joint angle producing the same speed variation as a driveshaft system of two or more joints is called the *torsional equivalent angle*, and its usefulness in driveline design is discussed in the section on *Torsional Excitation*.

If the yokes d_1 and D_2 on the connecting or intermediate shaft as shown in Fig. 11(b) are phased at 90 deg or *crossed*, the residual joint angle or torsional equivalent angle of the system is:

$$\theta_{res} \approx \sqrt{\theta_1^2 + \theta_2^2}$$

This equation indicates the desirability to have parallel yoke phas-

American Axle v. Neapco - IPR2025-00091
PET_AAM_1012-0052

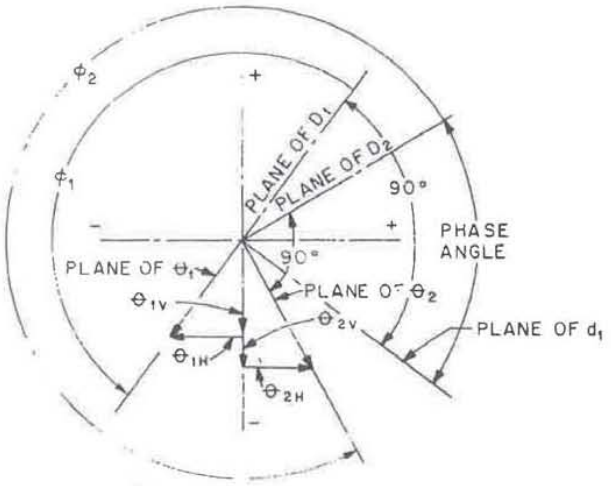


Fig. 14 — Joint angle and driving yoke plane relationships for best phasing

ing on the intermediate shaft of the driveshaft system as shown in Fig. 11(a).

Intersecting Shafts Arrangement — The second two-joint driveshaft system to be analyzed is the *intersecting shafts* arrangement shown in Fig. 12. As with the case of the previous parallel shafts arrangement, the input and output shafts as well as the intermediate shaft lie in the same plane when seen in the plan view. The input and output shafts in the side view, however, are not parallel and their centerlines intersect at some point inboard of joint centers. This arrangement produces the same torsional characteristics as the parallel shafts arrangement in Fig. 11 because the cancellation effect of one joint by another is identical at the same joint phase condition.

General Arrangement of Shafts not in the Same Plane — The third two-joint driveshaft system to be analyzed is the *general* arrangement or case where the shafts do not lie in the same plane. Fig. 13 shows this general arrangement. An angular offset in the plan view, which could be parallel as shown, is combined with an intersecting condition in the side view producing an out-of-plane condition.

The plane relationships of the joint angles and driving yokes can be shown by constructing an end view around the centerline of the intermediate shaft as shown in Fig. 14. This end view of the intermediate shaft can be seen in Fig. 13 when viewing the shaft from the direction of arrows A-A. The tangents of the joint angle horizontal and vertical components for the general two-joint driveshaft arrangement in Fig. 13 are plotted in the proper direction in Fig. 14 by using the right hand rule system. In Fig. 13, the angular disposition of the joint angle components is considered negative (−) when they are clockwise and positive (+) when they are counterclockwise as shown. Then, when the components are plotted in Fig. 14 from the origin, vertically upward and horizontally to the right is positive, while vertically downward and horizontally to the left is negative.

If the joint yokes are phased properly, the same cancellation condition exists as in the two simpler installations previously described. Fig. 14 shows the plane of driving yoke D_1 of joint 1 in line with the plane of joint angle θ_1 in the same rotational position

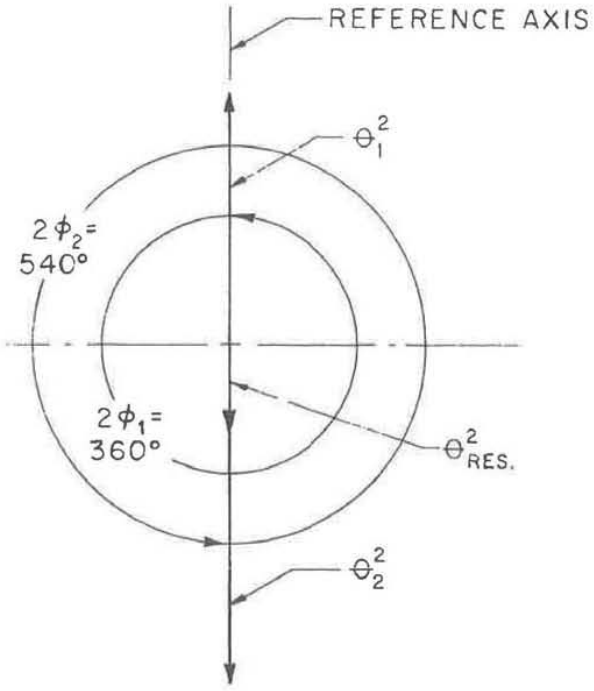


Fig. 15 — Vectorial solution for minimum θ_{res}^2

as when the plane of driving yoke D_2 of joint 2 is normal to the plane of joint angle 2. Under these conditions of phasing, the torsional resultant is a minimum and is based upon joint angle size in the same way as in the driveshaft arrangements of Figs. 11 and 12.

It can be determined vectorially or graphically that the optimum phasing condition shown in Fig. 14 produces a minimum torsional equivalent angle for the system. In this solution, the following steps are required:

A. In Fig. 14 establish angles ϕ_1 and ϕ_2 in the same direction of rotation. These angles extend from the plane of the joint angle for both joints 1 and 2. Also, these angles are arbitrarily assumed in the counterclockwise direction and represent the relative phase relationship of the joint driving yokes D_1 and D_2.

B. The actual vectorial solution for the torsional resultant can now be determined graphically as shown in Fig. 15. For this solution, a reference axis is established with the vertical axis arbitrarily chosen as this axis.

C. From the vertical reference axis, construct angles $2\phi_1$ and $2\phi_2$ in the previously assumed counterclockwise direction using the values of ϕ_1 and ϕ_2 found in Fig. 14. The values of these constructed angles in Fig. 15 are 360 deg for $2\phi_1$ and 540 deg for $2\phi_2$.

D. At this relative phase relationship, construct vectors equivalent in length to the magnitude of the joint angle squared. These vectors for the two joint angles are θ_1^2 and θ_2^2. For approximate solutions the joint angles in degrees or radians can be used. For exact solutions, the maximum amplitude of torsional vibration for each joint is used and can readily be adapted to computer programming.

American Axle v. Neapco - IPR2025-00091
PET_AAM_1012-0053

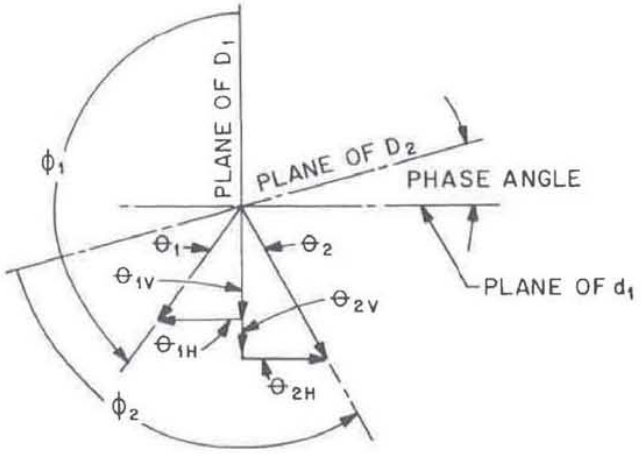


Fig. 16 — Joint angle and driving yoke plane relationships for any assumed phasing

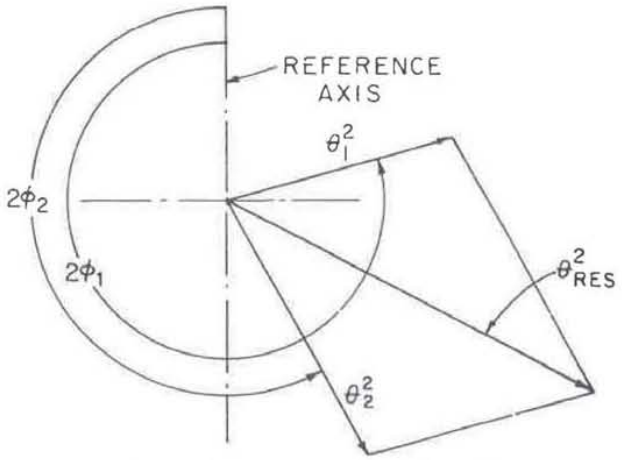


Fig. 17 — General vectorial solution for θ_{res}^2

E. The vectorial sum of these two vectors is proportional to the magnitude of the resultant joint angle squared. Since the individual vectors θ_1^2 and θ_2^2 are oppositely directed as shown in Fig. 15, the residual vector is a minimum. These individual vectors are oppositely directed because the optimum condition of phasing was used in Fig. 14 and if θ_1^2 and θ_2^2 are equal then the residual vector or torsional equivalent angle squared is zero.

It was previously indicated that under this condition of phasing, the torsional resultant is a minimum and is based upon joint angle size in the same way as shown in the driveshaft arrangements of Figs. 11 and 12. Hence, θ_{res}^2 is the numerical difference of θ_1^2 and θ_2^2. Therefore, θ_{res} is simply the square root of this difference and is expressed as follows:

$$\theta_{res} = \sqrt{\theta_1^2 - \theta_2^2}$$

As previously stated, only the arithmetical difference in these values is used and the negative sign possibility is ignored for the torsional equivalent angle.

When any relationship of joint angles as shown in Fig. 13 exists with any known or assumed phase relationship between joint yokes d_1 and D_2, a general solution can be obtained. To accomplish this solution, the planes of the joint angles are plotted as before in Fig. 14. The assumed plane relationships of the yokes are laid over this same plot. This procedure produces an end view of the intermediate shaft as shown in Fig. 16. This illustration is the same as Fig. 14, except for the relationship between the planes of the driving yokes D_1 and D_2. It is merely necessary to measure in the same direction of rotation in both cases the angle from the plane of the driving yoke to the plane of the joint angle for joints 1 and 2. This procedure produces angles ϕ_1 and ϕ_2 as shown in Fig. 16. These angles are arbitarily assumed in the counterclockwise direction.

The general vectorial solution for the torsional resultant can now be determined graphically as shown in Fig. 17. In this solution, the following steps are required:

A. Establish a reference axis. Note that the vertical axis is used here and is arbitrarily chosen.

B. From the vertical reference axis construct angles $2\phi_1$ and $2\phi_2$ in the previously assumed counterclockwise direction, using the values of ϕ_1 and ϕ_2 found in Fig. 16.

C. At this relative phase relationship, construct vectors equivalent in length to the magnitude of the joint angle squared. These vectors are θ_1^2 and θ_2^2. For approximate solutions, the joint angles in deg or rad can be used. For exact solutions, the maximum amplitude of torsional vibration for each joint is used and can be readily adapted to computer programming.

D. The vectorial sum of these two vectors is proportional to the magnitude of the resultant joint angle squared. θ_{res} can then be determined from the square root of this residual vector and represents the *torsional equivalent angle* of the system.

From this general vectorial solution for the torsional equivalent angle, it can be seen that in order to reduce the residual vector to a minimum, the intermediate shaft yokes d_1 and D_2 must be so phased that the individual vectors θ_1^2 and θ_2^2 are oppositely directed as shown in the solution in Figs. 14 and 15. Hence, if θ_1^2 and θ_2^2 are equal, the residual vector or torsional equivalent angle is zero as previously stated.

This same solution applies to any number of joints in series. In a system having n number of joints in series, the general solution can be expressed as follows:

$$\theta_{res}^2 \approx \theta_1^2 \pm \theta_2^2 \pm \theta_n^2$$

These torsional amplitudes of the joints are vector quantities and must be added vectorially. The general problem of joint angles and yoke phasing can be easily solved by this graphical method and the torsional excitation of a driveshaft system minimized as desired.

When a three-joint driveline is considered, it is noted that four principal phase relationships can exist if the three joint angles lie in a common plane. A *principal phase condition* is one where the yokes of the two intermediate shafts are either parallel (in line) or crossed (at 90 deg). Therefore, a three-joint shaft can have the following four principal phase relationships:

American Axle v. Neapco - IPR2025-00091
PET_AAM_1012-0054

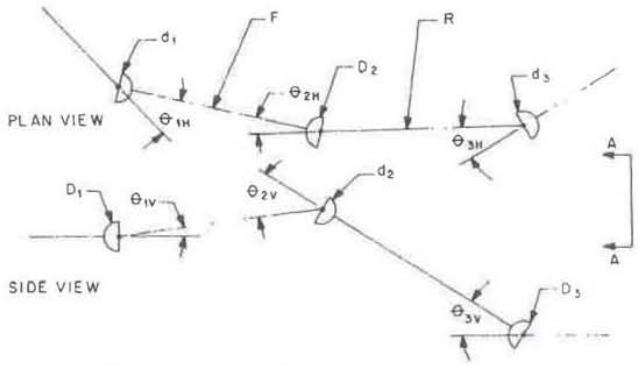


Fig. 18 — General three-joint shaft arrangement

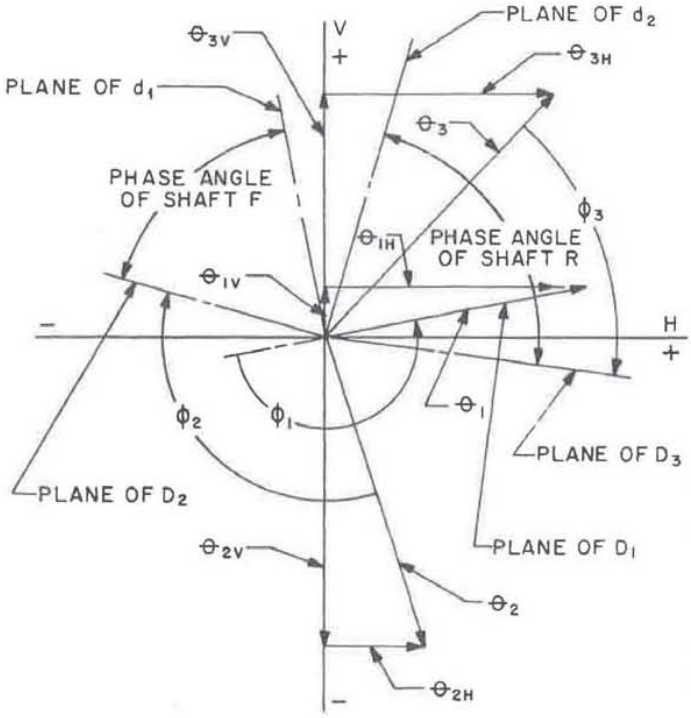
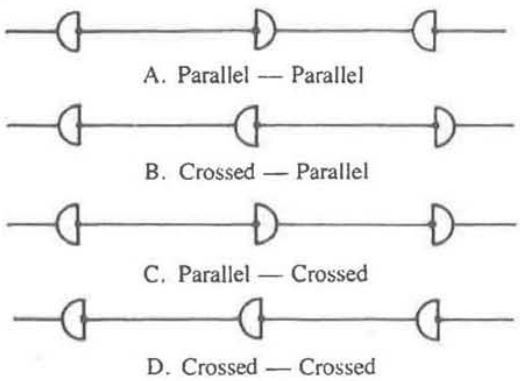


Fig. 19 — Joint angle and yoke plane relationships for optimum phasing



The residual joint angle or torsional equivalent angle of each of these four driveline phasing arrangements would be as follows:

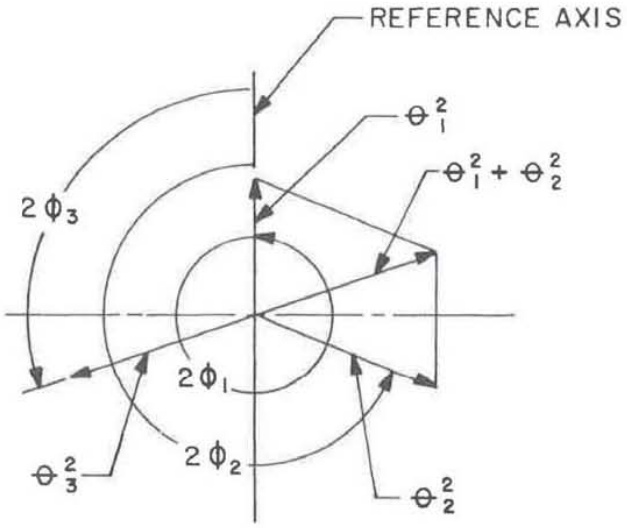


Fig. 20 — Vectorial solution for constant output velocity

Phasing Arrangement	Residual Joint Angle (Torsional Equivalent Angle)
Parallel — Parallel	$\sqrt{\theta_1^2 - \theta_2^2 + \theta_3^2}$
Crossed — Parallel	$\sqrt{\theta_1^2 + \theta_2^2 - \theta_3^2}$
Parallel — Crossed	$\sqrt{\theta_1^2 - \theta_2^2 - \theta_3^2}$
Crossed — Crossed	$\sqrt{\theta_1^2 + \theta_2^2 + \theta_3^2}$

If it is desired to achieve a zero output velocity variation (zero residual angle) of the system, an optimum or best phasing arrangement can be found by means of the graphical procedure previously described. Fig. 18 illustrates the general arrangement or case of a three-joint driveline where none of the shafts lie in the same plane. The solution for optimum or best phasing is accomplished by constructing views similar to Figs. 14-17.

Fig. 19 shows an end view of the two intermediate shafts where the planes of the joint angles are plotted and the planes of the yokes laid over this same plot. This end view can be seen in Fig. 18 when viewing the shafts from the direction of arrows A-A.

The plane of driving yoke D_1 of joint 1 is assumed in line with the plane of joint angle θ_1, while the planes of driving yokes D_2 and D_3 are unknown at this time. Angle ϕ_1 is measured in an assumed counterclockwise direction from the plane of the driving yoke to the plane of the joint angle for joint 1 as shown in Fig. 19. The vectorial solution for this three-joint driveline is shown graphically in Fig. 20. The vectors representing the joint angles of joints 1 and 2 are added vectorially in such a manner that their sum will be equal and opposed to the vector of the joint angle of joint 3. This procedure will result in a condition of constant output velocity for driven yoke d_3. In the solution, the following steps are required:

A. As in Fig. 15, a vertical reference axis is arbitrarily established.

B. Construct angle $2\phi_1$ in the previously assumed counterclockwise direction using the value of ϕ_1 found in Fig. 19.

C. At this location, construct a vector θ_1^2 equivalent in length

American Axle v. Neapco - IPR2025-00091
PET_AAM_1012-0055

to the magnitude of the joint angle squared. Also, at this time, the vectors θ_2^2 and θ_3^2 representing joints 2 and 3, respectively, should be determined and arbitrarily located on the diagram.

D. Since it is desired to achieve a zero residual joint angle of the system (constant output velocity), it is merely necessary to locate vector θ_2^2 in such a way that the vector sum of vector θ_1^2 and θ_2^2 is equal to vector θ_3^2. Now locate vector θ_3^2 so that it is oppositely directed from the resultant of vectors θ_1^2 and θ_2^2. This procedure will result in a zero residual joint angle for the system.

E. Construct angle 2 ϕ_2 to vector θ_2^2 and angle 2 ϕ_3 to vector θ_3^2 in the counterclockwise direction.

F. In Fig. 19, construct in the clockwise direction of rotation angles ϕ_2 and ϕ_3 from the planes of joint angles θ_2 and θ_3, respectively, as shown. This procedure locates the planes of driving yokes D_2 and D_3 of joints 2 and 3, respectively, at the instant when the plane of driving yoke D_1 of joint 1 lies in the plane of joint angle θ_1.

G. With all driving yokes now properly oriented with respect to each other in Fig. 19, construct driven yokes d_1 and d_2 of joints 1 and 2, respectively, and measure the phase angles of the appropriate yokes on the two intermediate shafts of the three-joint driveline. These are the phase angles required to achieve a constant output velocity or a zero residual joint angle for the system. As explained in the vectorial solution for the previous two-joint arrangement, this procedure is readily adapted to computer programming for exact solutions.

For drivelines with three or more joints, it should be pointed out that generally the optimum phasing required is determined by the necessity to minimize secondary couple forces which are usually more significant in vehicle applications.

Inertia Equivalent Angle—In a typical two-joint driveline, the portion of the driveshaft between joint centers rotates nonuniformly. The inertia effects of this nonuniform rotating shaft can be quite significant and limit the sizes of the continuous operating joint angles. The entire solution of this torsional system is a problem in torsional vibrations which will not be dealt with here. Only the basic principles involved and the practical limitations gained through experience will be discussed.

Fig. 21 shows a simulated two-joint system in a common plane with the following nomenclature:

J_1 = Mass moment of inertia of driveshaft portion between joint centers

M_1 and M_2 = Effective mass moment of inertia at the driveshaft ends

θ_1 and θ_2 = Joint angles

A basic equation of this system is:

$$T = J\alpha$$

where:

T = Exciting torque, lb-in

J = Mass moment of inertia, lb-in-s^2

α = Angular acceleration, rad/s/s

M_1 and M_2 are subject to the oscillating torque from the center of the driveshaft itself. This oscillation occurs even with equal

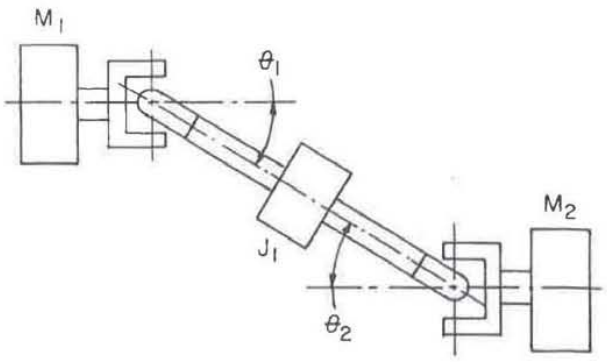


Fig. 21 — Simulated two-joint system

joint angles. If M_1 and M_2 are equal and large with respect to J_1, it is reasonable to assume that they will be subjected to oscillating torques equal to the maximum accelerating effects of the joint angle times the inertia J_1 of the center of the driveshaft. If M_1 and M_2 are small compared to J_1, then it is also reasonable to assume that the center of the driveshaft will turn uniformly while maximum amplitude and acceleration will occur through the end mass members. It can also be assumed that if M_1 or M_2 is large compared to the other, that the smallest mass would have the largest amplitude and vibration.

There are, therefore, many combinations of possibilities defining the relative effect of nonuniform motion of the center portion of the driveshaft. It is, however, generally true that a balance of torque loads must exist. The oscillating torque required to change the angular velocity of J_1 must be supplied by some equivalent oscillating torque on the rotating masses outside of J_1, namely, M_1 and M_2.

This brings up the situation that exists when the driveshaft operates at somewhat unequal joint angles. In this case, M_1 and M_2 are subject to torsional oscillation from inequality of the joint angles as well as from the nonuniform motion of J_1. In Fig. 21, θ_1 and θ_2 are assumed slightly unequal, while M_1 and M_2 are equal and large compared to J_1.

In this situation, the actual steady state condition could be estimated to be approximately as follows:

M_1 and M_2 are excited torsionally through one-half the amplitude of θ_{res}.

J_1 is torsionally excited through some joint angle which is probably about equivalent to the average of θ_1 and θ_2. An oscillatory torque is imposed on M_1 and M_2 equally from the oscillatory acceleration effects of J_1. The summation of these oscillatory torques show that they are out-of-phase relative to their effect on the end of the driveshaft with the smallest joint angle end, and in phase with each other relative to their effect on the largest joint angle end.

This leads to the following generalized conditions with unequal joint angles:

1. Torsional excitation effect is reduced on the member supporting the end of the driveshaft with the smallest joint angle.
2. Torsional excitation effect is increased on the member supporting the end of the driveshaft with the largest joint angle.

American Axle v. Neapco - IPR2025-00091
PET_AAM_1012-0056

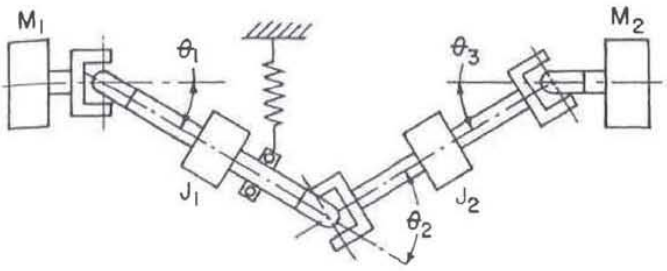


Fig. 22 — Simulated three-joint system

These situations are very useful in analyzing installations where the excitation created by nonuniform motion of the center of the driveshaft creates disturbances within one of the supporting members, such as a transmission. This excitation would usually appear as a disturbance when transmitting very light or no torque loads; a floating type of noise or disturbance, when under light or no torque loads, parts clatter through working clearances. To improve this situation, slightly unequal joint angles with the smallest angle at the disturbing element will often produce a much smoother operating drive system.

For purposes of expressing the inertia effects of this two-joint system the term *inertia equivalent angle* can be used. More specifically, in a two-joint system, the *inertia drive equivalent angle* is the joint angle of the first joint, while the *inertia coast equivalent angle* is the joint angle of the second joint. In this arrangement, the maximum inertia load is equivalent to the size of the largest joint angle.

The same situation described for the simple two-joint system applies to a multijoint system. The problem, while somewhat more complicated, still shows the same general solution if the multijoint combination is considered equivalent to a simple two-joint system. Fig. 22 shows a simulated three-joint system with the following nomenclature:

J_1 = Mass moment of inertia between joints 1 and 2.
J_2 = Mass moment of inertia between joints 2 and 3.
M_1 and M_2 = Effective mass moment of inertia at the system ends.
θ_1, θ_2 and θ_3 = Joint angles

It is possible to draw an analogy of an equivalent simple two-joint system. If J_1 and J_2 are approximately equal, the following assumptions can be made:

1. Relative to M_1, J_1 is subjected to torsional oscillations from the effects of θ_1.
2. Relative to M_1, J_2 is subjected to torsional oscillations from the sum of the effects of θ_1 and θ_2.
3. Relative to M_2, J_2 is subjected to torsional oscillations from the effects of θ_3.
4. Relative to M_2, J_1 is subjected to torsional oscillations from the sum of the effects of θ_2 and θ_3.

If the joint angles are all in a common plane and with parallel-parallel phasing of the yokes as shown in Fig. 22, the residual joint angle or *torsional equivalent angle* of the system was previously shown to be:

$$\theta_{res} = \sqrt{\theta_1^2 - \theta_2^2 + \theta_3^2}$$

For purposes of determining the inertia effects of this three-joint system, equations can be established by working from each end of the driveline. These expressions can be termed *inertia equivalent angles*. The *inertia drive equivalent angle* is the joint angle of a single joint which will produce the same maximum acceleration as the maximum of the sum of the accelerations of all but the last joint in the driveline. The *inertia coast equivalent angle* is the joint angle of a single joint which will produce the same maximum acceleration as the maximum of the sum of the accelerations of all but the first joint in the driveline. These two inertia equivalent angles are:

$$\theta_D = \sqrt{2\theta_1^2 - \theta_2^2}$$

$$\theta_C = \sqrt{2\theta_3^2 - \theta_2^2}$$

It was previously indicated that arithmetical values only are significant and that the negative sign possibility is ignored.

As an illustration, assume $\theta_1 = 5$ deg, $\theta_2 = 6$ deg, and $\theta_3 = 4$ deg.

$$\theta_{res} = \sqrt{(5)^2 - (6)^2 + (4)^2}$$

$$= \sqrt{5}$$

$$\theta_{res} = 2.24 \text{ deg}$$

$$\theta_D = \sqrt{2\,(5)^2 - (6)^2}$$

$$= \sqrt{14}$$

$$\theta_D = 3.74 \text{ deg}$$

$$\theta_C = \sqrt{2\,(4)^2 - (6)^2}$$

$$= \sqrt{4}$$

$$\theta_C = 2.00 \text{ deg}$$

From these results, the following obvious relationship can be established:

$$\theta_D^2 - \theta_C^2 = 2\,\theta_{res}^2$$
$$14 - 4 = 2 \times 5$$
$$10 = 10$$

This three-joint system, therefore, is equivalent to a one-piece driveshaft installation with $J = J_1$ or J_2 because they are assumed equal and with angles of 3.74 deg and 2.00 deg.

As with the case of the torsional equivalent angle, it is possible to express the inertia equivalent angles for the four principal phase relationships as follows, if the three joint angles lie in a common plane:

American Axle v. Neapco - IPR2025-00091
PET_AAM_1012-0057

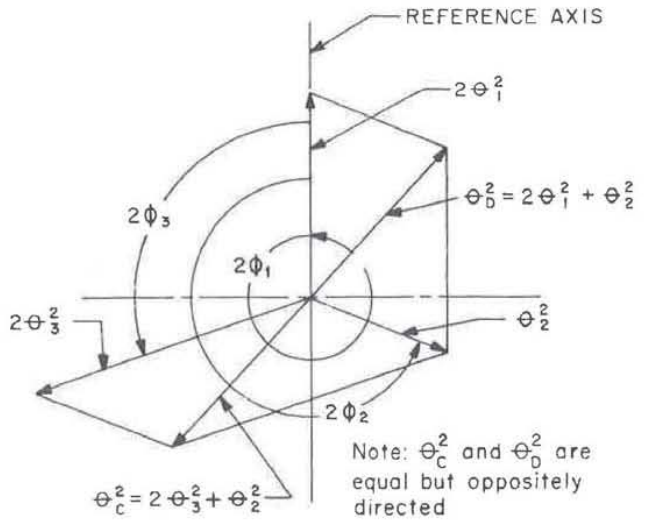


Fig. 23 — Vectorial solution for inertia equivalent angles

Phasing Arrangement	Inertia Equivalent Angle θ_D	Inertia Equivalent Angle θ_C
Parallel-Parallel	$\sqrt{2\theta_1^2 - \theta_2^2}$	$\sqrt{2\theta_3^2 - \theta_2^2}$
Crossed-Parallel	$\sqrt{2\theta_1^2 + \theta_2^2}$	$\sqrt{2\theta_3^2 - \theta_2^2}$
Parallel-Crossed	$\sqrt{2\theta_1^2 - \theta_2^2}$	$\sqrt{2\theta_3^2 + \theta_2^2}$
Crossed-Crossed	$\sqrt{2\theta_1^2 + \theta_2^2}$	$\sqrt{2\theta_3^2 + \theta_2^2}$

Also, any random selection of out-of-plane joint angles or phasing can be considered by expanding the vector solution to include these possibilities in very much the same way as was illustrated with the graphical procedure outlined for the torsional equivalent angle.

In illustrating the graphical procedure for determining the inertia equivalent angles, the same general three-joint driveline arrangement shown in Fig. 18 is used where none of the shafts lie in the same plane. An end view of the two intermediate shafts is shown in Fig. 19 where the planes of the joint angles are plotted and the planes of the yokes superimposed over this same plot. The phasing of the yokes is that which is required to produce constant output velocity or zero residual joint angle for the system. For these phase relationships of the yokes, Fig. 23 shows the vectorial solution for the inertia drive and inertia coast equivalent angles of the three-joint system. Since this vectorial solution is for the optimum phasing condition, the inertia drive and inertia coast equivalent angles are equal and oppositely directed or in phase opposition to each other as shown. The basic steps used are the same as for the vectorial solutions illustrated in Figs. 15, 17, and 20.

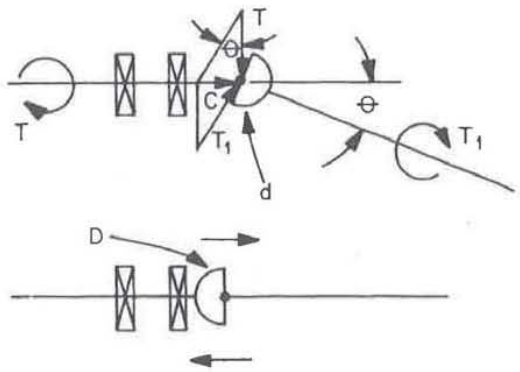
In a system having n number of joints in series, the general solution for the inertia drive equivalent angle can be expressed as follows:

$$\theta_D^2 = \overrightarrow{(n-1)\theta_1^2} \pm \overrightarrow{(n-2)\theta_2^2} \pm \ldots \pm \overrightarrow{(1)\theta_{(n-1)}^2} \pm \overrightarrow{(0)\theta_n^2}$$

where the torsional amplitudes of the joints are vector quantities and must be added accordingly. The general solution for the inertia coast equivalent angle can be similarly expressed as follows:

$$\theta_C^2 = \overrightarrow{(n-1)\theta_n^2} \pm \overrightarrow{(n-2)\theta_{(n-1)}^2} \pm \overrightarrow{(n-3)\theta_{(n-2)}^2} \pm \ldots \pm \overrightarrow{(0)\theta_1^2}$$

It was previously indicated that generally the optimum phasing required in multijoint drivelines is dictated by the necessity to minimize secondary couple excitation, which usually is more significant than torsional or inertia effects.



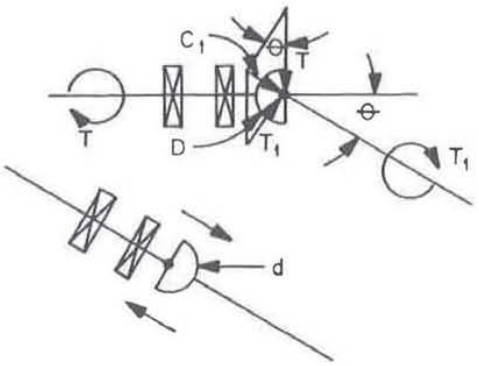
T = INPUT TORQUE
T_1 = OUTPUT TORQUE
Θ = JOINT ANGLE
C = SECONDARY COUPLE T TAN Θ
D = DRIVING YOKE.
d = DRIVEN YOKE
INPUT TORQUE T IS ASSUMED CLOCKWISE WHEN VIEWED FROM LEFT END.

Fig. 24 — Cardan joint secondary couple at rotational position (a)

Secondary Couple Forces—When a Cardan joint transmits torque at an angle, an oscillating bending moment is produced by this change in direction of torque. This bending moment, which is a function of torque and joint angle only, is called a *secondary couple* to distinguish it from the primary or torque transmitting couple. This bending moment differs from the primary or torque transmitting couple in that it acts in the axial plane of the driving and driven member yokes, is transferred into any connecting shaft member, and is reacted by the supporting bearings.

Fig. 24 shows a Cardan joint in rotational position (a). This position is one of the two *square* positions of a Cardan joint where one of the yokes lies in the plane of the joint angle, while the other yoke is normal or perpendicular to it. The secondary couple on the driving yoke has a maximum value of T tan θ, while on the driven yoke, it is zero. Fig. 25 shows the joint in rotational position (b) which is 90 deg of rotation from position (a) and is the other *square* position. In this position, the secondary couple on the driving yoke is zero, while on the driven yoke, it has a maximum value of T sin θ. Thus, it is seen that the couples, while remaining in the planes of the yokes, are cyclic in nature with a magnitude from zero to maximum twice per revolution, and the resultant couple forces react on supporting bearings with a complex excitation. Fig. 26 shows the basic characteristics of a secondary couple force on a supporting bearing. The result is equivalent to a static

American Axle v. Neapco - IPR2025-00091
PET_AAM_1012-0058



T = INPUT TORQUE
T_1 = OUTPUT TORQUE
θ = JOINT ANGLE
C_1 = SECONDARY COUPLE T SIN θ
D = DRIVING YOKE
d = DRIVEN YOKE
INPUT TORQUE T IS ASSUMED CLOCKWISE WHEN VIEWED FROM LEFT END.

Fig. 25 — Cardan joint secondary couple at rotational position (b)

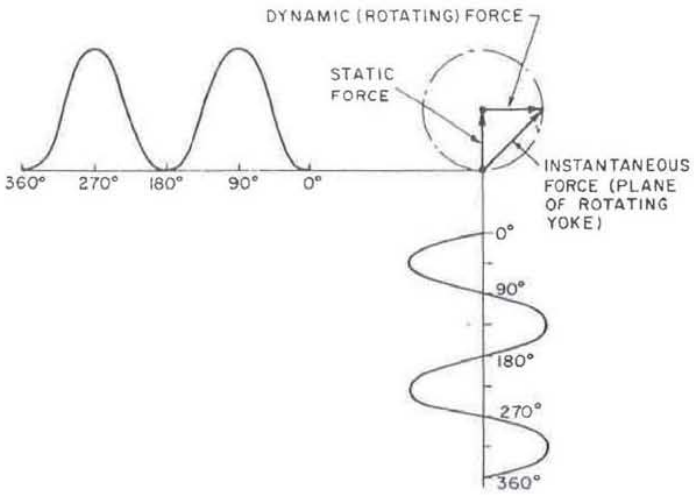


Fig. 26 — Secondary couple force characteristics on a supporting bearing

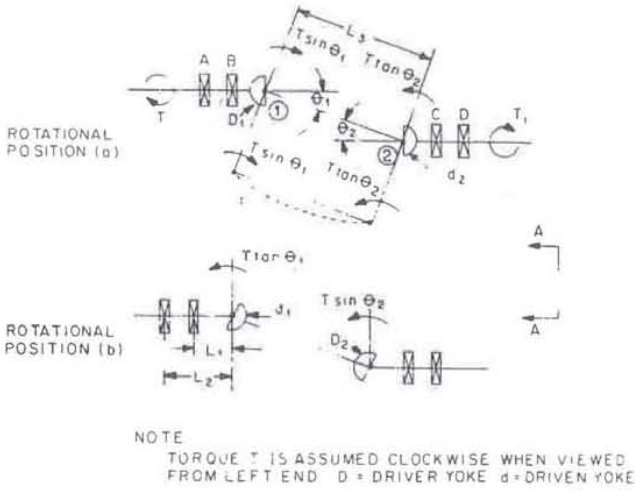


Fig. 27 — Parallel shaft arrangement with parallel intermediate shaft yokes

force constant in size and normal to the plane of the joint angle plus a dynamic force of equal magnitude with a rotational frequency of two cycles per revolution. It is the rotating force which produces a vibratory excitation on the bearing supports.

For small joint angles, the sine and tangent are approximately equal. Also, for small angles, the sine and tangent are approximately equal to the angle expressed in radians. Therefore, the couples within a joint are of essentially the same magnitude on the driving and driven yokes. Since the couple on each yoke varies from zero to maximum twice per revolution and since it is maximum on one yoke when it is zero on its mating yoke, the couples alternate between a maximum and zero twice each revolution 90 deg out of phase with each other. With respect to each of the rotating shafts, therefore, the couple stays in the plane of the yoke and varies from a maximum value in one direction to a maximum value in the opposite direction and back again once per revolution. These maximum values always occur normal to the plane of the joint angle.

For a given disposition or direction of the joint angle, the two couples of a joint are sensed in the same clockwise or counterclockwise direction. The direction of these couples can be reversed by reversing the direction of the applied torque or by reversing the direction of the joint angle.

When a second joint is added to a driveshaft, the resulting installed arrangement is generally described as either the parallel shafts or the intersecting shafts arrangement. Fig. 27 shows the parallel shafts arrangement with parallel phasing of the intermediate shaft yokes. Assuming equal angles at each end, this condition produces equal and opposite hand couples on the intermediate shaft, which cancel each other relative to supporting bearings. The only effect of these couples is, therefore, to produce an oscillating bending force on the intermediate shaft which results in the shaft being bent in an arc as shown in Fig. 27. This arc is a true radius since the joint angles are equal. Because the shaft is always bent in one direction from zero to maximum deflection, the intermediate member in the plane of its yokes is subjected to a completely reversed bending cycle at a frequency equal to the speed of rotation. With this parallel shaft arrangement, the support bearing structures must only withstand the couple forces from the adjacent joint yoke. For example, the maximum couple forces at bearing B in the two principal rotational positions are as follows:

$$\frac{\text{Couple T sin } \theta_1 \text{ (yoke d}_1\text{)}}{}$$

$$F = \frac{T \sin \theta_1}{L_3}$$

$$F_1 (L_2 - L_1) = FL_2$$

$$F_1 = \frac{T \sin \theta_1 L_2}{(L_2 - L_1) L_3}$$

American Axle v. Neapco - IPR2025-00091
PET_AAM_1012-0059

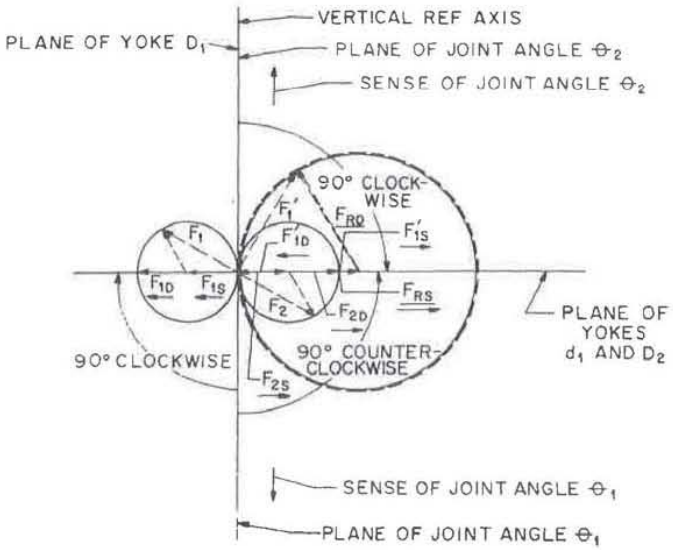


Fig. 28 — Vectorial solution for resultant static and dynamic forces

Couple T tan θ_2 (yoke D_2)

$$F = \frac{T \sin \theta_2}{L_3}$$

$$F_2 = (L_2 - L_1) = FL_2$$

$$F_2 = \frac{T \sin \theta_2 \, L_2}{(L_2 - L_1) L_3}$$

NOTE: For small angles, the sine and tangent are approximately equal. Arbitrarily, the sine is used here.

Couple T tan θ_1 (yoke D_1)

$$F_1' = \frac{T \sin \theta_1}{L_2 - L_1}$$

These couple forces may be summated at bearing B to determine the over-all effects. Fig. 28 shows the vectorial solution for the resultant static and dynamic forces accomplished by a graphical method with the following steps:

A. By viewing bearing B in Fig. 27 from the direction of arrows A-A, the vertical plane is established as the arbitrary vertical reference axis for Fig. 28. The planes of joint angles θ_1 and θ_2 lie in this plane with θ_1 sensed downward and θ_2 sensed upward. Also, the planes of yokes d_1 and D_2 are located in the horizontal plane. This procedure is arbitrary.

B. The maximum value of a couple force occurs normal to the plane of its joint angle. Since the planes of joint angles θ_1 and θ_2 lie on the vertical reference axis, the maximum vector values of the three couple forces are on the horizontal axis. In Fig. 27, the maximum couple force at bearing B resulting from couple T sin θ_1 is directed to the left from the vertical plane when viewed from the direction of arrows A-A, while the maximum couple force resulting from couple T tan θ_2 is directed to the right. Likewise, the maximum couple force resulting from couple T tan θ_1 is also directed to the right. Therefore, in Fig. 28, the maximum value of couple force F_1 is located 90 deg clockwise from the plane and sense of joint angle θ_1. The maximum value of couple force F_2 is located 90 deg clockwise from the plane and sense of joint angle θ_2. The maximum value of couple force F_1' is located 90 deg counterclockwise from the plane and sense of joint angle θ_1.

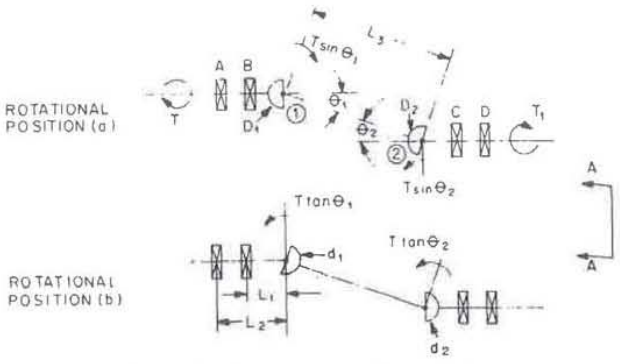


Fig. 29 — Parallel shaft arrangement with crossed intermediate shaft yokes

C. It was previously shown in Fig. 26 that with reference to a supporting bearing, the couple force is equivalent to a static force constant in size and normal to the plane of the joint angle plus a dynamic force of equal magnitude with a rotational frequency of two cycles per revolution. Therefore, in Fig. 28, the static force vectors F_{1S}, F_{2S}, and F_{1S}' are located as shown normal to their respective joint angles and added vectorially without regard to yoke phasing. The vectorial sum is the resultant static force F_{RS} and is located as shown.

D. When adding dynamic force vectors, yoke phasing is important. Yokes d_1 and D_2 are located in the same plane (parallel phasing), while yoke D_1 is located 90 deg from this plane. The dynamic force vector F_{1D} is directed horizontally to the left to the point where the circular trace of F_1 intersects the plane of yoke d_1, which lies on the horizontal axis. Vector F_{2D} is directed horizontally to the right to the point where the circular trace of F_2 intersects the plane of yoke D_2, which lies on the horizontal axis. Vector F_{1D}' is directed horizontally to the left to the origin where the circular trace of F_1' intersects the plane of yoke D_1, which lies on the vertical axis. The directions of all dynamic force vectors are now sensed correctly and can be added vectorially. The vectorial sum is the resultant dynamic force F_{RD} and originates at the end of F_{RS}.

When the previous parallel shafts arrangement is considered with crossed phasing of the intermediate shaft yokes, as shown in Fig. 29, the only effect is to increase the resultant dynamic force F_{RD}, while the resultant static force F_{RS} remains the same. This solution is shown in Fig. 30 for bearing B where the same steps were followed as outlined in the graphical solution shown in Fig. 28. The relocation of yoke D_2 from the horizontal to the vertical plane requires the reversal of the sense of the dynamic force

American Axle v. Neapco - IPR2025-00091
PET_AAM_1012-0060

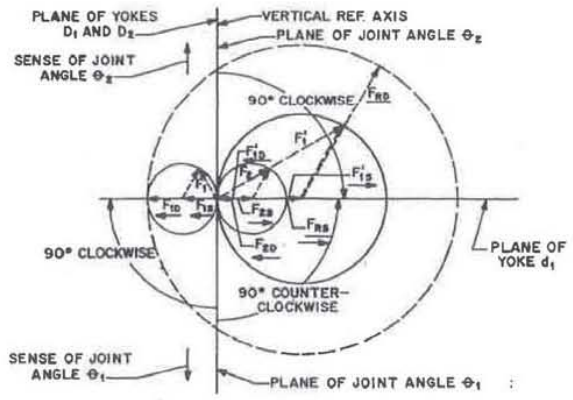


Fig. 30 — Vectorial solution for resultant static and dynamic forces

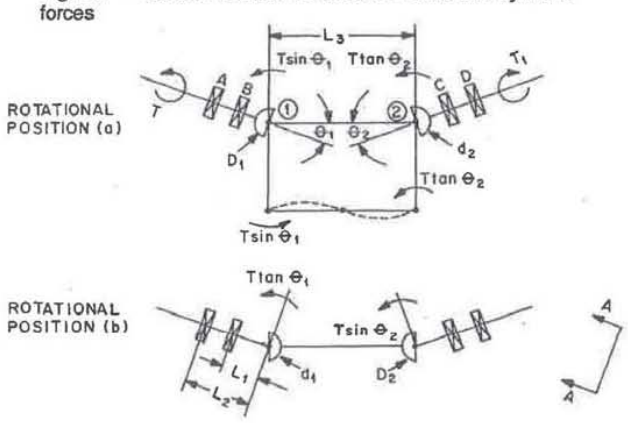


Fig. 31 — Intersecting shaft arrangement with parallel intermediate shaft yokes

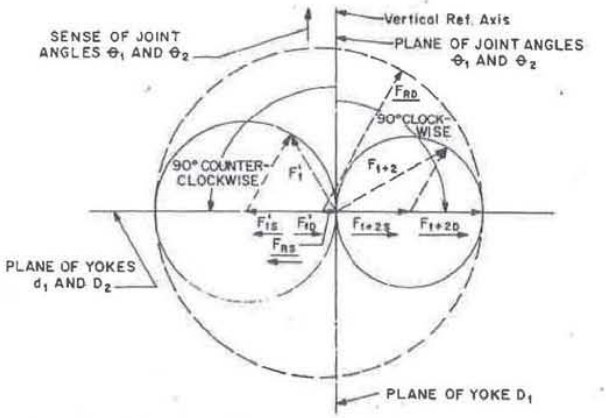


Fig. 32 — Vectorial solution for resultant static and dynamic forces

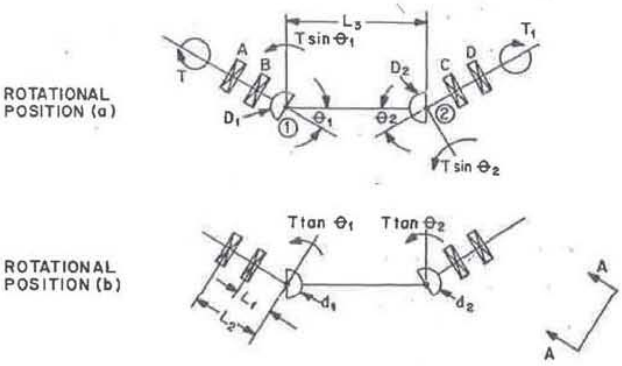


Fig. 33 — Intersecting shaft arrangement with crossed intermediate shaft yokes

vector F_{2D} and results in the increased resultant dynamic force. In studying these two solutions, it can be seen that for all conditions of joint phasing in a given driveshaft installation, the resultant static force always remains the same, while the resultant dynamic force varies.

Fig. 31 shows the intersecting shafts arrangement with parallel phasing of the intermediate shaft yokes and assuming equal angles at each end. Under this condition, the couples on the intermediate shaft are of the same hand and in phase with each other. These couples are supported through the length of the center portion of the driveshaft itself and result in the shaft being bent in an S shape having a nodal point at the middle of the shaft length as shown in Fig. 31. Because the shaft is always bent in a given S shape from zero to maximum deflection, it indicates that the intermediate member is subjected to a completely reversed bending cycle at a frequency equal to the rotational speed. With this intersecting shaft arrangement, the support bearing structures at each end must withstand the couple effect of the adjacent joint yoke as well as provide support for one of the force members from the couple around the length of the intermediate shaft. Fig. 32 shows the graphical solution for the resultant static and dynamic forces at bearing B where the same steps were followed as outlined in the previous solutions.

When the previous intersecting shafts arrangement is considered with crossed phasing of the intermediate shaft yokes, as shown in Fig. 33, the only effect is to reduce the resultant dynamic force F_{RD}, while the resultant static force F_{RS} remains unchanged. This solution is shown in Fig. 34 for bearing B. The relocation of yoke D_2 from the horizontal to the vertical plane requires the reversal of the sense of the dynamic force vector F_{2D} and results in the decreased resultant dynamic force.

The previous two-joint driveshaft arrangements were considered with both joint angles lying in the same plane. The graphical solution for the secondary couple effects can easily be extended to arrangements where the joint angles do not lie in a common plane.

Since all the previous two-joint driveshaft arrangements were considered with both joint angles in a common plane, it is also possible to determine the couple effects by mathematical equations which can be easily developed and used. Fig. 35 shows the parallel shafts arrangement with parallel phasing of the intermediate shaft yokes. The couples acting in this system are shown with the joint angles expressed in radians rather than with the sine or tangent. This procedure is permissible for small angles. The maximum couple forces at bearing B are as follows:

American Axle v. Neapco - IPR2025-00091
PET_AAM_1012-0061

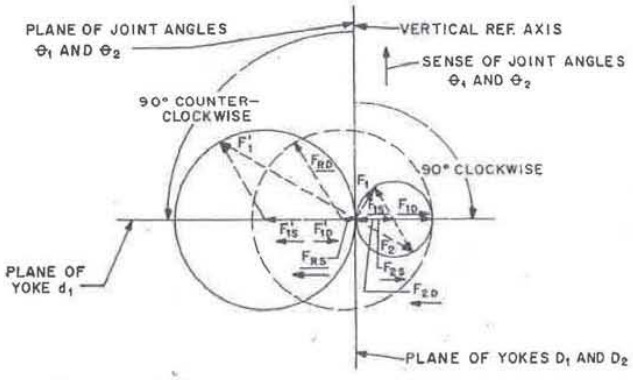


Fig. 34 — Vectorial solution for resultant static and dynamic forces

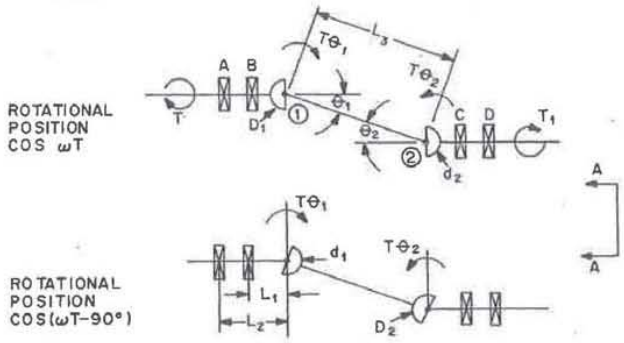


Fig. 35 — Parallel shaft arrangement with parallel intermediate shaft yokes

Couple $T\theta_1$ (yoke d_1)

$$F = \frac{T\theta_1}{L_3}$$

$$F_1(L_2 - L_1) = FL_2$$

$$F_1 = \frac{T\theta_1 L_2}{(L_2 - L_1)L_3}$$

Couple $T\theta_2$ (yoke D_2)

$$F = \frac{T\theta_2}{L_3}$$

$$F_2(L_2 - L_1) = FL_2$$

$$F_2 = \frac{T\theta_2 L_2}{(L_2 - L_1)L_3}$$

Couple $T\theta_1$ (yoke D_1)

$$F_1' = \frac{T\theta_1}{L_2 - L_1}$$

When viewing the driveshaft system of Fig. 35 from the direction of arrows A-A, the couple forces acting on bearing B will be arbitrarily considered positive (+) if they act left transversely (horizontally), and negative (−) if they act right transversely. Therefore, the couple forces in the two principal rotational positions can be summated as follows:

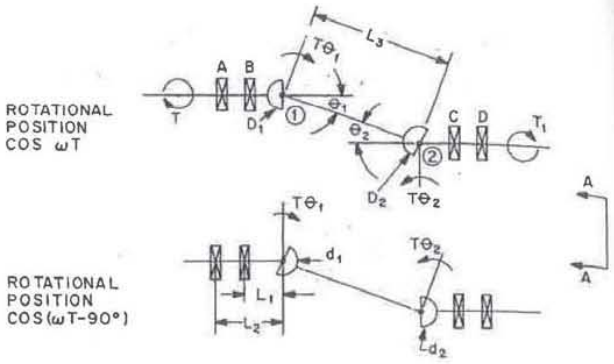


Fig. 36 — Parallel shaft arrangement with crossed intermediate shaft yokes

$$\text{Force at bearing B} = \frac{T\theta_1 L_2}{(L_2 - L_1)L_3}\cos\omega t - \frac{T\theta_2 L_2}{(L_2 - L_1)L_3}\cos\omega t - \frac{T\theta_1}{L_2 - L_1}\cos(\omega t - 90\text{ deg})$$

This equation of the resultant force at bearing B must now be expressed as a resultant static force and a resultant dynamic force. The resultant static force F_{RS} is simply the above expression divided by two as follows:

$$F_{RS} = \frac{T\theta_1 L_2}{2(L_2 - L_1)L_3} - \frac{T\theta_2 L_2}{2(L_2 - L_1)L_3} - \frac{T\theta_1}{2(L_2 - L_1)}$$

The resultant dynamic force is, however, affected by the location of the couples with regard to the two rotational position views in Fig. 35. If the view of rotational position cos ωt is assumed as the reference view, then the signs of all the couple forces originating in the view of rotational position cos (ωt − 90 deg) must be changed to their opposite sign. Also, as in the static force equation, all couple forces must be divided by two. Therefore, the resultant dynamic force is:

$$F_{RD} = \frac{T\theta_1 L_2}{2(L_2 - L_1)L_3} - \frac{T\theta_2 L_2}{2(L_2 - L_1)L_3} + \frac{T\theta_1}{2(L_2 - L_1)}$$

When the previous parallel shafts arrangement is considered with crossed phasing of the intermediate shaft yokes as shown in Fig. 36, the couple forces acting on bearing B can be summated as follows:

$$\text{Force at bearing B} = \frac{T\theta_1 L_2}{(L_2 - L_1)L_3}\cos\omega t - \frac{T\theta_2 L_2}{(L_2 - L_1)L_3}\cos(\omega t - 90\text{ deg}) - \frac{T\theta_1}{L_2 - L_1}\cos(\omega t - 90\text{ deg})$$

American Axle v. Neapco - IPR2025-00091
PET_AAM_1012-0062

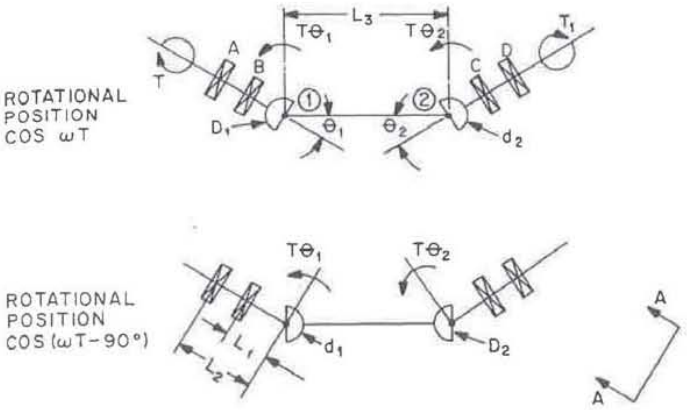


Fig. 37 — Intersecting shaft arrangement with parallel intermediate shaft yokes

From this equation, the resultant static force is:

$$F_{RS} = \frac{T\theta_1 L_2}{2(L_2 - L_1)L_3} - \frac{T\theta_2 L_2}{2(L_2 - L_1)L_3} - \frac{T\theta_1}{2(L_2 - L_1)}$$

and the resultant dynamic force is:

$$F_{RD} = \frac{T\theta_1 L_2}{2(L_2 - L_1)L_3} + \frac{T\theta_2 L_2}{2(L_2 - L_1)L_3} + \frac{T\theta_1}{2(L_2 - L_1)}$$

Fig. 37 shows the intersecting shafts arrangement with parallel phasing of the intermediate shaft yokes. The couple forces acting on bearing B can be summated as follows:

$$\text{Force at bearing B} = -\frac{T\theta_1 L_2}{(L_2 - L_1)L_3}\cos\omega t - \frac{T\theta_2 L_2}{(L_2 - L_1)L_3}\cos\omega t + \frac{T\theta_1}{L_2 - L_1}\cos(\omega t - 90\text{ deg})$$

From this equation, the resultant static force is:

$$F_{RS} = -\frac{T\theta_1 L_2}{2(L_2 - L_1)L_3} - \frac{T\theta_2 L_2}{2(L_2 - L_1)L_3} + \frac{T\theta_1}{2(L_2 - L_1)}$$

and the resultant dynamic force is:

$$F_{RD} = -\frac{T\theta_1 L_2}{2(L_2 - L_1)L_3} - \frac{T\theta_2 L_2}{2(L_2 - L_1)L_3} - \frac{T\theta_1}{2(L_2 - L_1)}$$

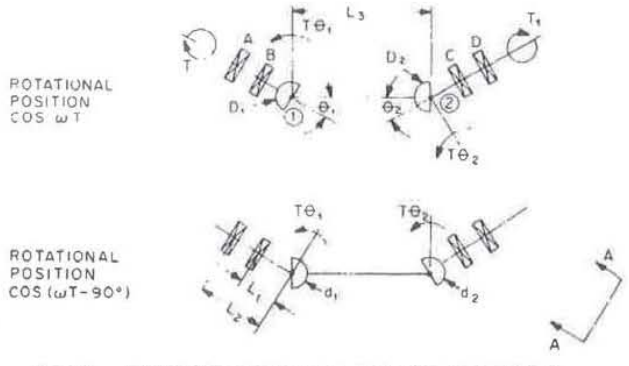


Fig. 38 — Intersecting shaft arrangement with crossed intermediate shaft yokes

When the previous intersecting shafts arrangement is considered with crossed phasing of the intermediate shaft yokes as shown in Fig. 38, the couple forces acting on bearing B can be summated as follows:

$$\text{Force at bearing B} = -\frac{T\theta_1 L_2}{(L_2 - L_1)L_3}\cos\omega t - \frac{T\theta_2 L_2}{(L_2 - L_1)L_3}\cos(\omega t - 90\text{ deg}) + \frac{T\theta_1}{L_2 - L_1}\cos(\omega t - 90\text{ deg})$$

From this equation, the resultant static force is:

$$F_{RS} = -\frac{T\theta_1 L_2}{2(L_2 - L_1)L_3} - \frac{T\theta_2 L_2}{2(L_2 - L_1)L_3} + \frac{T\theta_1}{2(L_2 - L_1)}$$

and the resultant dynamic force is:

$$F_{RD} = -\frac{T\theta_1 L_2}{2(L_2 - L_1)L_3} + \frac{T\theta_2 L_2}{2(L_2 - L_1)L_3} - \frac{T\theta_1}{2(L_2 - L_1)}$$

The graphical and mathematical procedures for the secondary couple effects used in the previous two-joint driveshaft arrangements can also be applied to drivelines having three or more joints in series. In fact, in multijoint drivelines, these couple effects are usually more significant than torsional or inertia excitations. Therefore, optimum phasing is generally dictated by the desire to minimize secondary couple disturbances at the relatively sensitive shaft support bearings in multijoint drivelines.

The driveline, however, assumes a varying geometry due to suspension movements and various driving modes to which a vehicle may be subjected. Hence, a compromise on phasing must be made in order to minimize the major disturbance for a specific dynamic driveline condition.

Fig. 39 shows a typical three-joint driveline in two principal rotational positions with the four secondary couples which influence the resultant forces on the shaft support bearing. Fig. 40

American Axle v. Neapco - IPR2025-00091
PET_AAM_1012-0063

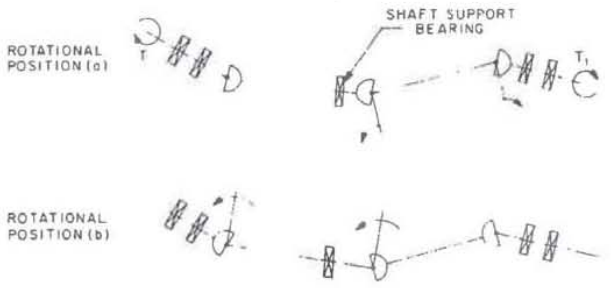


Fig. 39 — Secondary couples which influence shaft support bearing

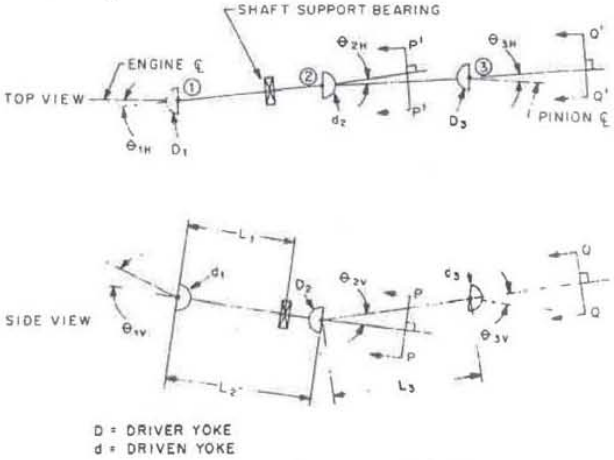


Fig. 40 — Typical three-joint driveline

shows a typical three-joint driveline in top and side views. The vectorial solution is used in an illustrative problem to determine and compare the secondary couple effects at the support bearing for various yoke phasing combinations.

For a four-passenger load wide-open throttle (WOT) forward start or maximum wheel slip (tractive effort) condition in a typical small passenger car, the following driveline data is assumed:

$T = 5000$ lb-in (assumed clockwise when viewed from front of car)

$\theta_{1H} = 0°53'03''$

$\theta_{1V} = 2°12'24''$

$\theta_{2H} = 0°$

$\theta_{2V} = 5°18'00''$

$\theta_{3H} = 0°53'03''$

$\theta_{3V} = 1°22'24''$

$L_1 = 26.33$ in

$L_2 = 29.26$ in

$L_3 = 34.32$ in

The true joint angles are found as follows:

$$\tan \theta_1 = (\tan \theta_{1H})^2 + (\tan \theta_{1V})^2$$

$$= (0.015433)^2 + (0.038533)^2$$

$$\tan \theta_1 = 0.041509$$

$$\theta_1 = 2°22'37''$$

$$\theta_2 = 5°18'00'' = \theta_{2V} \ (\theta_{2H} = 0 \text{ deg})$$

$$\tan \theta_3 = (\tan \theta_{3H})^2 + (\tan \theta_{3V})^2$$

$$= (0.015433)^2 + (0.023974)^2$$

$$\tan \theta_3 = 0.028512$$

$$\theta_3 = 1°37'59''$$

The maximum couple forces on the shaft support bearing are as follows:

Couple $T \sin \theta_1$ (yoke d_1)

$$F_1 = \frac{T \sin \theta_1}{L_1}$$

$$= \frac{5000 \times 0.041474}{26.33}$$

$$F_1 = 7.876 \text{ lb}$$

Couple $T \tan \theta_2$ (yoke D_2)

$$F_2 = \frac{T \sin \theta_2}{L_1}$$

$$= \frac{5000 \times 0.092371}{26.33}$$

$$F_2 = 17.541 \text{ lb}$$

Couple $T \sin \theta_2$ (yoke d_2)

$$F_2' = \frac{T \sin \theta_2 L_2}{L_1 L_3}$$

$$= \frac{5000 \times 0.092371 \times 29.26}{26.33 \times 34.32}$$

$$F_2' = 14.955 \text{ lb}$$

American Axle v. Neapco - IPR2025-00091
PET_AAM_1012-0064

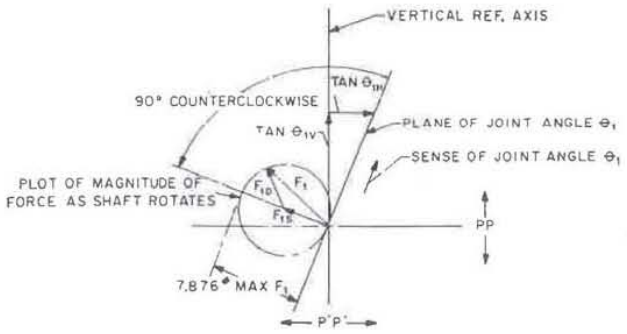


Fig. 41 — Secondary couple force vectors

$$F_3 = \frac{\text{Couple T sin } \theta_3 \text{ (yoke D}_3\text{)}}{L_1 L_3}$$

$$= \frac{T \sin \theta_3 L_2}{L_1 L_3}$$

$$= \frac{5000 \times 0.028498 \times 29.26}{26.33 \times 34.32}$$

$$F_3 = 4.614 \text{ lb}$$

NOTE: For small angles, the sine and tangent are approximately equal. Arbitrarily, the sine is used here.

Although they can be constructed as one figure in the following vectorial solution, the single vectors and the various combinations on the two shafts are shown separately in sequence for convenience of explanation.

Fig. 41 shows the trace of the force F_1 on the support bearing from the couple at yoke d_1. Because the couple varies as the sine of the angle of rotation of the driving yoke, the force must also vary at this angle, and makes the trace of the force a circle which passes through zero. The maximum value of this trace occurs normal to the plane of the true joint angle, and gives the effect of a static force equal to one-half of the maximum force plus a dynamic force equal to one-half of the maximum force acting at the end of the static force. This dynamic force has a rotational frequency of twice shaft speed. When viewing the front shaft from the right or rear end in Fig. 40, and using the vertical plane as the arbitrary vertical reference axis, locate the plane and sense of joint angle θ_1 upward and to the right. As shown, the plane of this angle is determined by constructing the tangents of the side and top view component angles. The maximum value of force F_1 is located 90 deg counterclockwise from the plane and sense of joint angle θ_1. The vector representing this force may be more readily visualized as the two vectors previously described. One vector is a static force F_{1S} at 90 deg counterclockwise from the plane and sense of the joint angle and the other vector is a dynamic force F_{1D} of the same magnitude beginning at the end of F_{1S}.

Fig. 42 shows the trace of the force F_2 on the support bearing from the couple at yoke D_2. The same vertical reference axis in Fig. 41 must be used here. Also, the plane and sense of joint angle θ_2 coincide with this axis as seen in Fig. 40. The maximum value

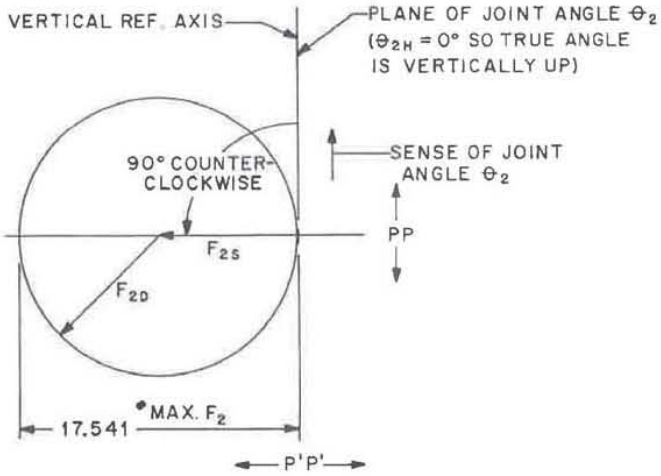


Fig. 42 — Secondary couple force vectors

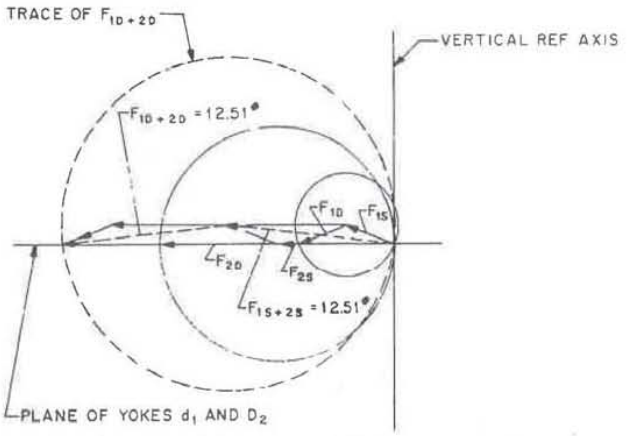


Fig. 43 — Vectorial solution for front shaft secondary couple forces

of F_2 is located 90 deg counterclockwise from the plane and sense of this angle. Therefore, the static force F_{2S} is also located in the same 90 deg counterclockwise position and the dynamic force F_{2D} of the same magnitude starts at the end of F_{2S}.

It is now possible to combine the static and dynamic vectors of forces arising from the two yokes on the front shaft to obtain the net effect of these forces on the support bearing. The first results to be shown are for the case of yokes d_1 and D_2 lying in the same plane (parallel phasing). This solution is shown in Fig. 43, where these yokes lie in the horizontal plane, which, is arbitrary. Since the angular setting of yoke d_1 relative to yoke D_2 does not alter the relationship of F_{1S} and F_{2S}, these vectors may be added without regard to yoke phasing. Thus, the resultant front shaft static force $F_{1S+2S} = 12.51$ lb.

In adding dynamic force vectors, phasing is important. The vector F_{1D} is angled downward and to the left from the end of F_{1S} to the point where the circular trace of F_1 intersects the plane of yoke d_1, which lies in the horizontal plane. Vector F_{2D} is directed horizontally to the left to the point where the circular trace of F_2 intersects the plane of yoke D_2, which lies in the horizontal plane. With the directions of the dynamic force vectors now sensed correctly, they can be added vectorially. Thus, the resultant front

American Axle v. Neapco - IPR2025-00091
PET_AAM_1012-0065

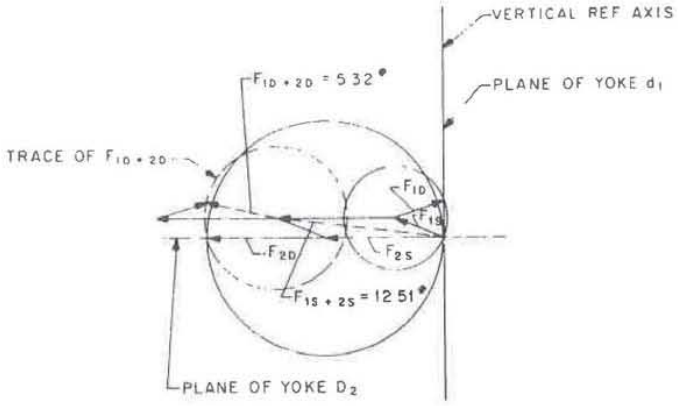


Fig. 44 — Vectorial solution for front shaft secondary couple forces

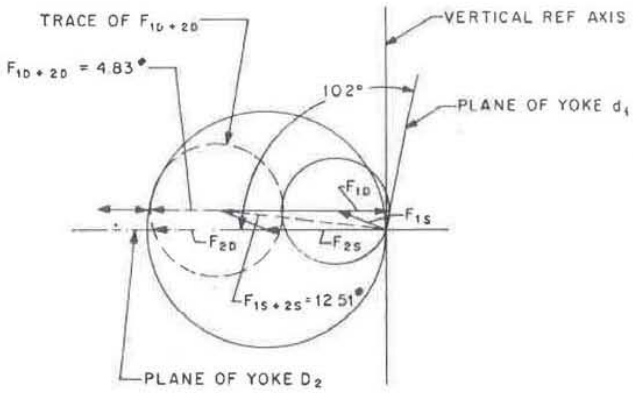


Fig. 45 — Vectorial solution for front shaft secondary couple forces

shaft dynamic force $F_{1D+2D} = 12.51$ lb and originates at the end of F_{1S+2S}.

Fig. 44 shows the net effect of the front shaft forces on the support bearing for yokes d_1 and D_2 at 90 deg (crossed phasing). F_{1S+2S} remains the same as before at 12.51 lb. The plane of yoke D_2 is maintained in the horizontal plane, while the plane of yoke d_1 is relocated to the vertical axis. Therefore, vector F_{2D} remains sensed horizontally to the left, but vector F_{1D} is angled upward and to the right from the end of F_{1S} to the point where the circular trace of F_1 intersects the plane of yoke d_1, which lies on the vertical axis. Thus, $F_{1D+2D} = 5.32$ lb and originates at the end of F_{1S+2S}.

If an absolute minimum vibrating force is desired, the yokes should be phased so that F_{1D} and F_{2D} are exactly opposite in sense. Fig. 45 shows the yoke phasing necessary in order to minimize the sum of these dynamic force vectors. F_{1S+2S} remains the same as before at 12.51 lb. The plane of yoke D_2 is maintained in the horizontal plane with vector F_{2D} sensed horizontally to the left. Therefore, the trace of F_1 must intersect the plane of yoke d_1 at a point horizontally to the right of the end of F_{1S}. With F_{1D} and F_{2D} now sensed at 180 deg to each other, the minimum $F_{1D+2D} = 4.83$ lb and originates at the end of F_{1S+2S}. The angle between yokes d_1 and D_2 is measured as 102 deg and is the phase angle required at the front shaft to obtain the minimum couple disturbance from this

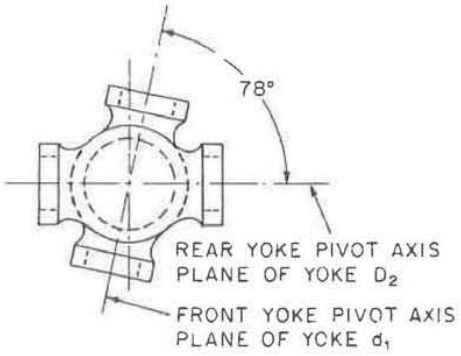


Fig. 46 — Front shaft yoke phasing

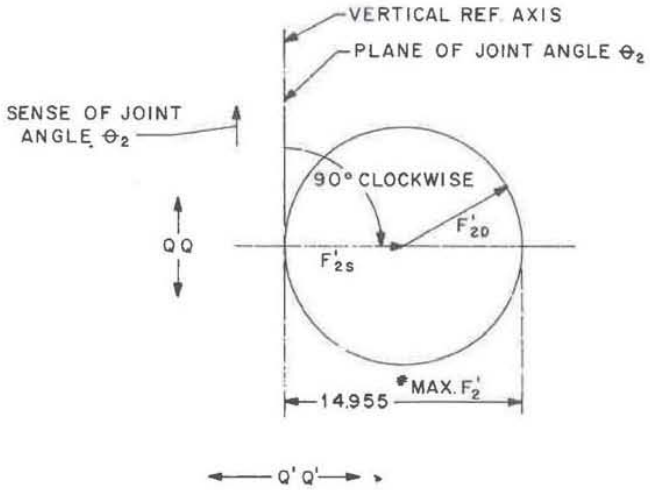


Fig. 47 — Secondary couple force vectors

shaft at the four-passenger load wide open throttle start condition. Fig. 46 shows this yoke phasing when the front shaft is viewed from the rear. The plane of the front yoke d_1 is 78 deg counterclockwise from the plane of the rear yoke D_2.

The influence of the rear shaft couples on the support bearing disturbance are determined vectorially applying the same methods used for the front shaft. Fig. 47 shows the trace of the force F_2' on the support bearing from the couple at yoke d_2. When viewing the rear shaft from the right or rear end in Fig. 40, the same vertical reference axis as before must be used, since the effects of the two shafts have to be considered in proper phase with each other in order to obtain the final net effect of both shafts. Obviously, the planes of yokes D_2 and d_2 must be at 90 deg to each other, and if Fig. 39 is reconsidered, it is evident that the couple force of D_2 acting at the support bearing is opposite to the couple force of d_2. Since joint angle θ_2 lies in the vertical plane, the maximum value of F_2' is located 90 deg clockwise from the plane and sense of this angle. Therefore, the static force F_{2S}' is also located in the same 90 deg clockwise position, and the dynamic force F_{2D}' of the same magnitude starts at the end of F_{2S}'.

American Axle v. Neapco - IPR2025-00091
PET_AAM_1012-0066

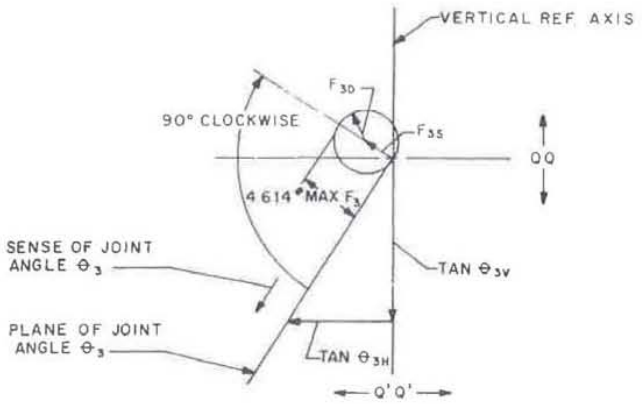


Fig. 48 — Secondary couple force vectors

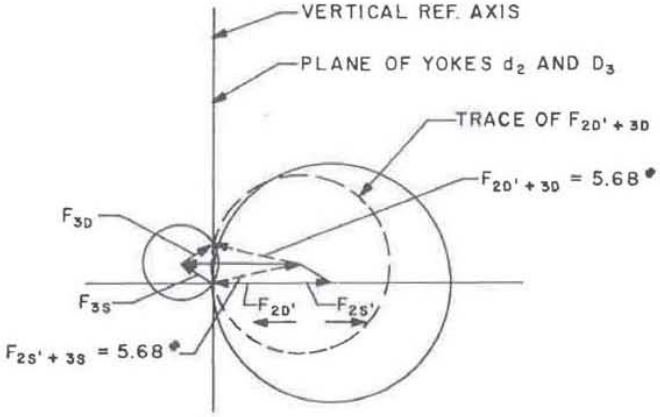


Fig. 49 — Vectorial solution for rear shaft secondary couple forces

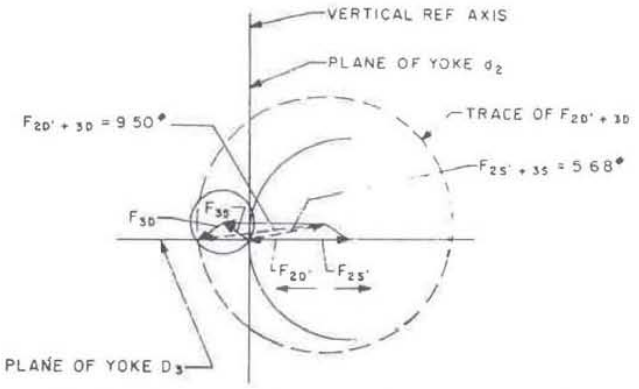


Fig. 50 — Vectorial solution for rear shaft secondary couple forces

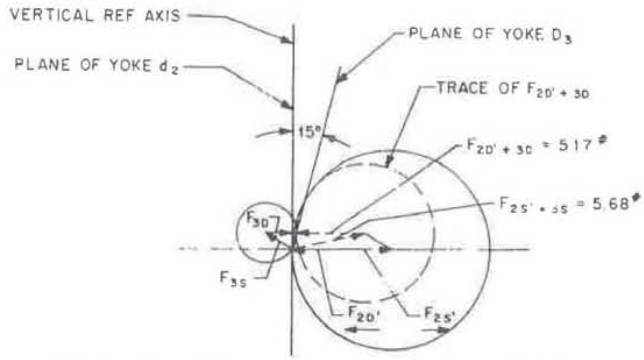


Fig. 51 — Vectorial solution for rear shaft secondary couple forces

Fig. 48 shows the trace of the force F_3 on the support bearing from the couple at yoke D_3. The same vertical reference axis as before must again be used here. As seen in Fig. 40, the plane and sense of joint angle θ_3 is located downward and to the left. As shown, the plane of this angle is determined by constructing the tangents of the side and top view component angles. The maximum value of F_3 is located 90 deg clockwise from the plane and sense of joint angle θ_3. Therefore, the static force F_{3S} is also located in the same 90 deg clockwise position and the dynamic force F_{3D} of the same magnitude starts at the end of F_{3S}.

The vectors for the rear shaft forces can now be combined in the same manner as the net front shaft forces were resolved. Fig. 49 shows the case of yokes d_2 and D_3 lying in the same plane (parallel phasing). Since the plane of yoke D_2 was maintained horizontal in Figs. 43-45, the plane of yoke d_2 and D_3 must be vertical in Fig. 49. The resultant rear shaft static force $F_{2S'+3S}$ = 5.68 lb and the resultant rear shaft dynamic force $F_{2D'+3D}$ = 5.68 lb.

Fig. 50 shows the net effect of the rear shaft forces on the support bearing for yokes d_2 and D_3 at 90 deg (crossed phasing). $F_{2S'+3S}$ remains the same as before at 5.68 lb. The plane of yoke d_2 is maintained on the vertical axis, while the plane of yoke D_3 is relocated to the horizontal plane and thus $F_{2D'+3D}$ increases to 9.50 lb.

Fig. 51 shows the yoke phasing necessary in order to minimize the sum of the dynamic force vectors. As before, $F_{2S'+3S}$ remains the same at 5.68 lb. The plane of yoke d_2 is maintained on the vertical axis with $F_{2D'}$ sensed horizontally to the left. Therefore, the trace of F_3 must intersect the plane of yoke D_3 at a point horizontally to the right of the end of F_{3S}. With $F_{2D'}$ and F_{3D} now sensed at 180 deg to each other, $F_{2D'+3D}$ is a minimum at 5.17 lb. The angle between yokes d_2 and D_3 is measured as 15 deg and is the phase angle required at the rear shaft to obtain the minimum couple disturbance from this shaft at the four-passenger load wide-open throttle start condition. Fig. 52 shows this yoke phasing when the rear shaft is viewed from the rear. The plane of the rear yoke D_3 is 15 deg clockwise from the plane of the front yoke d_2.

To obtain the combined effect on the support bearing of the couples from both shafts, the net front and rear shaft static and dynamic forces can be added vectorially in any phasing combination desired. The best combination for minimum resultant dynamic force would be from Figs. 45 and 51 and is shown in Fig. 53. The resultant static force F_{RS} = 7.40 lb. The resultant dynamic force F_{RD} = 10.00 lb and originates at the end of F_{RS}. (Since this is an illustrative problem, it should be noted that this value for the resultant dynamic force is generally too high to be acceptable in a passenger car as is shown in the section on *Secondary Couple Excitation*. Therefore, changes in the driveline geometry must be made in order to reduce this force.)

Since there is a possibility of confusion in setting yokes at odd

American Axle v. Neapco - IPR2025-00091
PET_AAM_1012-0067

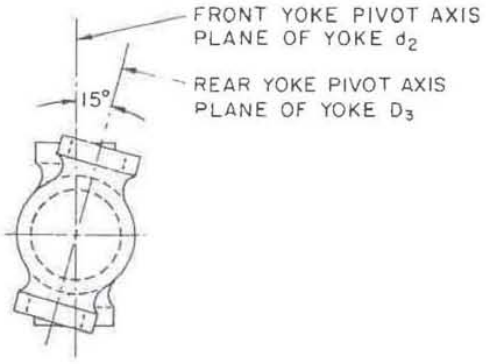


Fig. 52 — Rear shaft yoke phasing

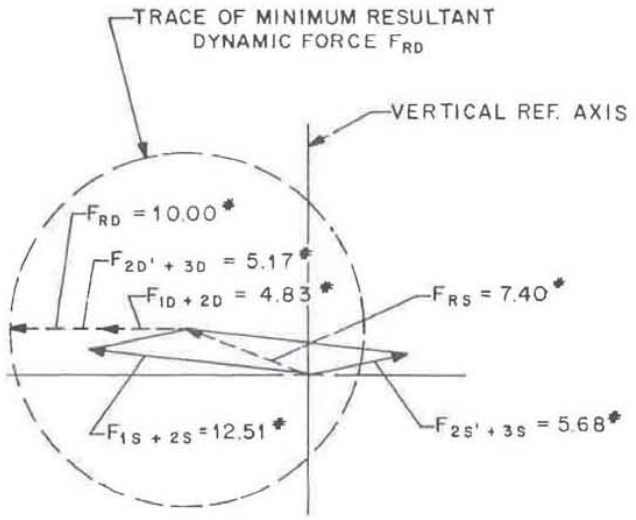


Fig. 53 — Vectorial solution for resultant static and dynamic forces

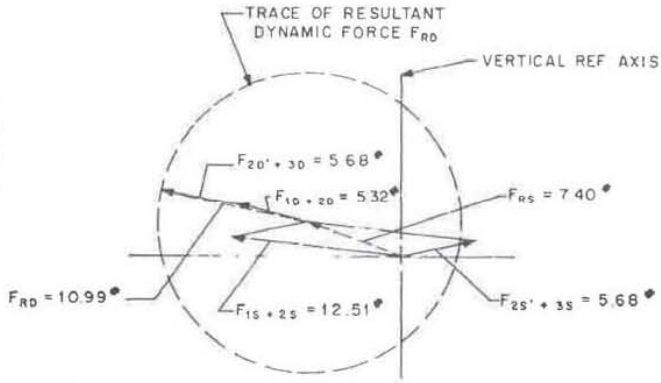


Fig. 54 — Vectorial solution for resultant static and dynamic forces

angles when the shafts are manufactured, it is of interest to know what percentage increase in disturbance might be expected if the yokes are placed at the nearest 90 deg setting to the optimum position. In studying Figs. 43, 44, 49, and 50, it is evident that the crossed (90 deg) phasing of the front shaft shown in Fig. 44 and the parallel phasing of the rear shaft shown in Fig. 49 would be the next most desirable arrangement. Fig. 54 shows the solution for this arrangement. F_{RS} remains at 7.40 lb and F_{RD} increases to 10.99 lb. Since the vibrating force increase is only 9.90%, it appears reasonable to accept the crossed-parallel phasing combination for the driveline at the drive condition studied.

Various other operating conditions must be analyzed by the preceding vectorial method to complete a study of the couple disturbance and finalize on the yoke phasing combination to be used. In order to achieve an acceptable low disturbance level, it may be necessary to make various adjustments in the driveline geometry including revised engine and pinion shaft angles. In addition, it may be necessary to substitute one or more constant velocity joints, such as double Cardan joints in place of Cardan joints. The use of a constant velocity joint may be especially required next to the sensitive support bearing in a three joint driveline for a passenger car application. The same procedure used in analyzing the couple forces on the support bearing can be applied, if desired, at the bearing supports on the transmission and pinion shaft ends of the driveline.

In order to accurately determine the couple forces acting on the supporting bearing structures, the dynamic operating condition of the drivetrain should be simulated with a computer program. High torque loads, when applied to the drivetrain, cause the various drivetrain components to shift to new positions from their initial static locations. The dynamic position of the drivetrain is needed if the true couple forces on the supports are to be predicted. Also, the true torsional and inertia equivalent angles can then be determined.

Excitation and Effects

The nonuniform angular motion characteristics of the Cardan joint produce fluctuating speeds and torques, which cause excitation in the driveshaft and its supporting members. This excitation can be classified generally into one of three basic types, each with its own distinctive characteristics and effect. The disturbances resulting from these different excitations can be identified by these characteristics and general maximum limits of allowable excitation established based upon experience in similar installations.

Torsional Excitation — The nonuniform velocity obtained when a Cardan joint operates at an angle produces a torsional vibration. In a driveline having two or more joints in series, it is desirable to have the individual joint angles arranged such that the net result produces uniform velocity characteristics over the system when optimum yoke phasing is employed. Since it is practically impossible to maintain the desired joint angles throughout the operating range, it is necessary to determine some maximum limit of torsional excitation which can be considered as generally acceptable. The effect of two or more joints operating in a driveline can be combined and expressed as an equivalent single joint angle called the *torsional equivalent angle*. The procedure for determining this equivalent angle of a driveline system was described previously.

The amplitude of torsional oscillation which can be accepted without causing excessive disturbance depends upon operating speed and characteristics of supporting structures and other units in the driveline and drivetrain system. It has been found that if this

American Axle v. Neapco - IPR2025-00091
PET_AAM_1012-0068

excitation is maintained under approximately 400 rad/s/s maximum angular acceleration in any continuous operating position and speed, the driveline is generally satisfactory in passenger car and most truck installations. This excitation level is equivalent to driving the system with a single joint at an angle not exceeding approximately 3 deg at 3600 rpm. Certain other highway as well as off-highway vehicles, agricultural equipment, power take-off, and stationary installations may tolerate other and generally higher levels of excitation. Fig. 9 shows the effect of rotational speed and joint angle on maximum angular acceleration and can be used in analyzing various driveline systems.

Excessive torsional excitation can be identified usually by the following characteristics:

A. Torsional vibration produces oscillating reaction torque on major supports. This vibration can excite the engine and transmission mounts and rear axle suspension supports especially through any resonant frequency of these mountings. The disturbance is usually frequency and torque sensitive. Often extreme peaks of disturbance will occur through a short speed range under specific loading conditions. This disturbance very often occurs under full drive or full coast where angles are more severe and deflected supporting mounts have their highest vibration transmitting characteristics.

B. The torsional fluctuation of the supporting shafts can cause load and unload cycles on the driving members. This characteristic tends to accentuate gear noises and clatter which otherwise may not be noticeable.

C. Rotating components not under load are often oscillated within their backlash limitations. This characteristic can be especially disturbing where these rotating members have a response frequency that corresponds with two cycles per revolution within the operating range.

Inertia Excitation — This excitation is produced by the oscillating torque loads resulting from the driveshaft inertia being accelerated through nonuniform motion. This condition exists in any driveshaft operating at a joint angle and exists even when torsional excitation is eliminated by exactly equal angles in a two-joint installation. The inertia of the intermediate member in a driveshaft produces fluctuating torque loads due to its changes in angular velocity. The level of torsional fluctuation depends upon the size of the joint angle and the inertia of the intermediate member. This type of fluctuation limits the size of the maximum joint angle which is acceptable in an installation.

It has been found that automotive vehicle installations are extremely sensitive to this type of excitation and to the disturbance it creates. Generally, for average passenger car and light-duty truck installations which have a relatively large driveshaft inertia, the acceptable excitation level must be kept under a maximum acceleration of approximately 1000 rad/s/s in any continuous operating position. This maximum acceleration is equivalent to operating the shaft with a single joint at an angle not exceeding approximately 4¾ deg at 3600 rpm. A long one-piece, two-joint driveline generally falls into this class of installation. Where the driveshaft inertia is relatively small, as is the case often in many multipiece truck driveline systems, the maximum acceleration can be increased to 2000 rad/s/s for reasonable limits of excitation from the inertia on nonrotating members. This maximum acceleration is equivalent to an angle not exceeding approximately 8 deg at 3000 rpm.

Extremely short, small diameter driveshafts used in some truck applications allow this increased acceleration, due to the relatively small inertia of the driveshaft. Certain other highway as well as off-highway vehicles, agricultural equipment, power take-off, and stationary installations may tolerate other and generally higher levels of excitation. Fig. 9 can be referred to when analyzing inertia problems in drivelines. Also, the procedure for determining the *inertia equivalent angles* of a driveline system was described previously.

In multipiece shaft installations, it is possible to arrange the joint angles in the system with proper yoke phasing so that the acceleration of the shafts are in phase opposition to each other and reduce the effect on the over-all system. This type of arrangement can allow the use of larger joint angles for those applications where cancellation can be achieved. The typical three-joint installation in an automotive vehicle generally does not allow full advantage of this cancellation due to the joint angle arrangement and yoke phasing required to cancel or reduce secondary couple forces at the shaft support bearing.

Inertia excitation usually produces disturbances in the unloaded or very lightly loaded drive condition. The effects are quite similar to that of torsional excitation except usually being identified with unloaded operating conditions. This excitation shows up most often during a float down condition. Under these light loads, components in the driving system are allowed to reverse and clatter through their backlash and clearance limitations. The resulting disturbance is usually extremely disturbing due to the generally low noise level of the operating condition where inertia excitation occurs. Since response characteristics of the vehicle must resonate the inertia excitation, the disturbance is frequency sensitive.

Secondary Couple Excitation—The *secondary couple* is a bending moment which results from a Cardan joint transmitting torque at an angle. In a driveline, the secondary couples react on both the supporting structures and the intermediate shaft or shafts. They can produce an effect like critical speed by shaking the supports twice per revolution. The vibration of the supports can cause a response of the driveline itself at one-half of the frequency where a normal critical speed would occur. The couple effect on the intermediate shaft or shafts is a one per revolution excitation and only adds to other one per revolution effects such as unbalance. The couple effect is also evident in joint assemblies having end clearance in the bearings. Here, the yokes are forced back and forth endwise on the cross trunnions by the couple force at a cyclic frequency of once per revolution.

Support response itself can be a major cause of disturbance. Disturbances resulting from the couple force reactions will usually occur during some frequency response range and increase directly with the transmitted torque. Shaft support bearings of multipiece drivelines for automotive vehicles are quite critical to this excitation. The couple forces will excite this support bearing when the driveline is rotating at a speed equivalent to one-half of the support bearing natural frequency. A low frequency, low damping support bearing required to produce good isolation at

American Axle v. Neapco - IPR2025-00091
PET_AAM_1012-0069

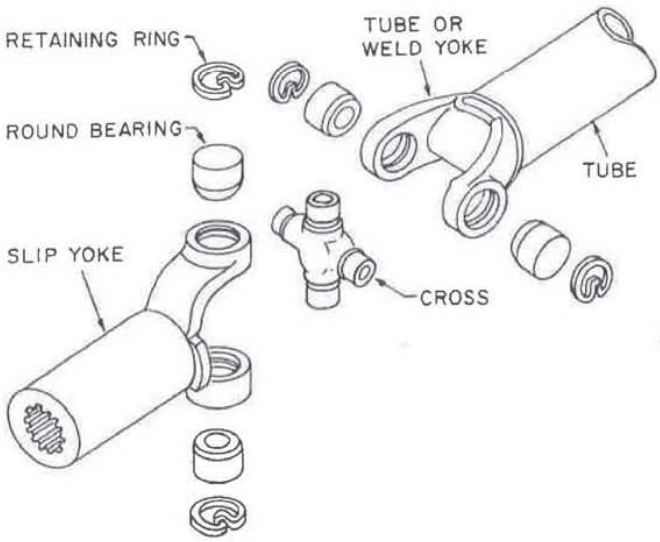


Fig. 55 — Cardan universal joint

high speeds will often respond to these couple forces at low speeds. Support bearings of this type usually have a critical or natural frequency of 1000 to 2000 cpm and, therefore, they will be excited at 500 to 1000 rpm driveline speed.

Experience in driveline installations having shaft support bearings has shown that the dynamic or rotating couple force should be maintained under a certain maximum value in order to prevent an objectionable shudder-type of vibration. In Table 1 are shown the limits on the oscillating force, which have been found to be generally acceptable at maximum transmitted torque. These rotating couple forces act twice per driveshaft revolution on the shaft support bearing.

Table 1 — Maximum Dynamic Couple Forces

Installation	Maximum Dynamic (Rotating) Couple Force, Pounds
Passenger Cars	8
Light-Duty Trucks	15
Medium-Duty Trucks	25
Heavy-Duty Trucks	75

A shaft support bearing must be studied primarily to obtain acceptable cancellation. The procedure for determining the secondary couple forces on the support bearing was shown previously in an illustrative problem. Since these forces are torque and rear suspension jounce (or load) sensitive, the wide open throttle start condition of the driveline is generally most important.

Design

The various components of a typical Cardan joint, shown in an exploded view in Fig. 55, must be designed to provide the necessary joint angularity, strength, and life requirements for a given application. In a typical Cardan joint, the yoke is the basic torque and motion input and output member with drivable means

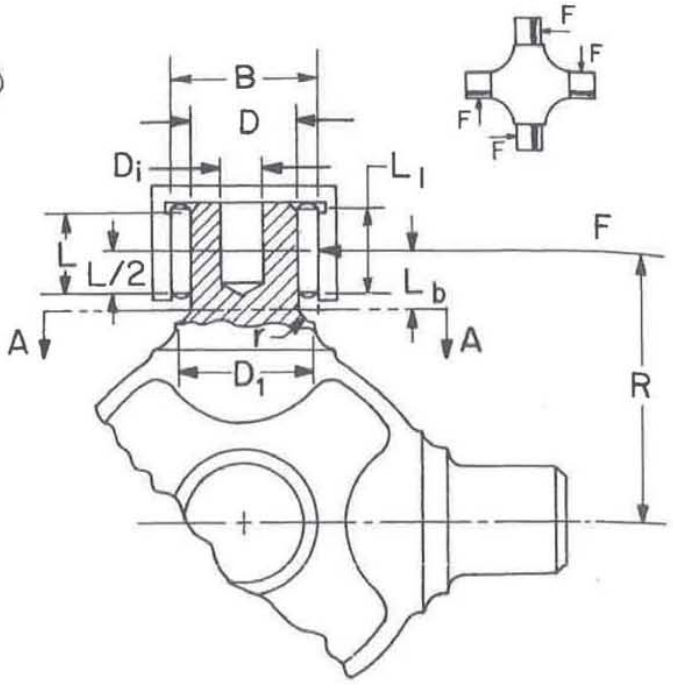


Fig. 56 — Needle roller bearing and cross trunnion

of attachment, while the cross is the intermediate drive member which has four equally spaced trunnions in the same plane. The ultimate strength of the joint must be safely in excess of the maximum applied torque which can be developed by various loading modes discussed in the chapter on *Basic Driveline Requirements*. The ultimate strength is the maximum applied torque at which failure of any of the joint's components will occur.

Initially, a tentative bearing size with a given number of needle rollers, as the rolling elements, must be determined. The bearing configuration must have the dynamic capacity to transmit power for a required period of time at various torques, speeds, and joint angles. Generally, this tentative bearing size selection is determined by analytical means. In the section on *Rating Procedure and Joint Size Selection*, a method is shown for determining this dynamic capacity. In addition, the desired yoke ear, cross trunnion, and bearing seal configuration must be assumed. If the components can be assembled with ease, it is then possible to proceed with other computations and design procedures.

Fig. 56 shows a cross sectional view of the assumed needle roller bearing and cross trunnion. The bearing is acted upon by the torque couple force F which is assumed to be concentrated at the centroid of the projected bearing area on the cross trunnion, formed by the trunnion diameter D and the effective length L of the needle rollers. For a given torque T acting on the joint, the torque couple force is:

$$F = \frac{T}{2R}$$

American Axle v. Neapco - IPR2025-00091
PET_AAM_1012-0070

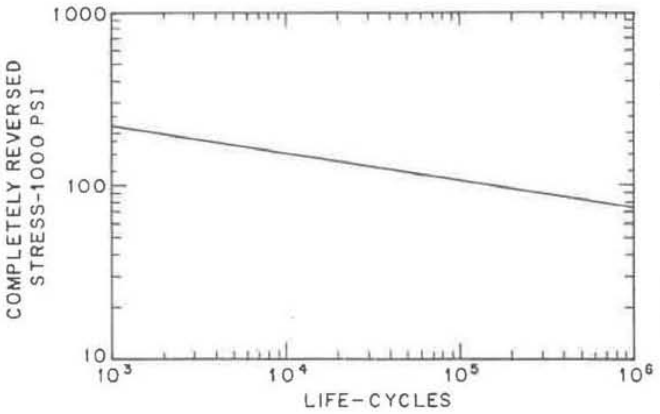


Fig. 57 — S-N curve for cross

where:

T = Torque, lb-in

R = Torque radius, in

F = Torque couple force, lb

When the joint is operated at a zero degree joint angle and has equal length torque radii in both driving and driven yokes, the two pairs of couple forces are equal and opposed. The bending strength of the cross trunnion at section A-A due to the torque couple force can be determined. Section A-A is assumed at the tangent point of the fillet radius, r, with the trunnion or journal diameter, D. If the cross has one or more stepped diameters such as D_1 with blending fillet radii connecting the trunnion to the body, these sections also must be analyzed for strength. The fillet radii act as points of stress concentration and, therefore, must be considered in the design of the cross. The nominal bending stress at section A-A has a maximum value at the outermost fiber and is:

$$S_b = \frac{FL_b}{Z}$$

where:

L = Bending moment arm, in

Z = Area section modulus, in^3

For a round solid section, the section modulus is:

$$Z = \frac{\pi D^3}{32}$$

where:

D = Trunnion diameter, in

However, some cross trunnions have lubrication reservoirs or holes which extend below the trunnion area into the center of the body. For this hollow section trunnion configuration, the section modulus is:

$$Z = \frac{\pi}{32} \frac{(D^4 - D_i^4)}{D}$$

where:

D_i = Inside diameter of trunnion, in

The nominal bending stress applies to a trunnion without a point of stress concentration or a stress raiser. When a trunnion with a stress raiser is considered, the maximum or effective stress S_b' is affected by the geometric or theoretical stress concentration factor K_t and is expressed as follows for a solid section trunnion:

$$S_b' = K_t S_b = \frac{K_t FL}{Z} = \frac{32 K_t FL}{\pi D^3}$$

Therefore, it is possible to compute the maximum or effective stress from static ultimate and yield torque test data for a given cross trunnion. This limiting stress value can then be used with sufficient accuracy to predict the strength of other cross designs which have the same material and heat treatment as well as similar geometric configurations. *Appendix D* shows values of K_t for various shoulder fillet radii. In the case of the hollow section trunnion, consideration must also be given to the machining and heat treatment effects in the hole on the overall value of K_t.

For a carburized and hardened cross trunnion, a typical ultimate bending stress of 220 000 psi, which includes the effect of the shoulder fillet stress concentration factor, can be used in estimating the required trunnion size. Also, it is possible to predict the fatigue life of a cross at various stress levels with the use of an S-N curve. Fig. 57 shows such a typical curve based on B_{10} fatigue test data for fully reversed bending of a carburized and hardened cross where failures were concentrated in the area of the critical trunnion fillet radius, which represented a given theoretical stress concentration factor.

When the ultimate strength of the cross trunnion is determined, it is possible to finalize the tentative bearing design. The basic bearing design can be either the full complement needle roller or the caged needle roller type as shown in Fig. 58. The commonly used full complement needle roller bearing has proven more successful in the smaller joint sizes, while the caged needle roller bearing has been used to some degree in the larger joint sizes for severe service. Also, in certain very lightly loaded and very slow speed applications, such as steering shafts, no needle rollers have been used at all in the bearings of some joints.

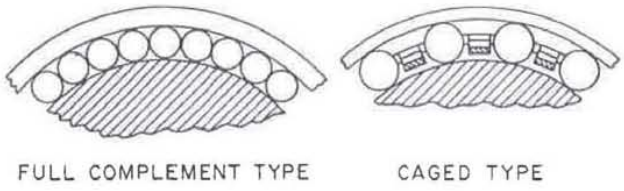


Fig. 58 — Needle roller bearing types

American Axle v. Neapco - IPR2025-00091
PET_AAM_1012-0071

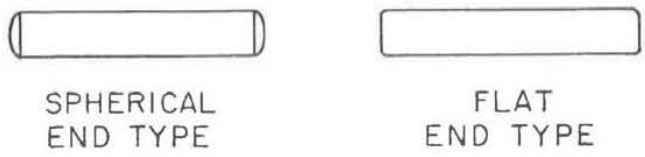


Fig. 59 — Full complement bearing needle roller types

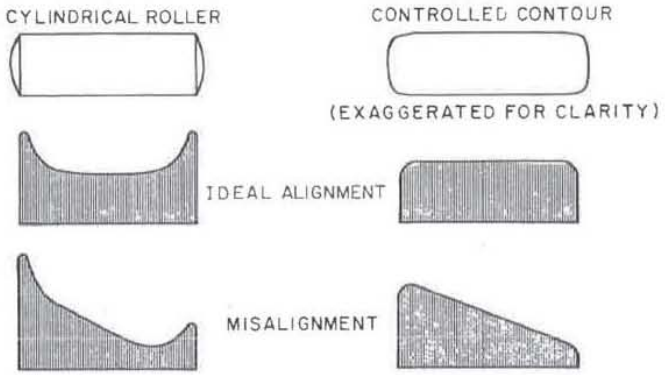


Fig. 60 — Cylindrical and controlled contour needle rollers with comparative contact stress patterns

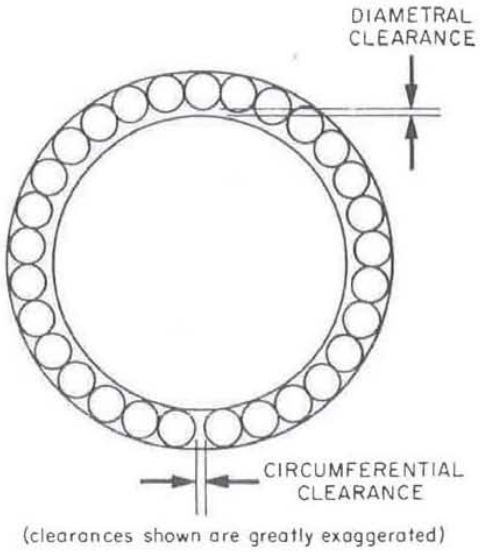


Fig. 61 — Circumferential and diametral clearances for a full complement needle roller bearing

Both the spherical end rollers and the flat end rollers shown in Fig. 59 have been generally used in full complement bearings. The spherical end type has been most widely used and is the most economical type. The flat end type of roller provides the maximum effective contact length for a given roller length.

In the case of the spherical end roller, it can be made as a cylindrical roller or as a controlled contour or relieved end roller as shown in Fig. 60. Also shown in this figure are the comparative contact stress patterns for ideal bearing alignment and for a misaligned bearing when the mating bearing raceways in the bearing cup and on the cross trunnion are cylindrical. It has been found that bearing life can be extended when using relieved end rollers because the stress concentrations at the roller ends are decreased as shown in Fig. 60. The effects of manufacturing inaccuracies or misalignment caused by deflections due to the transmitted torque are minimized. The use of a crowned raceway in the bearing cup, or on the cross trunnion, or on both components with cylindrical rollers, has also proven beneficial for much the same reasons.

With regard to needle roller proportions, the length-to-diameter ratio generally has been in the relatively wide range of 3.50 to 8.50. The minimum permissible diameter of the roller is determined by its compressive strength value. In passenger car applications rollers as small as 0.0625 in diameter have been successfully used, while in heavy-duty truck applications, rollers as large as 0.125 in diameter or larger are employed. The roller length can vary considerably in the different bearing designs. Theoretically, universal joint capacity increases with roller length, suggesting that as long a roller as possible should be used. However, practical limitations are imposed by cross and yoke deflections and by bearing clearances employed. These clearances will affect the skewing tendency of the rollers which can result in bending forces imposed on them and lead to subsequent roller failure.

For a full complement needle roller bearing, the circumferential and diametral clearances are shown in Fig. 61. Certain minimum values are desirable for optimum bearing life. For passenger car applications, a total minimum circumferential clearance (c.c.) of 0.0012 in is generally recommended to obtain the ultimate in needle roller guidance. Since the bearing motion is oscillatory, the diametral clearance (d.c.) can also be quite small. The usual recommended minimum diametral clearance is 0.0001 in. *Appendix C* illustrates a bearing computation procedure using typical automotive Cardan joint component dimensional tolerances and minimum bearing clearances. The total dimensional tolerances for the cross trunnion diameter and bearing cup bore are 0.001 in and for the needle roller diameter it is 0.0002 in. These tolerances were selected because of economic factors. The computed results show a wide variation of circumferential and diametral clearances, and therefore, a wide variation in test results may be possible. For larger size joints or those used in applications other than automotive drivelines, usually higher minimum clearance values as well as larger component tolerances may be used. Other dimensional features of the cross trunnion and bearing cup bore, such as taper and out-of-roundness within the operating length of the rollers, must be controlled within given limits, otherwise bearing life can be impaired.

After the dimensions and tolerances of a tentative bearing design have been selected and computed, it is possible to proceed with a computation of the Hertz contact stresses between the needle rollers and cross trunnion, and between the rollers and the bearing cup bore. In Fig. 56 is shown a needle roller bearing and

American Axle v. Neapco - IPR2025-00091
PET_AAM_1012-0072

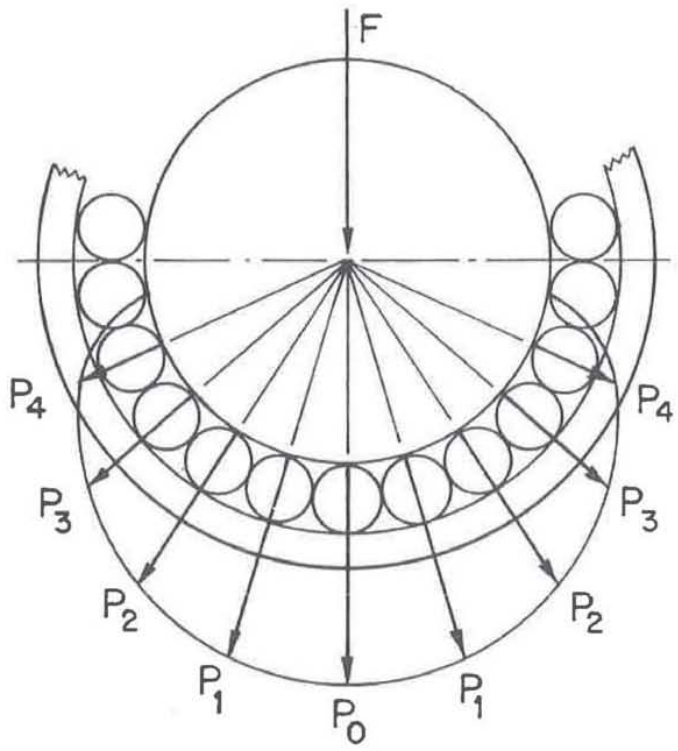


Fig. 62 — Needle roller radial load distribution

cross trunnion with the torque couple force F acting at the centroid of the projected bearing area on the cross trunnion. This couple force is assumed to be a pure radial load and when applied to the needle roller bearing it is not evenly distributed on all the rollers as shown in Fig. 62. With the rollers assumed to be positioned as shown, and the torque couple force F applied at the center of the trunnion, the individual radial forces at the rollers are as indicated. In this bearing design, it is assumed that some radial clearance exists. Therefore, the individual radial forces range from a maximum value directly under the applied load to a zero value at some angle less than 90 deg on either side. In the remaining arc of the bearing, the rollers are completely unloaded. The force at the highest loaded roller can be computed with the following load distribution equation:

$$P_o = \frac{5.00F}{n}$$

where:

P_o = Force on highest loaded needle roller, lb

F = Torque couple force, lb

n = Number of needle rollers per bearing

5.00 = Constant for needle roller bearing with radial play or clearance. When a needle roller bearing has zero radial clearance, the constant is 4.08 (per Stribeck and Palmgren)

Following computation of the force on the highest loaded needle roller at maximum torque, it is possible to determine the Hertz contact or mean compressive stress between this roller and the trunnion with Eq. A-22 shown in *Appendix A*. For convenience, this equation can be expressed in terms of the diameters rather than the radii as follows:

$$S_m = 2464\sqrt{\frac{P_o}{L}\left(\frac{1}{d}+\frac{1}{D}\right)}$$

where:

S_m = Mean surface compressive (Hertz contact) stress, psi

P_o = Force on highest loaded needle roller, lb

L = Effective needle roller length on cross trunnion, in

d = Needle roller diameter, in

D = Cross trunnion diameter, in

The Hertz contact stress between the roller and the bearing cup bore can be computed with the following equation:

$$S_m = 2464\sqrt{\frac{P_o}{L_1}\left(\frac{1}{d}-\frac{1}{B}\right)}$$

where:

L_1 = Effective needle roller length on bearing cup bore, in

B = Bearing cup bore diameter, in

It is also possible to compute the contact stress between the roller and trunnion with the following approximate equation:

$$S_m = 2220\sqrt{\frac{T}{BF}}$$

where:

T = Torque, lb-in

BF = Bearing Factor (This factor is defined in the section on *Rating Procedure and Joint Size Selection*. Also, the constant of 5.00 for the load distribution equation is assumed to apply).

In most Cardan joint bearing designs, the contact stress between the roller and trunnion is higher than between the roller and bearing cup bore. The allowable limits of the mean contact stress at the maximum applied torque are discussed in detail in *Appendix A*. At normal operating load conditions much lower stresses must be employed.

American Axle v. Neapco - IPR2025-00091
PET_AAM_1012-0073

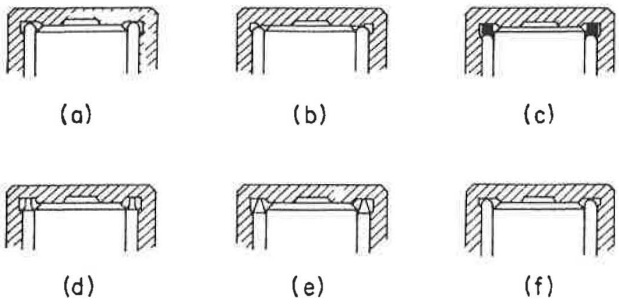


Fig. 63 — Bearing cup grind relief, trunnion chamfer and needle roller end design features

Bearing life is also affected by the surface finish used on the cross trunnion and bearing cup bore. Typical maximum roughness height values used on the cross trunnion and bearing cup bore are 30 and 35μ in (arithmetical average), respectively, where these finishes are based principally on economic considerations. A finer finish means better bearing performance, and insofar as it diminishes the progress of fretting corrosion, results in longer bearing life.

To take full advantage of the relatively high radial load capacity of needle rollers, the bearing components must be made of the proper materials, as discussed in the following section on *Materials Selection*, and have optimum metallurgical structures. The surface hardness, case hardness gradient, and core hardness range of the cross trunnion and bearing cup bore must be adequate as indicated in *Appendix A*.

Another characteristic which can add significantly to bearing life is precession. This term, as used in universal joint oscillatory bearing teminology, describes a condition where the rollers continually change position with respect to the bearing cup bore and the cross trunnion so that the raceway wear condition appears to be similar to that found in rotating bearings. Unfortunately, at this state of the art, it is not known how to design this desirable feature into an oscillatory bearing with any degree of reliability.

Also contributing significantly to bearing life, are the use of proper design techniques in the area of the bearing configuration containing the cup bore grind relief and the trunnion chamfer as shown in Fig. 63. In good bearing design, it is desirable that the cylindrical portion of the raceway in the cup bore and on the trunnion be greater than the effective roller length. If the cylindrical portion of the roller overhangs the grind relief in the cup or the chamfer on the trunnion, as shown in Fig. 63 (a), roller stress concentrations will occur which can cause premature bearing failure. This potential source of failure can be circumvented by maintaining minimum grind relief and chamfer length, as shown in Fig. 63 (b), or by employing a steel or plastic thrust washer in the bottom of the cup as shown in Fig. 63 (c). The thrust washer prevents the roller from contacting the grind relief or chamfer edges. Other design innovations which can prevent premature bearing failure are the crankpin end rollers shown in Fig. 63 (d), the conical end rollers shown in Fig. 63 (e), or the ball end rollers shown in Fig. 63 (f).

An additional important factor contributing to optimum bearing life is the provision of an adequate sealing means for the bearing. The principal function of the bearing seal is to prevent the escape of lubricating fluid from or entry of foreign matter into the bearing. In addition, the bearing seal which is a flexible member must be capable of operating under varying environmental conditions at various speeds, joint angles, and its design depends on joint usage. When moisture gets into the bearing and mixes with the products formed by normal lubricant breakdown, corrosive compounds can develop that will react on all surfaces. Often a joint failure which was initially attributed to bearing malfunction would upon closer examination point to acid corrosion as the contributing or primary cause. Corrosion in areas other than the bearing raceways is indicative of seal, rather than bearing failure.

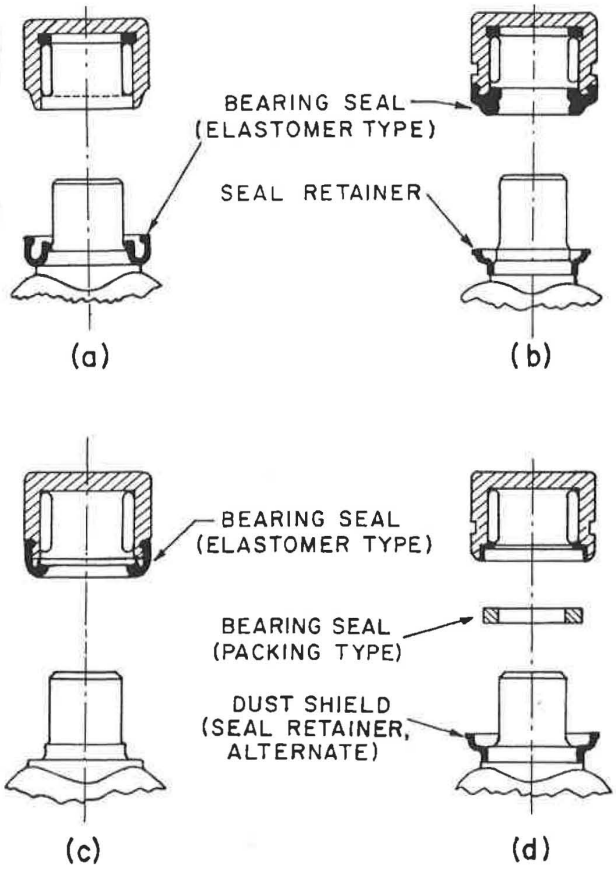


Fig. 64 — Typical bearing seal types

The typical bearing seal is generally of the elastomer or packing types as illustrated in Fig. 64. These seal types can be further classified as to venting or purging and nonventing or nonpurging types. The elastomer type seals shown in Fig. 64 (a) and (b) are typical of the nonventing types and are, therefore, generally used in joints which are lubricated for life. A lubrication fitting or plug cannot be used with the nonventing type seal and can only be used, if desired, with the venting type elastomer seal illustrated in Fig. 64 (c). The packing type seal, which is nonventing, is illustrated in Fig. 64 (d).

Another type of elastomeric seal shown in Fig. 3 (b) is a boot seal. In certain applications, this seal is used to enclose the entire joint.

American Axle v. Neapco - IPR2025-00091
PET_AAM_1012-0074

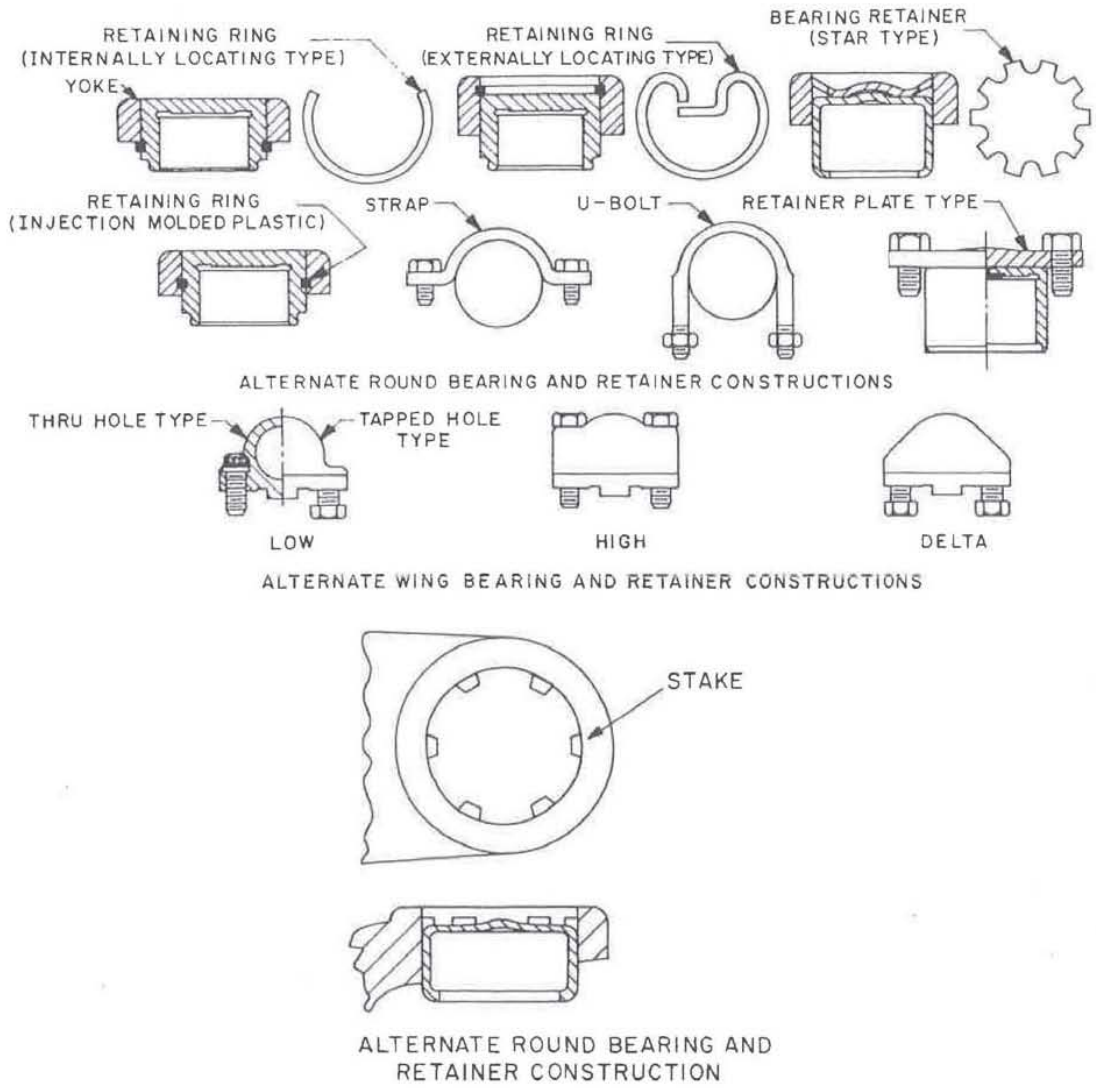


Fig. 65 — Typical bearing and retainer types

Bearing life is further influenced by the bearing retention means employed. Misalignment of the bearing cup with respect to the cross and end clearance between the cross and bearing cup thrust surfaces must be controlled to close tolerances to prevent premature bearing failure or unsatisfactory functioning of the joint. Also, if the fit between component parts is too tight, detrimental results will occur. Therefore, proper design of the bearing retention means is quite important. Fig. 65 shows the various types of typical bearing and retainer constructions.

In the design of a typical yoke, preliminary strength computations can be made. In general, the design of the yoke ears require special attention. These yoke ears are the projecting members of a yoke which must resist the torque couple forces applied at the joint bearings. The cross sections of the ears vary in size and shape from the bearing cross holes to the yoke body.

A typical section of the ear is subjected to both bending and torsional moments. Therefore, the combined stresses at various sections should be computed and analyzed. Together with experience factors and test results, the ears can be designed and proportioned for adequate strength. Since manual computations at numerous sections are tedious and time consuming, a computer stress and deflection analysis procedure using the finite element method can be readily applied to complex shaped components such as yokes.

The important load-deflection characteristics of the Cardan joint components and their effects on bearing life are often overlooked. The yoke ears will deflect due to the applied torque and the centrifugal force effects caused by the high rotational speeds. For adequate bearing life, it is highly desirable to provide for *balanced* yoke and cross deflection under torque loads so that the needle rollers will not be pinched at either end, but are uniformly loaded along their active length as shown in Fig. 66. This deflection characteristic can be accomplished by proper proportioning of the yoke ear and cross trunnion sections through the use of

American Axle v. Neapco - IPR2025-00091
PET_AAM_1012-0075

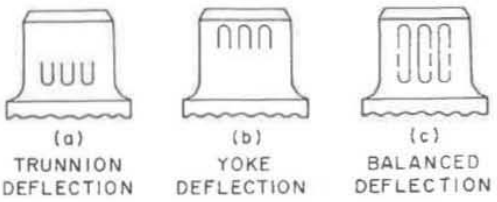


Fig. 66 — Deflection characteristics

mathematical procedures, but generally the solution can best be obtained by practical design experience and by analysis of test results.

When the trunnion in a bearing design is relatively small and the rollers are large in diameter, the trunnion is the weaker member and the rollers are loaded at the radially inner end as shown in Fig. 66 (a). The incorporation of smaller diameter rollers allows the use of a larger diameter and, hence, stiffer trunnion in the same space. This design procedure reduces the trunnion deflection. If the yoke is the weaker member, roller end loading can also result, but at the radially outer end as shown in Fig. 66 (b). When the deflections of both the cross trunnion and the yoke ear are *balanced*, the ideal loading condition shown in Fig. 66 (c) exists and results in improved bearing life.

Fig. 67 shows schematically the deflections of the cross trunnions and yoke ears due to the applied torque load. In using an approximate mathematical procedure for determining the deflection characteristics, basic deflection equations can be used. After computing the trunnion deflection, computations can be made at various sections of the ear to determine if the torsional rigidity at its weakest section is such so as to allow it to deflect with the trunnion and thereby not induce an additional twisting couple into the ear. This loading characteristic would occur if the ear were stiffer than necessary.

Since the joint may operate at substantial rotational speeds in certain applications, the yoke ears will also deflect radially outward due to centrifugal force effects acting on the ears and bearing cups as shown schematically in Fig. 68. This radial deflection characteristic results in increased end clearance between the cross trunnion and bearing cup thrust surfaces and can cause the driveshaft attached to the joint to rotate off its rotational center. The skewed thrust surfaces of the trunnion and bearing cup, combined with the centrifugal force, can produce galling-type failures on these surfaces. This type of failure generally does not occur in joints used in the smaller lightweight driveshafts. In large heavy-duty driveshafts, however, this condition can readily occur in improperly designed joints. In some heavy-duty joints, a trunnion thrust washer between the trunnion and bearing cup thrust surfaces may be necessary to withstand the centrifugal force and eliminate galling.

In the extremely wide variety of Cardan joint applications, the yokes assume numerous constructions. The detail design of each yoke is therefore dependent upon these applications, but in many instances, existing yokes are used if possible for economic and standardization considerations.

Yokes must be designed to permit the joint to operate at the maximum required joint angle. In addition, some joints such as in certain agricultural implement driveshafts and as steering shafts in vehicle tilt cabs, must have a hinge capability as high as approximately 90 deg, even though rotational operation is not encountered at this high an angle.

Fig. 65 shows typical bearing and retainer type constructions which can be incorporated in the yoke ear designs. Commonly used yoke constructions are the slip yoke, tube or weld yoke, end

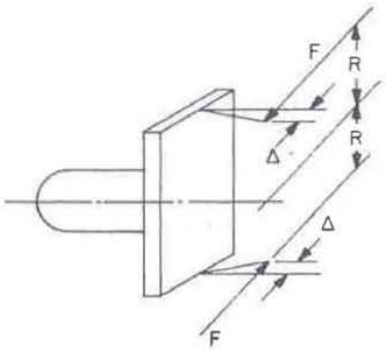


Fig. 67 — Yoke deflection due to torque

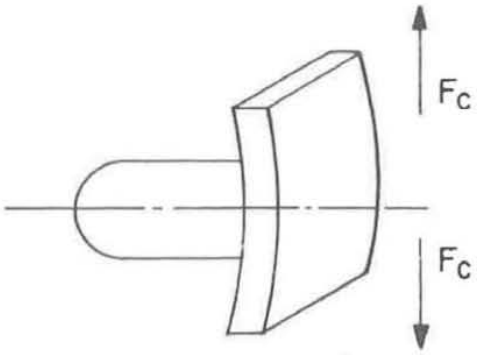


Fig. 68 — Yoke deflection due to centrifugal force

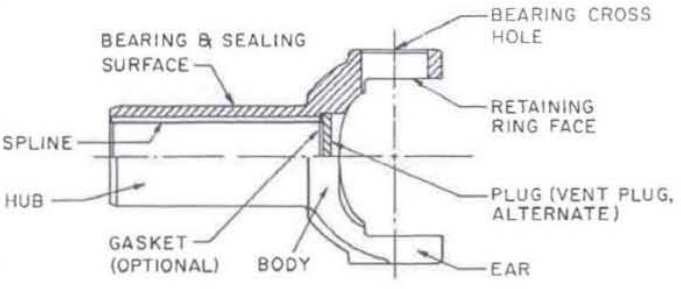


Fig. 69 — Slip yoke (internal splined type)

American Axle v. Neapco - IPR2025-00091
PET_AAM_1012-0076

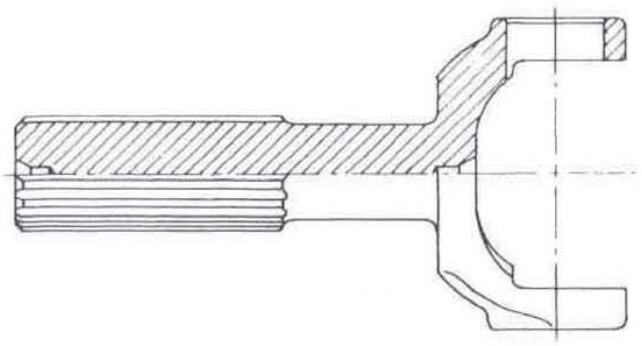


Fig. 70 — Slip yoke (external splined type)

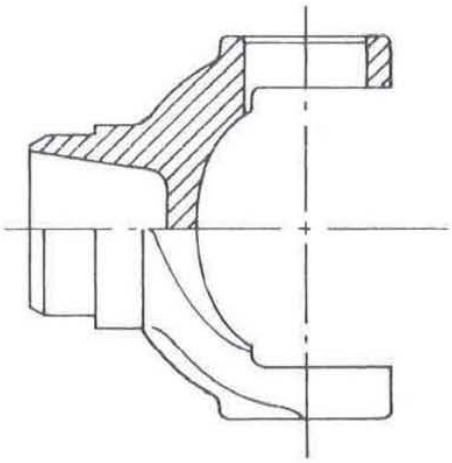


Fig. 71 — Tube or weld yoke

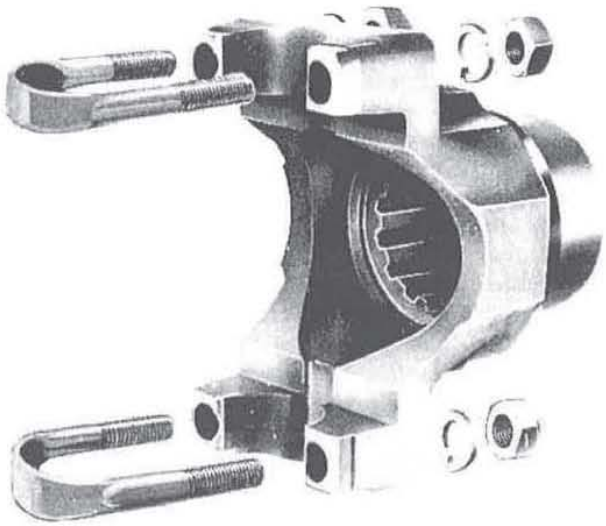


Fig. 72 — End yoke (U-bolt type)

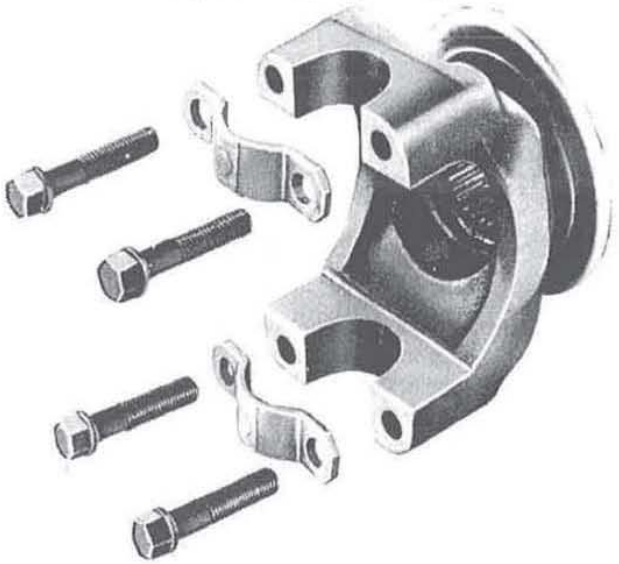


Fig. 73 — End yoke (strap type)

yoke, and flange yoke.

The slip yoke is a yoke which accommodates axial movement. It has a hub attached to the yoke body and is shown in Fig. 69 with appropriate descriptive nomenclature. The hub usually has an outer ground bearing and sealing surface and internal spline with the body end of the hub closed by a plug. The chapter on *Splines and Axial Motion Devices* discusses types of splines suitable for a slip yoke. The hub length and diameters required depend on the application and the transmitted torque. This length consists of the desired average engaged spline length plus the total spline travel required by the vehicle driveline. In passenger car and light-duty truck applications, the ratio of the average engaged spline length to the spline pitch diameter has been in the typical range of 2.25 to 2.75. The total spline travel includes not only the spline movement due to suspension motion and pinion windup or winddown, but also the build or assembly tolerance. An additional hub length may also be required to accommodate a counterbore which is used as an internal sealing surface in some applications, and a vented plug will, therefore, be necessary in place of a solid plug.

In some applications, especially in multishaft arrangements, a slip yoke is used having a solid hub or shaft with external spline as shown in Fig. 70. In passenger car and light-duty truck applications, the ratio of the average engaged spline length to the spline pitch diameter of this yoke has been in the typical range of 2 to 3. In slower speed applications, this ratio has been smaller.

The tube or weld yoke is a yoke with a piloting hub for attachment to a tube and is shown in Fig. 71. The pilot diameter of this hub supports the tube, and in order to obtain adequate fatigue life of the typical circumferential arc welded tube and yoke connection, the length and press fit of the pilot must be optimized. This optimum length is usually developed by experience and fatigue testing. If the tube is attached to the yoke by means other than welding, different or additional design considerations will have to be incorporated.

The end yoke is a yoke which attaches a driveshaft to another drivetrain component. It assumes numerous constructions with the specific design being dependent to a large degree on the application requirement. In passenger car and truck applications, the relatively short hub generally has an outer ground sealing surface and internal spline. The spline is of the interference fit or zero backlash type and the chapter on *Splines and Axial Motion*

American Axle v. Neapco - IPR2025-00091
PET_AAM_1012-0077

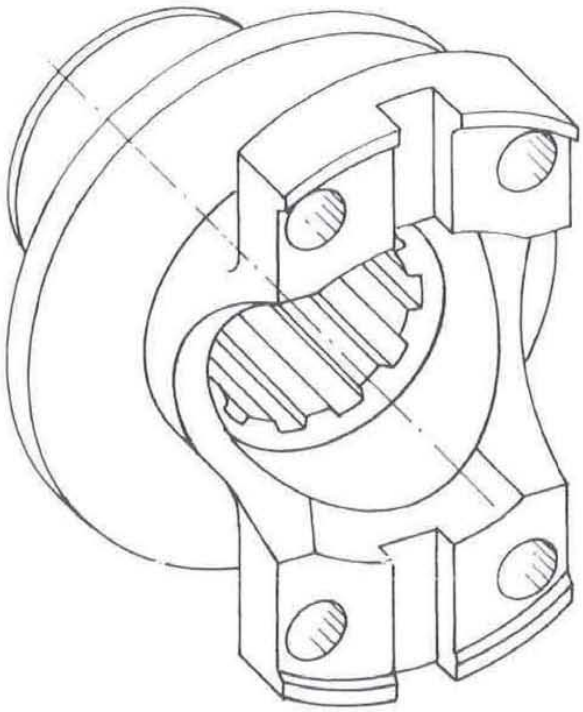


Fig. 74 — End yoke (wing bearing type)



Fig. 75 — End yoke (quick-disconnect type)

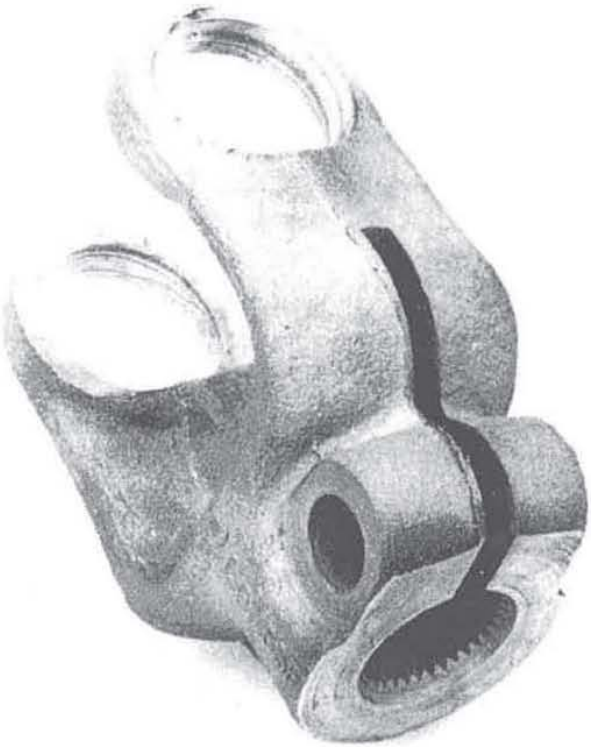


Fig. 76 — End yoke (clamp bolt type)

Devices discusses types of spline suitable for this yoke. The ratio of the engaged spline length to the spline pitch diameter has been in the typical range of 0.80 to 1.10.

The U-bolt and strap type end yoke constructions with a splined hole in the hub and using round bearings, shown in Figs. 72 and 73 respectively, are commonly used in passenger car and light-duty truck applications. The wing bearing type construction with a splined hole, shown in Fig. 74, is commonly used in heavy-duty trucks and off-highway vehicles. In all of these applications, the yoke is usually retained with a nut or bolt and washer at the splined connection when attached to another driveline or drive-train component. The thread size of these fasteners, as well as for the U-bolt, bolt, or cap screw fasteners, retaining the round or wing bearings to the yokes must be of sufficient size and strength to withstand the forces which may result from the functional and durability requirements of a given application. The quick-disconnect type construction with a splined hole, as shown in Fig. 75, is generally used in power take-off drive systems. The clamp bolt type construction with a partially serrated hole, shown in Fig. 76, is most commonly used in very slow speed applications such as steering shaft systems.

Other end yoke constructions with a splined hole or with a straight round hole and keyway are retained with a set screw or a nut. An end yoke can also have a tapered round hole and keyway and be retained with a nut. Still, other end yoke constructions have square, rectangular or hexagonal holes which are usually set screw retained.

A flange yoke is a yoke which attaches a driveshaft to a companion flange. The flange yoke is shown in Fig. 77 in two alternate constructions. These two types are the commonly used circular and rectangular configurations. For clarification purposes, the mating companion flange for each type is also shown. The yoke is held to the flange with bolts, and a pilot diameter is provided to maintain concentricity. The bolt size required is dic-

American Axle v. Neapco - IPR2025-00091
PET_AAM_1012-0078

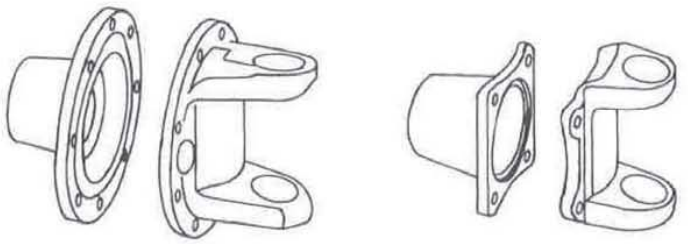


Fig. 77 — Flange yoke

tated by the clamping force necessary to withstand the forces which may result from the functional and durability requirements of a given application. The flange yoke is used in a wide variety of driveshaft applications.

Material Selection

The selection of optimum materials for the Cardan joint is based on ultimate strength, fatigue strength, and other functional and durability requirements for a given application, as well as economical processing advantages.

Because of the large variety of applications, the yokes may be made from a number of different materials and by various processing methods. The most commonly used yoke materials are steel forgings made of resulphurized or plain medium carbon steels which are heat treated to a typical range of BHN 228-255. Those yokes welded during assembly operations are generally machined from these forgings. Also, these medium carbon steels allow certain surfaces to be surfaced hardened by induction hardening when necessary, if the yoke has, for example, an integral spline on an external splined slip yoke. Yokes which are not subsequently welded to a connecting member, as a tube or shaft, or if they are made integral with a spline, as in an internal splined slip yoke, are frequently made from either pearlitic, malleable or nodular iron castings. These castings when heat treated to a typical range of BHN 241-269 for pearlitic, malleable iron and BHN 241-285 for nodular iron, allow the machining of yokes having the equivalent strength of forged steel components. In some cases, certain yokes are also formed from plain low carbon steel stampings or made by other means.

Since the cross serves the important function as the intermediate drive member of the Cardan joint, it is generally made from a low carbon alloy steel forging which is carburized to an adequate case depth and surface hardened to a typical R_c60 minimum to provide the required wear characteristics and torsional strength. The trunnions are then finish ground. In some applications, the cross is also shot peened prior to finish grinding. The necessary case depth of the cross trunnion is determined by the size of the Cardan joint and its application requirement. This requirement was discussed in the previous section on *Design* and is further explained in *Appendix A*.

The bearing cup is usually made of plain low carbon or low carbon alloy steel, which is carburized to an adequate case depth and surface hardened to a typical R_c60 minimum, to provide the required wear characteristics and strength. The necessary case depth is determined in a manner similar to that described for the cross trunnion. The cup is then finish ground. It can also be made of resulphurized medium carbon steel which is induction hardened in the bearing bore to an adequate case depth and a typical R_c60 minimum surface hardness before finish grinding.

The needle rollers used are made of chromium steel which are hardened to a typical range of R_c60-64 and finish lapped. In some joint bearing designs, components having low coefficients of friction are included, as desired, to improve bearing performance. Typical examples are the plastic needle thrust washer and seal washer used at the needle roller ends. Also, in certain cases, a trunnion thrust washer is incorporated between the bearing cup and cross trunnion thrust surfaces. This component is generally made of plastic or plastic with metal backing material.

The dust seal or seal retainer used in the bearing seal design is usually made from a plain low carbon steel stamping. The two common seal designs are generally either the packing or the elastomer types. The packing type of seal is usually made of cork neoprene coated with graphite or molydisulfide and must meet certain compressibility and recovery specifications. The elastomeric type of seal is generally a synthetic rubber. Both seal designs must exhibit specific resistance to the action of petroleum-based fluids and permit the seal to function satisfactorily for any environmental operating condition of the joint application.

The retaining ring is usually made of carbon spring steel. Also, in some applications an injected ring of plastic, such as glass-filled nylon, serves as the retaining ring.

Bearing retainer types other than the retaining ring are also commonly used. The U-bolt is one of these types and is generally made of medium carbon alloy steel, which is heat treated to a typical hardness range of BHN 302-352. The strap is another retainer and is usually made of plain low carbon steel, which may have a typical hardness of R_b70 minimum after forming.

Bolts and cap screws are used not only to retain various bearing constructions, but also to fasten an end or flange yoke to another driveline or drivetrain member. Therefore, these bolts and cap screws are generally made of medium carbon alloy steel and heat treated to conform to the SAE grade 8 bolt specifications.

Lubrication

In a Cardan joint the cross can be designed to hold an adequate supply of lubricant. This stored lubricant is supplied to the bearings by the centrifugal action of the rotating joint. The joint bearing and cross assemblies may be lubricated for life or provided with a lubrication plug or fitting for periodic replenishment of the lubricant. This lubrication procedure depends on the joint's specific design characteristics as well as the operating conditions encountered in an application. The lubricant type and grade are dependent primarily upon the application, the transmitted torque and speed, and the operating environment.

For most passenger car, truck, and other highway and off-highway vehicle driveline applications, a lubricating grease hav-

American Axle v. Neapco - IPR2025-00091
PET_AAM_1012-0079

ing an NLGI grade number 1 or 2, is generally preferred due to its ability to withstand relatively heavy loads. A typical lubricant of this type usually consists of a refined mineral oil and lithium 12 hydroxy stearate soap. Extreme pressure and other additives are incorporated, as required, to impart to, or enhance specific properties or performance characteristics of the lubricant. An added advantage of using an NLGI grade number 1 or 2 lubricating grease is that its consistency is firm enough to assist in maintaining the full complement of needle rollers in position against the inside diameter of the bearing cup until the joint is assembled.

In some lightly loaded applications, a more fluid lubricating grease having an NLGI grade number 0 may be desired. Also, in some axle driveshaft applications, the joint operates submerged in lubricant inside the closed steering knuckle of a vehicle's front live axle steerable wheel. This typical lubricant is a lubricating mineral oil of SAE viscosity number 90 or 140. In addition, in some very slow speed applications below 500 rpm, a lubricating mineral oil in the range of SAE viscosity number 140 or 250 has been used.

Typical basic performance requirements of a lubricating grease or oil which must be met, and its various properties, are described in the *SAE Handbook* under *Automotive Lubricating Greases*. In addition to providing for optimum joint life by reducing friction and wear at all bearing surfaces, the lubricant used must perform satisfactorily in all environmental conditions of the joint application.

Rating Procedure and Joint Size Selection

The following rating procedure for the Cardan joint applies to a complete universal joint assembly which consists of the cross, four bearings with full complements of needle rollers and bearing seals, as well as the attaching yokes. Also included are miscellaneous components such as bolts, cap screws, lockplates, U-bolts, retaining rings, and so forth, as required. It will be assumed that these miscellaneous attaching means as well as the driving yoke members have been designed with the comparable strength and life of the cross and bearing assembly.

The Cardan joint can be rated according to its static and operating capabilities in terms of such design parameters as torque, speed, and joint angle as described in *Appendix I*. Also, the joint can be rated in a manner which establishes a common size characteristic for comparison with other size Cardan joints. Fig. 78 shows a cross sectional view of the cross trunnion and bearing configuration of a joint. The bearing is acted upon by the torque couple force F which is assumed to be concentrated at the centroid of the projected bearing area on the cross trunnion, formed by the cross trunnion diameter D and the effective length L of the needle rollers. This couple force is at a distance R from the center of the cross and is called the torque radius.

The size characteristic of the joint can be expressed by a term called the *bearing factor*, BF, which is determined as follows:

$$BF = DLR$$

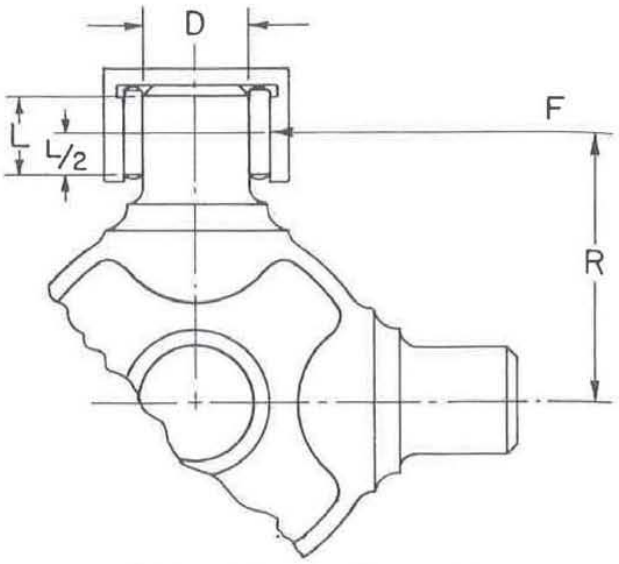


Fig. 78 — Needle roller bearing and cross

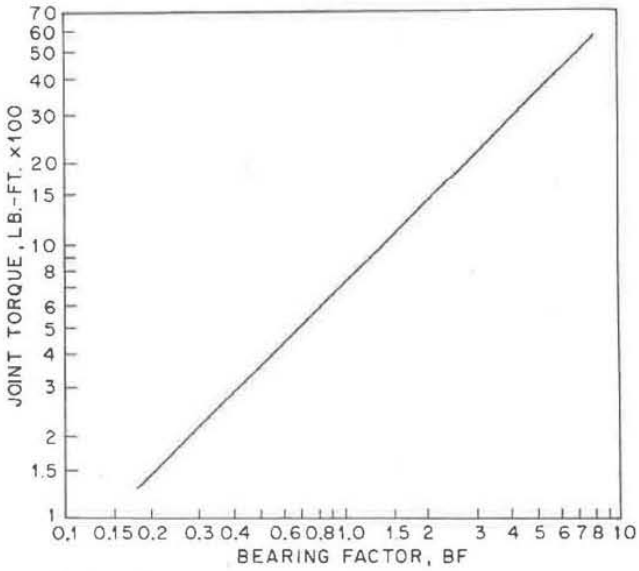


Fig. 79 — Basic joint torque rating at 3 deg angle, 1,000 rpm, and 3,000 h B_{10} life

where:

D = Trunnion diameter, in
L = Effective needle roller length on cross trunnion, in
R = Torque radius, in

Therefore, the *bearing factor* is simply the product of the projected bearing area on the cross trunnion times the torque radius, and serves as an *index* by providing a simple means for comparing various size joints with regard to relative bearing capacity.

The life of a Cardan joint is a function of the applied torque, speed, and joint angle. These three operating requirements can be shown on convenient curves. Fig. 79 shows a basic torque rating curve for a joint operating at 3 deg joint angle, 1000 rpm and 3000 h of B_{10} life. Fig. 80 shows correction factors for speed and joint

American Axle v. Neapco - IPR2025-00091
PET_AAM_1012-0080

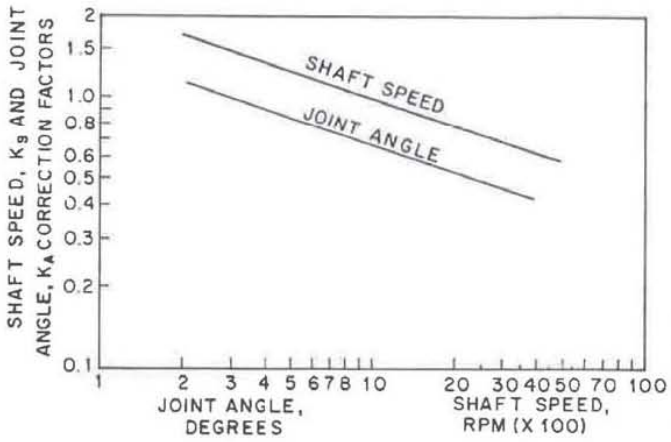


Fig. 80 — Shaft speed and joint angle correction factors

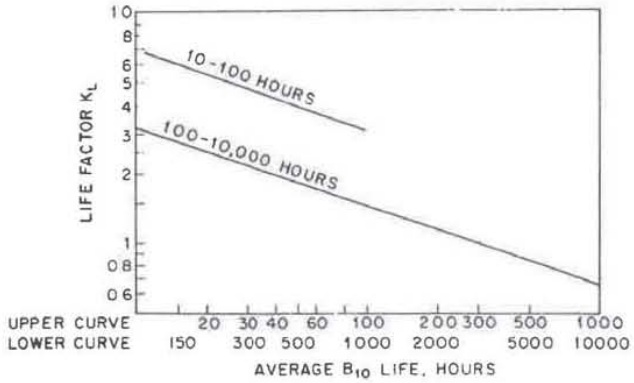


Fig. 81 — Life correction factors

angle while Fig. 81 is a life factor curve. The following typical problems illustrate the use of these curves:

Problem 1:

A Cardan joint with a bearing factor of 1.80 is assumed to operate in an application at 600 lb-ft torque, 6 deg joint angle, and 3000 rpm. Determine the estimated B_{10} life.

In Fig. 79, at a bearing factor of 1.80, the torque rating of the joint is 1300 lb-ft for a 3 deg joint angle, 1000 rpm, and 3000 h of B_{10} life.

A correction must now be made for the speed and joint angle of the required application. In Fig. 80, at 3000 rpm, the speed factor K_S is 0.70, and at 6 deg joint angle, the angle factor K_A is 0.78. Therefore, at the speed and joint angle required, the torque rating of the joint is:

$$T_2 = T_1 K_S K_A$$

$$= 1300 \times 0.70 \times 0.78$$

$$T_2 = 709 \text{ lb-ft}$$

The life factor is:

$$K_L = \frac{T}{T_2}$$

$$= \frac{600}{709}$$

$$K_L = 0.846$$

Then in Fig. 81, at a life factor of 0.846, the B_{10} bearing life is 4500 h.

Problem 2:

A vehicle application requires a Cardan joint which can operate at a continuous torque load of 400 lb-ft with a speed of 2000 rpm at 5 deg joint angle. The expected life is 300 000 miles at 3000 revolutions per mile. Determine the minimum size joint that should be used.

The expected life in hours can be computed as follows:

$$\text{Expected life} = \frac{300\,000 \times 3000}{2000 \times 60}$$

$$\text{Expected life} = 7500 \text{ h}$$

The basic torque rating at 3 deg joint angle, 1000 rpm and 3000 h of B_{10} life is:

$$T_1 = \frac{T_2}{K_L K_A K_S}$$

where:

$T_2 = 400$ lb-ft

$K_L = 0.73$ at 7500 h from Fig. 81

$K_A = 0.82$ at 5 deg from Fig. 80

$K_S = 0.80$ at 2000 rpm from Fig. 80

$$T_1 = \frac{400}{0.73 \times 0.82 \times 0.80}$$

$$T_1 = 835 \text{ lb-ft}$$

Then in Fig. 79 at 835 lb-ft, the bearing factor of the required minimum joint size is 1.22.

Problem 3:

In a truck application, the continuous torque is 300 lb-ft at 1800 rpm. The tire size used results in 506 wheel revolutions per mile and the axle ratio is 6:1. A Cardan joint with a bearing factor of 0.70 is used at a 3 deg operating angle. Determine the expected life in vehicle miles.

From Fig. 79, a joint with a bearing factor of 0.70 has a basic torque rating of 500 lb-ft at 3 deg joint angle, 1000 rpm and 3000 h of B_{10} life. This rating must be corrected to 3 deg and 1800 rpm.

American Axle v. Neapco - IPR2025-00091
PET_AAM_1012-0081

From Fig. 80, the speed factor is 0.80. Hence, at 3000 h, the corrected torque is:

$$T_2 = T_1 K_S$$

$$= 500 \times 0.80$$

$$T_2 = 400 \text{ lb-ft}$$

The continuous torque, however, is 300 lb-ft and the life must be corrected as follows:

$$K_L = \frac{T_3}{T_2}$$

$$= \frac{300}{400}$$

$$K_L = 0.75$$

From Fig. 81, the average B_{10} life is 7000 h. In order to express the life in miles, the vehicle speed must be computed as follows:

$$\text{Truck speed} = \frac{1800 \times 60}{6 \times 506}$$

$$\text{Truck speed} = 35 \text{ mph}$$

Therefore, the expected life is:

$$\text{Expected life} = 35 \times 7000$$

$$\text{Expected life} = 245\,000 \text{ miles}$$

Applications

The Cardan joint has been used in by far the widest range of applications of any universal joint in existence. Through the years, this joint has found nearly universal usage in passenger car, truck, and various other highway and off-highway vehicle driveline, axle driveshaft, power take-off, and steering shaft systems. In addition, the Cardan joint has been widely used in aircraft, railway, marine, agricultural, military, industrial, and stationary drive applications.

For passenger car and light-duty truck driveline applications, it has been found that the Cardan joint will operate satisfactorily with a minimum of disturbances at continuous operating joint angles up to about 4½ deg. In these applications, the minimum continuous operating angle should not be less than approximately ½ to ¾ of one degree. In other vehicles, varying joint angle limitations are usually required because of the numerous possible driveline configurations.

In axle driveshaft applications of four-wheel drive, light-duty trucks in particular, the Cardan joint has been used at the wheel position of live, rigid front axles where the maximum intermittent operating joint angles have reached approximately 40 deg during extreme steering movements. However, in this location, the normal operating angle is very low, and is in the range of ½-1½ deg.

The use of a single Cardan joint on a driveshaft is not advisable where the operating speed is very high, or where considerable power is to be transmitted because of its nonuniform motion characteristics. This undesirable condition can be corrected by using two joints in series in proper phase relationship and operating at or nearly equal joint angles. In addition to one-piece driveshafts, Cardan joints are also used in multipiece driveline arrangements with proper phasing and selection of joint angles.

The recommended maximum operating joint angle is governed by the rotational speed of the Cardan joint, and since the many joint applications cover a wide range of speeds, Table 2 is an application guide for operating joint angles where the angle and speed are continuous conditions and the maximum angular acceleration limit is 1000 rad/s/s. Also, the driveshafts have two joints with equal joint angles. In certain applications, the shaft length used, usually a very short or a very long center-to-center distance, may require a reduction of the recommended maximum operating angles, and whenever the joint angles are not equal, phasing of the joints with respect to one another may be necessary.

In very slow rotational speed applications such as steering shafts, for example, the joint angles should be such that the torsional equivalent angle of the system will not exceed approximately 25 deg for a generally smooth feel at the steering wheel rim. A higher torsional equivalent angle results generally in a "lumpy" feel or variable effort due to the lag and lead of the angular displacement of the steering gear input shaft.

Table 2 — Allowable Operating Joint Angles

Driveshaft Speed, rpm	Maximum Operating Angle, Degrees
5000	3°30′
4500	3°50′
4000	4°20′
3500	5°00′
3000	5°45′
2500	6°55′
2000	8°40′
1500	11°30′

References

1. H. O. Fuchs, *Notes on Universal Joints, Product Study,* GMC, October 6, 1939.

2. A. Y. Dodge, "Bearing Loads Due to Universal Joint Action," *Automotive Industries,* December 15, 1940, pp. 636-639.

3. H. I. F. Evernden, "The Propeller Shaft or Hooke's Coupling and the Cardan Joint," *Proceedings of the Institution of Mechanical Engineers,* October, 1949, pp. 100-110.

4. P. J. Mazziotti, *Universal Joints and Propeller Shafts,* Dana Corp. Bulletin J-1371, October 15, 1954.

5. M. Olley and J. Valukonis, *Propeller Shaft and Universal Joint Notes,* Chevrolet R & D, GMC, 1954.

6. *Method for Minimizing Couple Forces at Center Bearing Support of Three-Joint Propeller Shaft,* Engineering Staff, GMC, 1956.

American Axle v. Neapco - IPR2025-00091
PET_AAM_1012-0082

7. R. R. Burkhalter and P. J. Mazziotti, *The Low Silhouette Drive Line*, SAE Paper 691, 1956.

8. N. J. Denil, *Analysis of Multi-Universal Joint Drive Lines*, Vol. I and II, Cadillac Motor Car Division and General Motors Institute, 1957.

9. J. A. Kayser, *Drivelines for Heavy Equipment*, SAE Paper 403A, 1961.

10. W. T. Condon, *Application of Universal Joints to Construction and Industrial Machinery*, SAE Paper 403B, 1961.

11. M. C. Kaye, *Some Aspects of the Truck Drive Train Vibration Problem*, SAE Paper 402A, 1961.

12. T. C. Stott, *Notes on Propeller Shafts and Universal Joints*, February 13, 1962.

13. H. R. Pickford, "Hints on How to Reduce Truck Drive Train Vibration," (Written Discussion on SAE Paper 402A), *SAE Journal*, April, 1962, pp. 70-73.

14. W. Ker Wilson, "Practical Solution of Torsional Vibration Problems," *Amplitude Calculations*, Vol. 2, London: Chapman and Hall Ltd., 1963, pp. 299-308.

15. P. J. Mazziotti, *Dynamic Characteristics of Truck Driveline Systems*, Published in SAE SP-262, 1964.

16. *Universal Joint Layout and Selection Data Book*, Rockwell-Standard Corp., 1964.

17. B. R. Reimer, *Design and Application Considerations for Agricultural P. T. O. Drivelines*, SAE Paper 650680, 1965.

18. C. E. Cooney, *Design and Application of Universal Joints for Off-Highway Vehicles*, SAE Paper 650681, 1965.

19. L. J. DiFrancesco, *Better Needle Bearings for Universal Joints*, SAE Paper 660159, 1966.

20. C. E. Cooney, *Practical Procedures for Designing and Analyzing a Tandem Truck Driveline*, SAE Paper 660413, 1966.

21. D. P. Marquis, *The Composite Universal Joint*, SAE Paper 690256, 1969.

22. C. W. Haines, *Drivelines for High Performance*, SAE Paper 700742, 1970.

23. J. W. Macielinski, "The Design and Selection of Universal Joints. Part I: The Hooke's Joint," *The Journal of Automotive Engineering*, May 1970, pp. 14-18.

American Axle v. Neapco - IPR2025-00091
PET_AAM_1012-0083

Section 3.1.2
Ball and Trunnion Universal Joint

J. Koinis — Chrysler Corp.
E.R. Wagner, P. E. — Saginaw Steering Gear Div., GMC

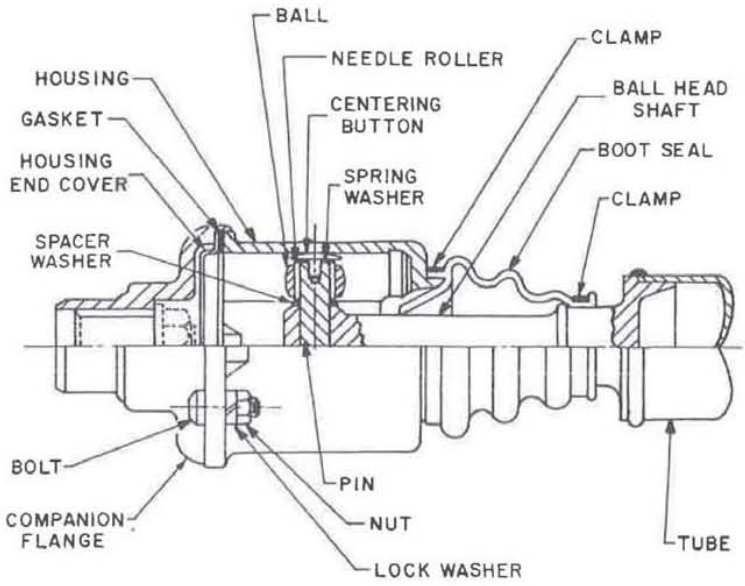


Fig. 1 — Ball and trunnion universal joint

Introduction

The patent literature shows that the concept of the ball and trunnion universal joint was developed as early as 1914 and that patents on various applicable features were issued through the early 1930s. This joint has also been commonly called a *bipot* joint. It was used as the inboard joint in an early American front wheel drive passenger car built in the late 1920s, and then used extensively in some American passenger car driveshafts from 1932 until the middle 1960s. The joint has also been used in independently sprung European rear drive passenger cars as either the axle driveshaft inboard or outboard joint. Other limited usage of this joint has been in some American military vehicles and various industrial applications.

The ball and trunnion universal joint, shown in Fig. 1 in a typical design for a driveshaft application, is a nonconstant velocity universal joint radially self-supported, and permitting axial movement, which consists of a housing drivably connected to a ball head shaft through a pair of diametrically opposed trunnion mounted balls. The principal advantage of this joint is the relatively low axial thrust force required for end motion when compared with a conventional sliding spline. This joint characteristic minimizes thrust forces on supporting driveline structures due to shaft length changes and eliminates the undesirable spline noise or *grunt* problems of some sliding spline installations when subjected to relatively high torque. The joint also has a self-aligning feature when stroked axially and angulated within its design limitations. When compared with a Cardan joint, the ball and trunnion joint has a relatively large lubricant capacity, and if adequate sealing means are provided, no relubrication during normal life is required.

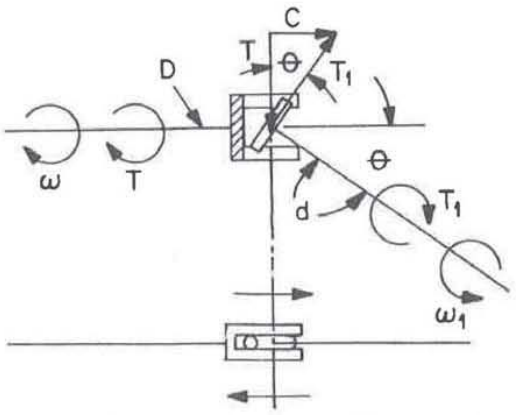
There are several limiting characteristics inherent with this type of joint. It has a larger swing diameter and less joint angular capability than a Cardan joint of comparable torque capacity. Also, the maximum joint angle required can limit the axial travel available within the joint. Therefore, the ball and trunnion joint is generally used in low angle applications so that sufficient end motion is available.

Kinematics

An analysis of the ball and trunnion joint indicates that it exhibits the same, nonconstant velocity, kinematic characteristics as a Cardan joint. It is important to correctly specify whether the joint housing or the trunnion pin is the driving or input member in a particular driveline system. This will affect the phase relationship required when the joint is used in series with either another ball and trunnion joint, or a Cardan joint.

American Axle v. Neapco - IPR2025-00091
PET_AAM_1012-0085

Case 1
Rotational Position (a)



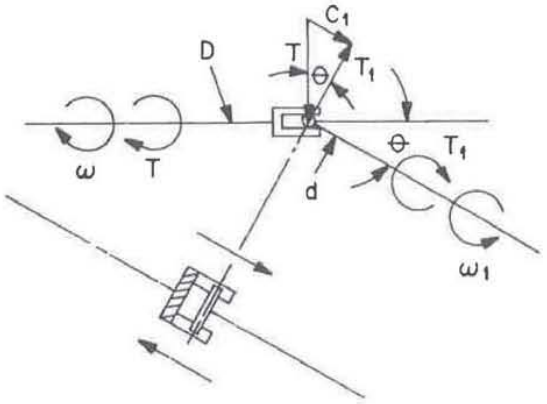
D = Driving Member (Housing)
d = Driven Member (Pin)
θ = Joint Angle

Input Torque T is Assumed Clockwise When Viewed from Left End.

	Joint Member	
	D	d
Angular Velocity	ω = const.	$\omega_1 = \omega \cos\theta$
Torque	T = const.	$T_1 = T/\cos\theta$
Secondary Couple	$C = T\tan\theta$	$C_1 = 0$

Fig. 2 — Ball and trunnion joint kinematic relationships

Case 1
Rotational Position (b)



D = Driving Member (Housing)
d = Driven Member (Pin)
θ = Joint Angle

Input Torque T is Assumed Clockwise When Viewed from Left End.

	Joint Member	
	D	d
Angular Velocity	ω = const.	$\omega_1 = \omega/\cos\theta$
Torque	T = const.	$T_1 = T\cos\theta$
Secondary Couple	C = 0	$C_1 = T\sin\theta$

Fig. 3 — Ball and trunnion joint kinematic relationships

Simplified motion, torque, and secondary couple relationships are shown in Figs. 2, 3, 4, and 5. The housing is the driving member in Figs. 2 and 3, while in Figs. 4 and 5 the pin is the driving member. Fig. 6 shows the velocity variation characteristics in the driven shaft of a ball and trunnion joint and Cardan joint for a 15 deg joint angle. Figs. 7 and 8 show the driving and driven member secondary couple characteristics, respectively, of both joints. In Figs. 6, 7, and 8, the joints are shown in various rotational positions with the ball and trunnion joint being shown with both the housing and the pin as the driving members. In addition, the same joint internal geometry which provides for angular motion also allows simultaneous axial movement.

Phasing

Since the kinematic characteristics of the ball and trunnion joint and Cardan joint are identical, the same phasing procedures outlined for Cardan joint driveline systems can be used. As indicated in the previous section on *Kinematics*, attention, however, must be given to the orientation of the housing or pin of one ball and trunnion joint relative to another ball and trunnion joint, or a Cardan joint when they are used in series.

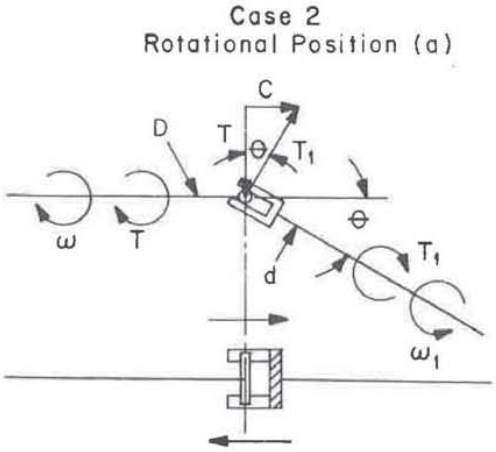
For example, in Fig. 9, the ball and trunnion joint is used with a Cardan joint on a one-piece driveshaft in an intersecting shaft arrangement. The shaft is shown schematically in two rotational positions 90 deg apart, and the joint angles are true angles. The housing of the ball and trunnion joint is the driving member, and the pin is phased parallel or in line with the driving yoke of the Cardan joint.

For this phasing arrangement, the torsional equivalent angle or residual joint angle of the system is:

$$\theta_{res.} = \sqrt{\theta_1^2 - \theta_2^2}$$

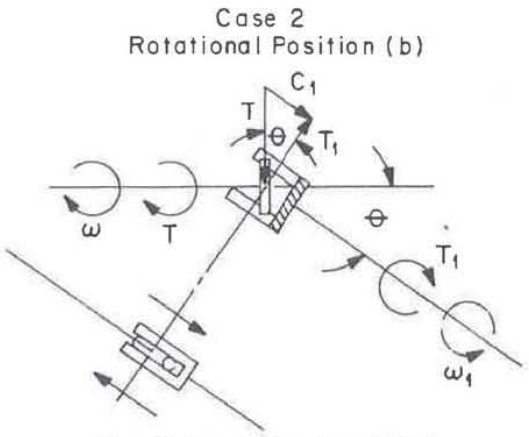
This residual joint angle characteristic is the same as for a one-piece driveshaft having Cardan joints with parallel intermediate shaft yokes. If the shaft lengths, joint angles, and the supporting bearing locations of these two driveshafts with intersecting shafts are identical, the secondary couple forces on the bearing structures are also the same. By referring to the kinematic characteristics shown in Figs. 2 thru 8, various driveline configurations using ball and trunnion joints can be analyzed with regard to optimum joint phasing.

American Axle v. Neapco - IPR2025-00091
PET_AAM_1012-0086



	Joint Member	
	D	d
Angular Velocity	ω = const.	$\omega_1 = \omega \cos \theta$
Torque	T = const.	$T_1 = T/\cos \theta$
Secondary Couple	$C = T \tan \theta$	$C_1 = 0$

Fig. 4 — Ball and trunnion joint kinematic relationships



	Joint Member	
	D	d
Angular Velocity	ω = const.	$\omega_1 = \omega/\cos \theta$
Torque	T = const.	$T_1 = T \cos \theta$
Secondary Couple	C = 0	$C_1 = T \sin \theta$

Fig. 5 — Ball and trunnion joint kinematic relationships

Design

The various components of a typical ball and trunnion joint shown in an exploded view in Fig. 10, must be designed to provide the necessary joint angularity, axial travel, strength, and life requirements for a given application. The ultimate strength of the joint must be safely in excess of the maximum applied torque which can be developed by various loading modes discussed in the chapter on *Basic Driveline Requirements*. Initially, the size of the ball head shaft is determined as outlined in the chapter on *Axle Driveshafts*. Then the ball head shaft assembly consisting of the ball head shaft, pin, needle rollers, balls, spacer washers, spring washers, and centering buttons, as well as the housing configuration, can be designed to meet the various joint application parameters.

Proper considerations for designing the joint bearing elements are necessary for adequate joint life. The ball-to-housing bore wear can be minimized by the selection of optimum comparable component materials, dimensions, Hertz contact stresses, surface hardnesses, and surface finishes or coatings, as well as an optimum hardness gradient of the housing bore case depth. In addition, an optimum lubricant must be utilized which is compatible with the overall ball-to-housing bore design selected, and also must meet the requirements of the joint application. The op-

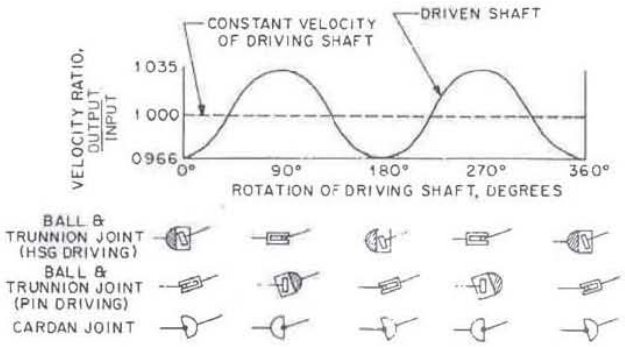


Fig. 6 — Velocity variation in driven shaft for a 15 deg joint angle

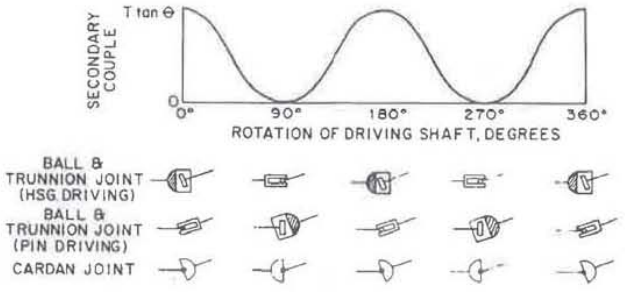


Fig. 7 — Secondary couple on driving shaft

American Axle v. Neapco - IPR2025-00091
PET_AAM_1012-0087

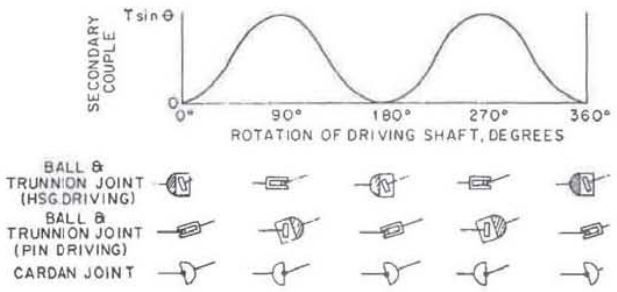


Fig. 8 — Secondary couple on driven shaft

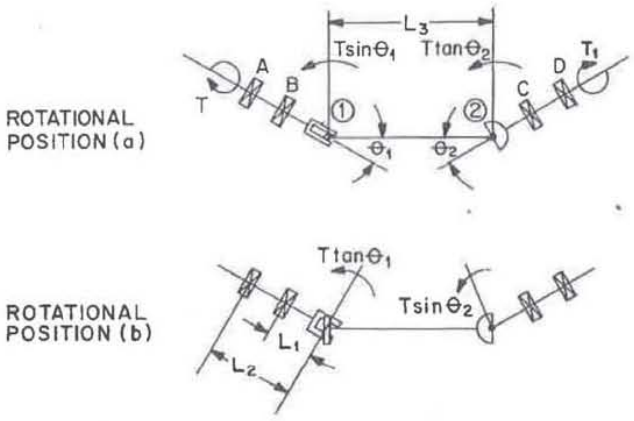


Fig. 9 — Intersecting shaft arrangement with parallel intermediate shaft pin and yoke

timized design should provide for an adequate precession of the balls in the housing bores and of the needle rollers relative to the pin and ball bore. This precession characteristic is also described in the section on the *Cardan or Hooke Universal Joint*.

The needle roller length-to-diameter ratio employed is usually at the high end of the range or somewhat higher than the range used in a typical Cardan joint. The needle roller bearing load distribution and Hertz contact stress computation is discussed in the section on the *Cardan or Hooke Universal Joint*. For the entire bearing configuration, the permissible Hertz contact stress, including the associated computaton procedure, is also shown in *Appendix A*. With regard to needle roller bearing design, the selection of optimum size and tolerances, as well as diametral and circumferential clearances is generally the same as for a Cardan joint in similar applications. *Appendix C* illustrates a typical bearing computation procedure for determining these clearances.

The ball head shaft assembly configuration with an adequate ball circle diameter must be optimized by trial computations. The ball head shaft is a member which provides for the transversely located pin and has drivable means of attachment. Strength computations can be made by assuming the ball head cross section at the pin to be circular with a transverse hole. For a tentative assumed bearing design with sufficient capacity, the bending strength of the finish ground pin is of primary importance. The pin is a member pressed through the ball head shaft which provides trunnions for the needle rollers, balls, centering buttons, and

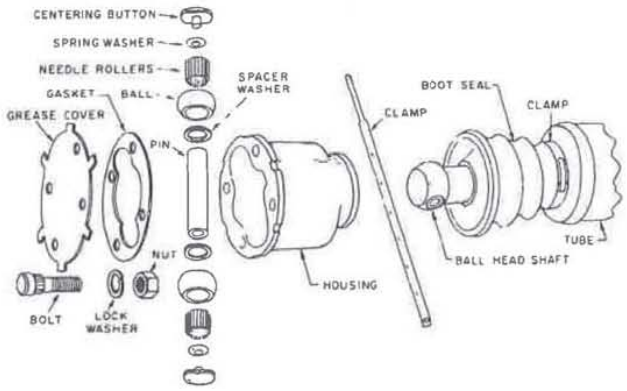


Fig. 10 — Ball and trunnion universal joint

associated components. The pin bending strength is computed in the same manner as the Cardan joint cross trunnion. Generally, the press fit in the spherical-shaped hub of the ball head is a typical 0.0002-0.0015 in total interference, which has an important effect on joint fatigue life. The interference fit used must be sufficient to prevent relative movement, commonly called "chafing" or "fretting", between the pin and hole in the hub when torque is transmitted. This interference fit results in a compressive stress in the pin and also imposes a stress concentration due to discontinuity at each end where the pin protrudes from the hub. This stress concentration can be minimized somewhat by chamfering both ends of the hole passing through the hub. Therefore, the application of a torque load on the joint results in a complex stress state, which is at a maximum in the pin just inside the hub edge. For passenger car and other similar applications, a typical allowable bending stress of 150 000 psi can be used at the maximum applied torque to determine the size of the pin which is carburized, hardened, and finish ground. The use of this stress value allows for the indicated stress concentration effects. With respect to the ball head shaft axis, the pin is usually centered within 0.004 in total indicator reading for automotive applications. At each end of the pin, a bearing assembly is mounted which consists typically of a ball, needle rollers as the rolling elements, spacer washer, spring washer, and centering button. These bearing assemblies mate with the housing, which is a member with two diametrically opposed, partly cylindrical axial ball bores on the cylindrical inner clearance surface, and with drivable means of attachment. Fig. 11(a) illustrates a typical housing construction used in a driveshaft application, while Fig. 11(b) shows a typical housing configuration for axle driveshaft usage.

The ball is a partly spherical shaped member which pivots and transmits torque from the housing to the ball head shaft through needle rollers and the pin, and permits axial movement. Instead of being true spherical, the outer profile surface of the ball may also be made toroidal in shape, as shown in Fig. 12, in order to control the contact area length and thus prevent edge contact in the housing ball bores during high torque load applications. For this toroidal-shaped ball, the generating radius is smaller than the equatorial radius and results in an elliptical spot contact in the cylindrical bore instead of the long and narrow elliptical contact

American Axle v. Neapco - IPR2025-00091
PET_AAM_1012-0088

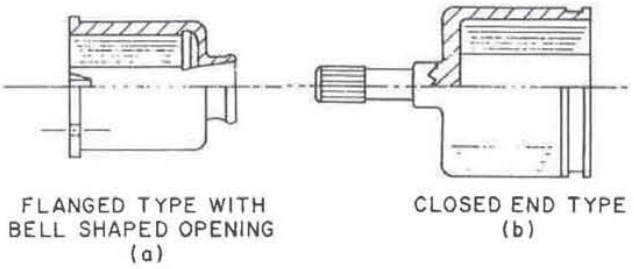


Fig. 11 — Typical ball and trunnion joint housing constructions

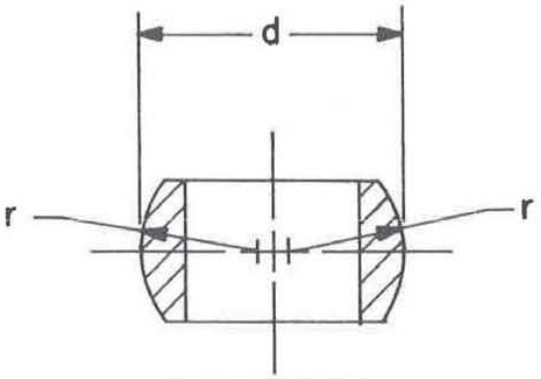


Fig. 12 — Toroidal ball

condition of the spherical ball, which actually runs off or extends beyond the ball edges during high torque loads.

The generating radius-to-equatorial diameter ratio of a typical toroidal ball may be approximately 0.46-0.48 and not result in contact run-off. For a given torque load, the smaller elliptical contact area produced by the toroidal ball increases the Hertz contact stress and the required case depth over that resulting from a spherical ball. However, the smaller contact area resulting from less conformity or wrap around of the bore on the toroidal ball reduces sliding and scuffing produced by the longer contact area of the spherical ball, as well as the edge contact and, hence, may improve housing ball bore wear life when other optimum design procedures are incorporated, even though the contact stress is higher. In a typical driveshaft design, the total clearance between the ball and housing cylindrical ball bore may be in the range of 0.0005-0.0025 in, whereas for an axle driveshaft application this clearance may be approximately 0.001-0.004 in.

The spacer washer is a member which positions the needle rollers inside the ball. The spring washer is a member which maintains contact of the centering buttons with the housing bore radial thrust surfaces. The centering button is a thrust-loaded member which locates the ball head shaft assembly during its various movements and radially retains the needle rollers. With a centering button and spring washer assembled to each end of the pin, the resulting total radial clearance in the housing axial bores is in the typical range of 0.000-0.006 in.

Depending on the maximum joint angle requirement, adequate clearance must be provided between the centering button flat surface and ball, while at zero joint angle clearance must exist

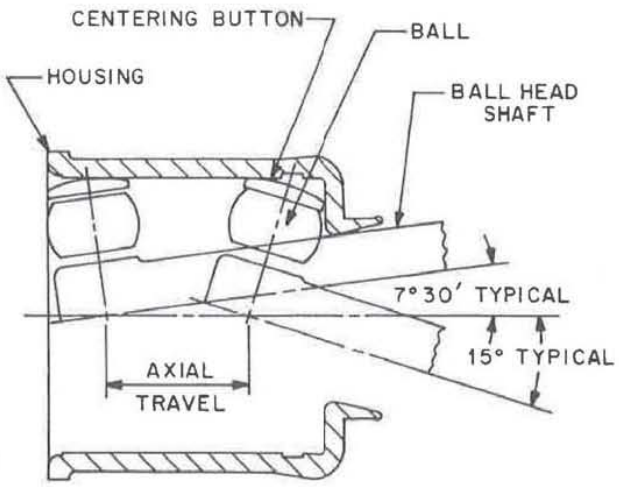
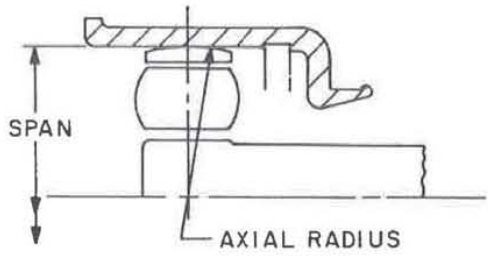
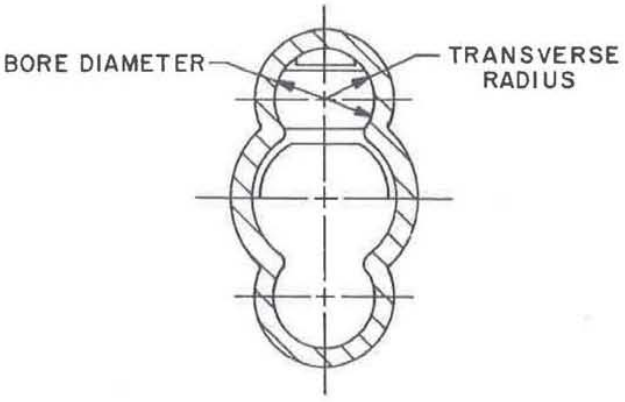


Fig. 13 — Determination of joint angularity and clearances



$$\text{AXIAL RADIUS} = \frac{1}{2}\ (\text{SPAN OF HOUSING BORES})$$



$$\text{TRANSVERSE RADIUS} = \frac{1}{2}\ (\text{BORE DIAMETER})$$

Fig. 14 — Centering button design radii

between the ball and spacer washer adjacent to the ball head. Figs. 13 and 14 show these clearances and the required radii of the centering button thrust surface in both axial or longitudinal, as well as transverse planes. These illustrations clearly show the design studies which must be made for a typical joint before the design can be finalized and are affected by joint angularity and axial movement requirements. Fig. 13 shows the highest joint angles possible at the extreme ends of the required end motion. At

American Axle v. Neapco - IPR2025-00091
PET_AAM_1012-0089

the maximum joint angle position the ball is shown adjacent to the bottom of the centering button, indicating the necessity of the clearance illustrated in Fig. 14 to prevent interference. At the maximum joint angle position also, the required length of the centering button is shown. Good design practice allows a length sufficient to provide for 2 deg-3 deg joint angle over travel before edge contact is reached. Since the button is subjected to sliding motion as well as thrust forces, it must be surface hardened. Therefore, the resulting minimum thickness at the edges of the toric curved surfaces must be adequate to prevent brittle fracture. Also, the necessary minimum length of the button stem protruding into the pin end for support can be determined at the maximum joint angle position.

In performing its principal function of keeping the lubricant in, and foreign matter out of the joint, the boot seal, which is a flexible member, must be capable of operating under varying environmental conditions at various speeds, joint angles, and end motion positions, and its design depends on the joint usage. For high-speed automotive driveshaft applications, a typical convoluted conical-shaped seal with an internal baffle is used. This internal baffle prevents the lubricant from working out of the joint housing and into the seal area. For slower speed applications, such as vehicle axle driveshafts, the baffle is generally not required. Also, for typical high speed driveline applications, the boot seal configurations illustrated for the cross groove and end motion type double offset joints for such installations can be used. Both ends of the seal are usually held in position with clamps which are thin metallic or nonmetallic adjustable bands. If the joint axial movement is relatively high, joint venting means may be required. When the closed end type of housing is employed, axial stroke limitation means can be incorporated in the seal design to prevent accidental disassembly.

In the flanged housing design commonly used in automotive driveshaft applications, the open flanged end is closed by a housing end cover and sealed with a gasket. This housing end cover is a member which protects the joint from contamination and loss of lubricant during shipping and handling. When a ball and trunnion joint is used on both ends of a driveshaft, a conical spring has been used between the housing end cover and ball head shaft to keep the joints centered at each end. If a Cardan joint is used with a ball and trunnion joint, then no centering spring is required. The maximum angular design capability of the joint for its entire axial stroke range can be determined by plotting a chart as described in *Appendix G*.

As previously indicated, the principal advantage of the ball and trunnion joint is that it requires a relatively low axial thrust force during end motion when compared with a conventional sliding spline. Fig. 15 shows the static (nonrotating) axial force characteristics for a typical joint.

Material Selection

The selection of optimum materials for the ball and trunnion joint components is based on ultimate strength, fatigue strength, and other functional and durability requirements for a given application, as well as economical processing advantages.

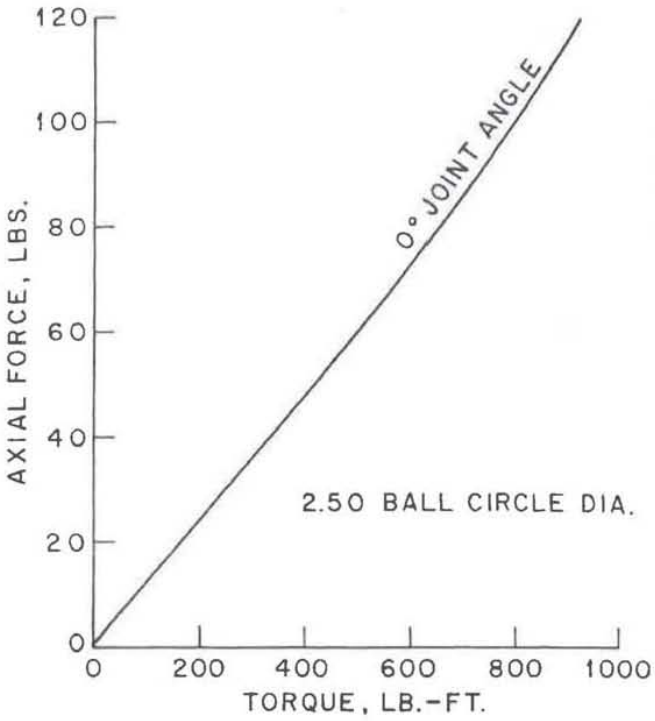


Fig. 15 — Ball and trunnion joint axial force characteristics

The housing is usually made from a low carbon alloy or plain low carbon steel forging which is carburized to an adequate case depth and surface hardened to a typical R_c60 minimum to provide the required wear characteristics and torsional strength. The necessary case depth required in the axial ball bores after finish grinding is relatively deeper when a toroidal ball is used than when a spherical ball is utilized, and is determined by the contact load requirement explained in *Appendix A*.

The pin is generally made from cold drawn low carbon alloy steel bar stock which is carburized to an adequate case depth and surface hardened to a typical R_c60 minimum and finish ground. The necessary case depth is determined by the joint size and its application requirement and is essentially the same as discussed for the Cardan Joint cross trunnion, and is also explained in *Appendix A*.

The finish ground balls are usually made of low carbon alloy steel which are carburized to an adequate case depth and surface hardened to a typical R_c60 minimum. The balls can also be made of chromium steel which are hardened to a typical range of R_c62-65. After basically providing for adequate surface hardness and case depth in the housing ball bores, the bore wear can sometimes be reduced by modifying the ball surface finish by, for example, grit or vapor blasting or lapping. Also, a phosphate type coating can be applied to the housing, if desired.

The needle rollers are made of chromium steel which are hardened to a typical range of R_c60-64 and finish lapped. The spacer washers are generally made of plain low carbon steel, which can be cyanided to a typical surface hardness of R_c60 minimum. The spring washers are usually made from spring steel stampings.

American Axle v. Neapco - IPR2025-00091
PET_AAM_1012-0090

The centering buttons are generally made of cold formed, low carbon alloy steel, which are carburized to an adequate case depth and surface hardened to a typical R_c60 minimum and finish ground on the toric curved thrust faces and the piloting stem.

The ball head shaft when used in driveshaft applications, is usually made from a resulphurized medium carbon steel forging, which is heat treated to a typical hardness range of BHN 255-285. For heavy duty or axle driveshaft applications, typical materials and heat treatments are the same as discussed for axle shafting in the chapter on *Axle Driveshafts*.

The elastomeric material of the boot seal is generally a synthetic rubber which must exhibit specific resistance to the action of petroleum based fluids, and permit the seal to function satisfactorily for any environmental operating condition requirements of the joint application. The clamps are usually made of plain low carbon steel. The gasket is generally made from gasket paper and the housing end cover is usually made from a plain low carbon steel stamping. The spring, when used, is generally made from carbon spring steel wire.

Lubrication

The ball and trunnion joint has a relatively large capacity for lubricant and is generally lubricated for life. In high speed driveshaft applications, approximately one half of the available volume of the assembled joint cavity is filled. The lubricant should be evenly distributed in the housing since it will not transfer from one ball bore to the other during operation. If too much lubricant is used, it may work past the boot seal baffle and cause failure of the convoluted seal due to centrifugal force effects. In slower speed applications such as axle driveshafts, generally most of the assembled joint cavity is filled with lubricant and the presence of lubricant in the seal area is not detrimental to seal life.

A lubricating grease having an NLGI grade number 1 or 2 is usually used. A typical lubricant of this type generally consists of a refined mineral oil and lithium 12 hydroxy stearate soap. Extreme pressure and other additives are incorporated, as required, to impart to or enhance specific properties or performance characteristics of the lubricant.

Typical basic performance requirements of a lubricating grease, which must be met, and its various properties are described in the *SAE Handbook* under *Automotive Lubricating Greases*. In addition to providing for optimum joint life by reducing friction and wear at all bearing surfaces, the lubricant used must perform satisfactorily in all environmental conditions of the joint application.

Rating Procedure

The ball and trunnion joint can be rated on the same basis as the Cardan joint where the term *bearing factor* is used in rating and comparing joint sizes. In addition, the joint can also be rated as described in *Appendix I*.

Applications

The ball and trunnion joint found its most common usage as the front joint in many past, one-piece passenger car driveshafts where there was a need for a joint providing low effort end motion in addition to a relatively low joint angle capability. Also, the joint has been used in axle driveshafts of front and rear drive vehicles where axial movement was required along with the necessary intermittent joint angle capability during suspension movements. Additional usage of this joint has been in aircraft, military vehicles, and industrial applications. Depending on the axial stroke requirement of an application, the maximum angular design capability of this joint is approximately 15 deg.

The normal design operating angle of the joint will depend on the specific application, while the maximum intermittent operating angle, throughout its entire axial stroke range, must be within the limit lines of the angular capability chart for a given joint design as described in *Appendix G*. For passenger car and light duty truck applications, normal operating angles of approximately 3 deg have been used in driveshafts. If this angle is decreased to less than 1½-2 deg, the bearing life is affected. Rotational movement or oscillation of the needle rollers and balls becomes erratic, which can cause brinelling of the trunnion pin and housing ball bores.

References

1. R. M. Heldt, "Propeller Shafts and Universal Joints," *The Automotive Chassis*, Chapt. VI, 1948, pp. 140-169.

2. R. V. Hutchinson, Notes on "Pot-Type" Universal Joints, General Motors Engineering Staff, February 27, 1958.

3. D. P. Marquis, *Future High Angle Joints*, SAE Paper S 218, 1959.

4. W. H. Crouse, "Drive Lines," *Automotive Mechanics*, Chapt. 27, McGraw-Hill Book Co., Inc., 1960, pp. 583-590.

5. D. P. Marquis, *Low Tunnels Mean High Angles*, SAE Paper 320C, 1961.

6. P. J. Mazziotti, *Dynamic Characteristics of Truck Driveline Systems*, Published in SAE SP-262, 1964.

7. E. R. Wagner, P.E., *Driveline Splines and Axial Motion Mechanisms*, SAE Paper 740670, 1974.

American Axle v. Neapco - IPR2025-00091
PET_AAM_1012-0091

Section 3.1.3
Roller and Trunnion Universal Joint

E. R. Wagner, P.E. — Saginaw Steering Gear Div., GMC

Introduction

The roller and trunnion universal joint was patented by Lipe in 1909 and was used in some European front wheel drive passenger cars as the inboard joint. This joint, which is similar to the ball and trunnion joint, is another type of *bipot* joint construction.

The roller and trunnion universal joint, shown in Fig. 1 in a typical design, is a nonconstant velocity universal joint radially self-supported, and permitting axial movement, which consists of a housing drivably connected to a shaft through a pair of diametrically opposed trunnion mounted rollers. Its advantages and disadvantages are essentially the same as for the ball and trunnion joint except for a somewhat higher axial thrust force during end motion which is, however, still lower than conventional sliding spline.

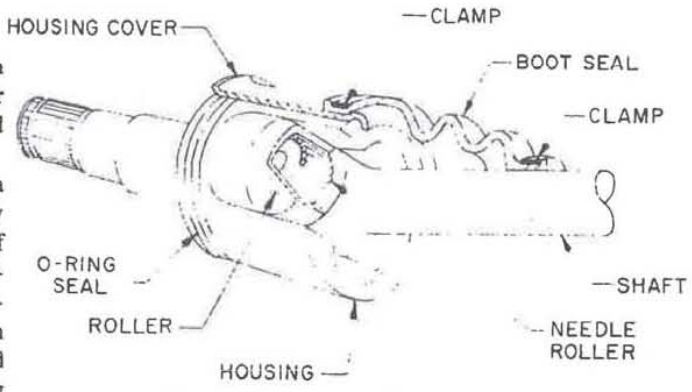


Fig. 1 — Roller and trunnion universal joint

Kinematics

The kinematics of the roller and trunnion joint are the same as for the Cardan and ball and trunnion joints, which both transmit nonconstant velocity. As in the ball and trunnion joint, the same internal geometry which provides for angular motion also allows for simultaneous axial movement. The joint phasing procedure is the same as described for the ball and trunnion joint.

Design

The various roller and trunnion joint components must be designed to provide the necessary joint angularity, axial travel, strength, and life requirements for a given application. The ultimate strength of the joint must be safely in excess of the maximum applied torque which can be developed by various loading modes discussed in the chapter on *Basic Driveline Requirements*. Initially, the shaft size is determined as outlined in the chapter on *Axle Driveshafts*. Then the housing, pin, needle roller, and roller configuration can be designed to meet the various joint application parameters.

The needle roller bearing load distribution and Hertz contact stress computation procedure is discussed in the section on the *Cardan or Hooke Universal Joint*. For the entire bearing configuration, the permissible Hertz contact stress, including the associated computation procedure, is also shown in *Appendix A*. With regard to needle roller bearing design, the selection of optimum size and tolerances as well as diametral and circumferential clearances is generally the same as for a Cardan, or ball and trunnion joint in similar applications. *Appendix C* illustrates a typical bearing computation procedure for determining these clearances.

The roller and trunnion joint is very similar in design to the ball and trunnion joint except that cylindrical rollers are used in place of balls. The roller is a cylindrical-shaped member which pivots and transmits torque from the housing to the shaft through needle rollers and the pin, and permits axial movement. Centering buttons, spacer washers, and spring washers are not used. The function of the centering buttons in providing radial thrust support is incorporated in the closed spherical end of the roller itself, or the pin is spherically shaped at the ends when open end rollers are employed. The radius of the spherical-shaped end of the roller or pin is equal to one-half of the span of the housing roller tracks or slots. Needle rollers are generally used with both roller designs. The closed end roller design allows a maximum joint angle capability of approximately 17 deg, while the open end roller permits approximately 10 deg of maximum angular capability.

For similar applications, the selection of various clearances and tolerances is generally the same as for the ball and trunnion joint. Also, the allowable pin strength and its interference fit with the mating shaft member are essentially the same as employed in the ball and trunnion joint. Fig. 2 shows two typical housing constructions used. The housing is a member with two diametrically opposed axial roller slots on the cylindrical inner clearance surface and with drivable means of attachment. In the tulip type housing, these roller slots extend through its periphery.

The boot seal is a flexible member, and in performing its principal function of keeping the lubricant in and foreign matter out of the joint, it must be capable of operating under varying environmental conditions at various speeds, joint angles, and end motion positions. When the closed type of housing is used, the seal is generally connected to the housing with a seal adapter and held in position with a seal retainer. An O-ring seal is usually

American Axle v. Neapco - IPR2025-00091
PET_AAM_1012-0093

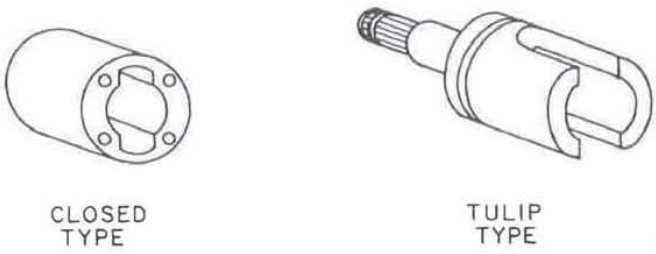


Fig. 2 — Typical roller and trunnion joint housing constructions

employed between the housing and seal adapter. Generally, a clamp is used to hold the boot seal in position on the shaft. When the tulip type of housing is used, a housing cover must be employed. This housing cover is a sleeve-like member which encloses the housing and provides for attachment of the boot seal and bearing surfaces for radial support of the joint. Usually, the housing cover has an interference fit with the housing outside surface and an O-ring provides sealing between these two members. The boot seal is generally held in position on the housing cover and shaft with clamps. To prevent accidental disassembly of the joint, the seal adapter and seal retainer for the closed type of housing and the housing cover for the tulip type of housing can be designed to limit the maximum axial movement. The maximum angular design capability of the joint for its entire axial stroke range can be determined by plotting a chart as described in *Appendix G*.

As previously indicated, a principal advantage of the roller and trunnion joint is that it requires a relatively low axial thrust force during end motion which is somewhat higher than for a ball and trunnion joint, but still much lower than for a conventional sliding spline. Fig. 3 shows the static (nonrotating) axial force characteristics for a typical joint.

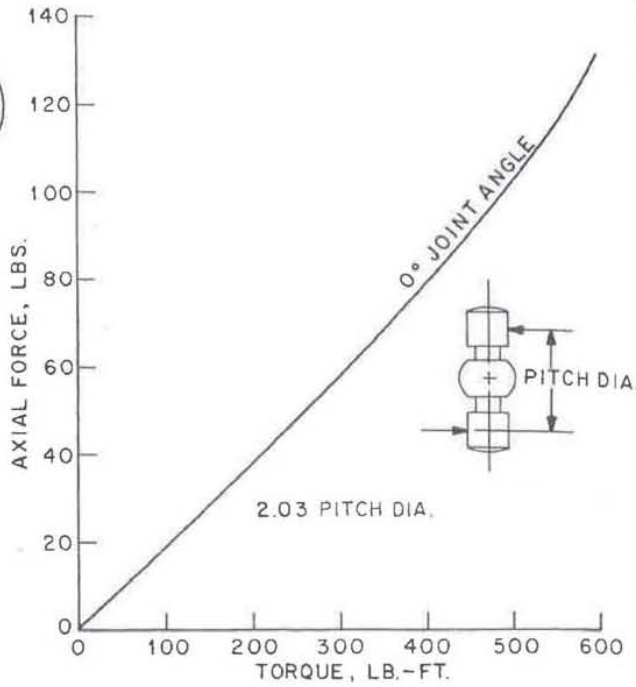


Fig. 3 — Roller and trunnion joint axial force characteristics

Material Selection

The selection of optimum materials for the roller and trunnion joint components is based on ultimate strength, fatigue strength, durability, and other functional requirements for a given application, as well as economical processing advantages.

The housing is generally made of plain, medium carbon steel. After finish broaching of the roller tracks or slots, the housing is induction hardened to an adequate case depth and a typical R_c60 minimum surface hardness in the roller slots and other selected areas to provide the required wear characteristics and torsional strength. The case depth in the roller slots must be sufficient to meet the contact load requirement explained in *Appendix A*. The housing can also be made of low carbon alloy steel which is carburized to an adequate case depth and surface hardened to a typical R_c60 minimum to meet the functional and durability requirements.

The pin is usually made from low carbon alloy steel bar stock, which is carburized to an adequate case depth and surface hardened to a typical R_c60 before finish grinding. The necessary case depth is determined by the joint size and application requirement and is essentially the same as discussed for the Cardan joint cross trunnion, and is also explained in *Appendix A*.

The finish ground closed end rollers are generally made of low carbon alloy steel which are carburized to an adequate case depth and surface hardened to a typical R_c60 minimum. The finish ground open end rollers are usually made of chromium steel which are hardened to a typical range of R_c60-64. The needle rollers are made of chromium steel which are hardened to a typical range of R_c60-64 and finish lapped.

The choice of typical steels and heat treatments for the shaft are the same as discussed for axle shafting in the chapter on *Axle Driveshafts*. The elastomeric material of the boot seal is generally a synthetic rubber, which must exhibit specific resistance to the action of petroleum based fluids and permit the seal to function satisfactorily for any environmental operating condition of the joint application. The housing adapter, seal retainer, and clamps are usually made of plain, low carbon steel. The housing cover is generally made of plain, low carbon steel which can be surface hardened to a typical R_c60 minimum and an adequate case depth. The O-ring seal material is usually a synthetic rubber.

Lubrication

The roller and trunnion joint has a relatively large capacity for lubricant and is generally lubricated for life with an NLGI grade number 1 or 2 lubricating grease. A typical lubricant of this type usually consists of a refined mineral oil and lithium 12 hydroxy stearate soap. Extreme pressure and other additives are incorporated, as required, to impart to or enhance specific properties or performance characteristics of the lubricant.

American Axle v. Neapco - IPR2025-00091
PET_AAM_1012-0094

Typical basic performance requirements of a lubricating grease which must be met, and its various properties are described in the *SAE Handbook* under *Automotive Lubricating Greases*. In addition to providing for optimum joint life by reducing friction and wear at all bearing surfaces, the lubricant used must perform satisfactorily in all environmental conditions of the joint application.

Rating Procedure

The roller and trunnion joint can be rated on the same basis as the Cardan and ball and trunnion joint, where the term *bearing factor* is used in rating and comparing joint sizes. In addition, the joint can also be rated as described in *Appendix I*.

Applications

The roller and trunnion joint has found usage as the inboard joint in axle driveshafts of front drive vehicles where there has been a need for a joint providing end motion capability. Depending on the axial stroke requirement of an application, the joint employing the open end rollers allows a maximum angular design capability of approximately 10 deg, while the joint incorporating the closed end rollers permits approximately 17 deg. The normal design operating angle of the joint will depend on the specific application, while the maximum intermittent operating angle, throughout its entire axial stroke range, must be within the limit lines of the angular capability chart for a given joint design as described in *Appendix G*.

References

1. E. Cordiano, *Autobianchi Primula Transverse Power Plant*, SAE Paper 670002, 1967.

2. "Austin Maxi, Part 2," *Automobile Engineer*, June, 1969, pp. 250-260.

3. E. R. Wagner, P.E., *Driveline Splines and Axial Motion Mechanisms*, SAE Paper 740670, 1974.

American Axle v. Neapco - IPR2025-00091
PET_AAM_1012-0095

Section 3.1.4
Sliding Block and Trunnion Universal Joint

E. R. Wagner, P.E. — Saginaw Steering Gear Div., GMC

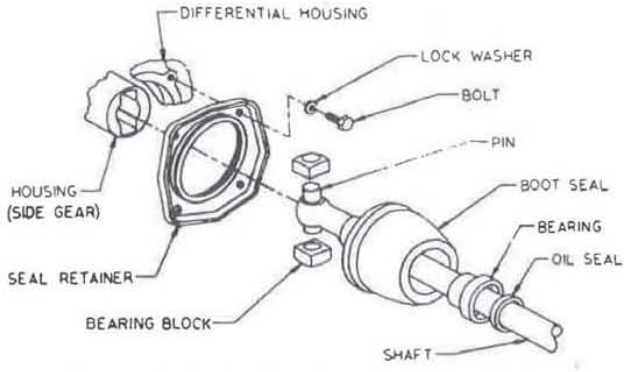


Fig. 1 — Sliding block and trunnion universal joint (axle driveshaft application)

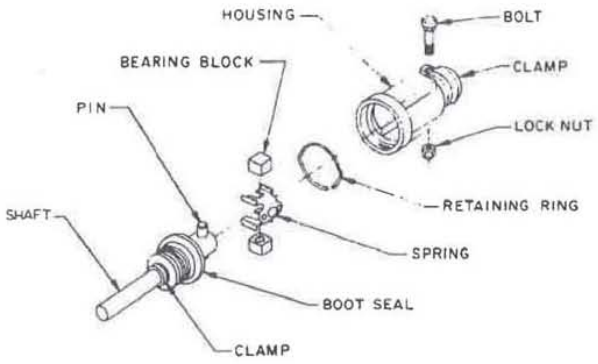


Fig. 2 — Sliding block and trunnion universal joint (steering shaft pot coupling application)

Introduction

The sliding block and trunnion universal joint was used as the axle driveshaft inboard joint in some small low-powered European rear drive passenger cars with independent swing axle suspensions. This joint is another type of *bipot* joint construction and is similar to the ball and trunnion and roller and trunnion joints. Since the late 1950s, this joint has found widespread usage in steering shaft systems of American passenger cars and some trucks where it has commonly been called a *pot coupling*.

The sliding block and trunnion universal joint, shown in Fig. 1, in a typical design for an axle driveshaft application, is a nonconstant velocity universal joint, radially self-supported and permitting axial movement which consists of a housing drivably connected to a shaft through a pair of diametrically opposed trunnion mounted bearing blocks. Fig. 2 shows this joint as used in a typical steering shaft application. Its advantages and disadvantages are essentially the same as for the ball and trunnion and the roller and trunnion joints except that its axial thrust force characteristics during end motion are approximately the same as for a conventional sliding spline.

Kinematics

The kinematics of the sliding block and trunnion joint are the same as for the Cardan, ball and trunnion, and roller and trunnion joints which all transmit nonconstant velocity. As in the ball and trunnion, and roller and trunnion joints, the same internal geometry which provides for angular motion also allows for simultaneous axial movement. The joint phasing procedure is the same as described for the ball and trunnion joint.

Design

The various sliding block and trunnion joint components must be designed to provide the necessary joint angularity, axial travel, strength, and life requirements for a given application. The ultimate strength of the joint must be safely in excess of the maximum applied torque which can be developed by various loading modes discussed in the chapter on *Basic Driveline Requirements*. Initially, the shaft size is determined as outlined in the chapter on *Axle Driveshafts*. Then the housing, pin, and bearing block configuration can be designed to meet the various joint application parameters.

This joint is more simple in construction than either the ball and trunnion or roller and trunnion joints. The housing design is basically the same as for the roller and trunnion joint housing. It is a member with two diametrically opposed axial bearing block slots on the cylindrical inner clearance surface and with drivable means of attachment. In axle driveshaft applications, the housing generally is integral with the differential side gear, while in steering shaft applications, it is the common enclosed construction.

The bearing block is a square or rectangular-shaped member, which pivots and transmits torque from the housing to the shaft through the pin and permits axial movement. As in the roller and trunnion joint, the function of providing radial support for this joint is incorporated in the closed spherical end of the bearing block, or the pin is spherically shaped at the ends when open end bearing blocks are employed. The radius of this spherical shape is equal to one-half of the span of the housing bearing block slots. When a closed end bearing block is used, a maxium joint angle capability of approximately 15 deg can be reached. When the open end bearing block is employed, the maximum angular capability is reduced to approximately 10 deg. Needle rollers are not

American Axle v. Neapco - IPR2025-00091
PET_AAM_1012-0097

used since the square or rectangular-shaped bearing blocks only slide in the housing slots.

The same general design procedure for the pin and shaft, as used in the ball and trunnion, and roller and trunnion joints can be followed. In axle driveshaft applications, the same press fit of the pin in the shaft can be used which is a typical 0.0002 - 0.0015 in total interference. In steering shaft applications, however, a typical total interference of 0.0007-0.002 in has been used because of the lower hardness materials employed. Therefore, lower levels of allowable stress for the pin and shaft are also used as compared to an axle driveshaft design.

In axle driveshaft applications, the boot seal, which is a flexible member, is generally a nonrotating design. Therefore, a bearing and a lip-type oil seal must be incorporated for the rotating shaft. The boot seal is usually held in position on the differential housing side with a seal retainer, small bolts, and lock washers, and must perform its principal function of keeping the lubricant in and foreign matter out of the joint under varying environmental conditions at various speeds, joint angles and end motion positions. In steering shaft applications, a conventional boot seal is used which is generally held to the housing with a retaining ring, and on the shaft with a clamp. In some steering shaft applications, a spring has been incorporated to dampen noise between the bearing blocks and housing slots due to the necessary clearances employed. To prevent accidental disassembly of the joint, the seal retainer in axle driveshaft applications and the boot seal in steering shaft applications can be designed to limit the maximum axial motion. The maximum angular design capability of the joint for its entire axial stroke range can be determined by plotting a chart as described in *Appendix G*.

As previously indicated, the axial thrust force during end movement for a sliding block and trunnion joint is approximately the same as for a conventional sliding spline. Fig. 3 shows the static (nonrotating) axial force characteristics for a typical joint.

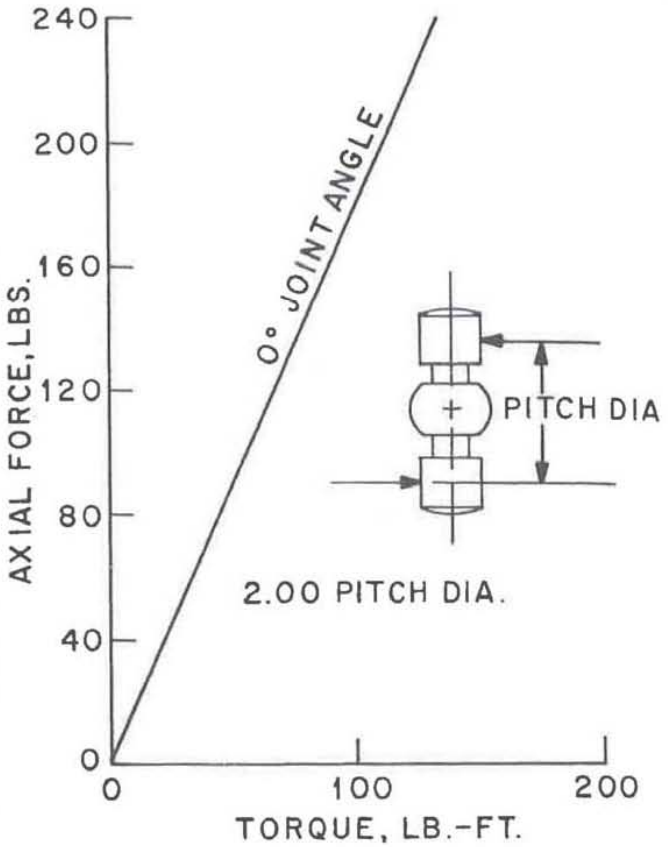


Fig. 3 — Sliding block and trunnion joint axial force characteristics

Material Selection

The selection of optimum materials for the sliding block and trunnion joint components is based on ultimate strength, fatigue strength, and other functional and durability requirements for a given application, as well as economical processing advantages.

For axle driveshaft applications, the housing is usually made from a low carbon alloy steel forging. After finish broaching of the bore and bearing block slots, the housing is carburized to an adequate case depth and surface hardened to a typical R_c60 minimum to provide the required wear characteristics and torsional strength. After heat treatment, the housing is generally phosphate coated.

The pin is usually made from low carbon alloy steel bar stock, which is carburized to an adequate case depth and surface hardened to a typical R_c60 minimum before finish grinding. The necessary case depth is determined by the joint size and application requirement and is essentially the same as discussed for the Cardan joint cross trunnion. The finish ground bearing blocks are generally made of low carbon alloy steel, which are carburized to an adequate case depth and surface hardened to a typical R_c60 minimum. The choice of typical steels and heat treatments for the shaft are the same as discussed for axle shafting in the chapter on *Axle Driveshafts*. The boot seal retainer is usually made from a plain low carbon steel stamping. The bearing can be made of various typical plain bearing materials, and the oil seal is generally of the elastomeric lip type.

For steering shaft applications, the housing is usually formed from plain low carbon steel tubing or is extruded from plain low carbon steel bar stock. The pin is generally made from medium carbon alloy steel or chromium steel bar stock which is hardened and tempered to a typical range of R_c40-45 before finish grinding. The bearing blocks are usually made of sintered ferrous powdered metal with specific density and hardness characteristics. The steering shaft is generally made from cold drawn, plain low carbon steel coil stock having a typical hardness of R_b85 minimum. For retaining the boot seal, the retaining ring is usually made from carbon spring steel wire, while the clamp is generally made of plain low carbon steel. The spring is usually made from carbon spring steel sheet or strip stock.

For both axle driveshaft and steering shaft applications, the elastomeric material of the boot seal is generally a synthetic rubber, which must exhibit specific resistance to the action of petroleum based fluids and permit the seal to function satisfactorily for any environmental operating condition of the joint application.

American Axle v. Neapco - IPR2025-00091
PET_AAM_1012-0098

Lubrication

The sliding block and trunnion joint has a relatively large capacity for lubricant and is generally lubricated for life. In axle driveshaft applications where the joint operates within the differential, it is lubricated with the same lubricating mineral oil used in the differential, which is generally of SAE viscosity number 90, and incorporates various additives, as required, to impart to or enhance specific properties or performance characteristics of the lubricant.

In steering shaft applications, the lubricating grease used is usually an NLGI grade number 2. A typical lubricant of this type generally consists of a refined mineral oil, lithium 12 hydroxy stearate soap and tacking agents.

Typical basic performance requirements of a lubricating oil or grease which must be met and its various properties are described in the *SAE Handbook* under *Automotive Lubricating Greases*. In addition to providing for optimum joint life by reducing friction and wear at all bearing surfaces, the lubricant used must perform satisfactorily in all environmental conditions of the joint application.

Rating Procedure

The sliding block and trunnion joint can be rated as described in *Appendix I*. Since needle rollers are not used with this joint, the term *bearing factor* as used with the Cardan, ball and trunnion, and roller and trunnion joints does not apply.

Applications

The sliding block and trunnion joint has found usage as the inboard joint in axle driveshafts of relatively small, low powered rear drive vehicles with swing axle-type suspensions where there was a need for a joint providing end motion capability at a relatively low joint angle. Depending on the axial stroke requirement, the open end bearing block design of the joint construction generally used in these axle applications allows a maximum angular design capability of approximately 10 deg.

The most extensively used application of this joint, however, has been as the *pot coupling* in vehicle steering shaft systems, where the relatively fixed operating joint angles have been in the range of 3-12 deg. Depending on the axial stroke requirement, the closed end bearing blocks generally employed in these applications can allow a maximum angular design capability of approximately 15 deg. The axial motion capability of the joint allows for relative movement between the body and frame of the vehicle and also for installation allowances. Whether the joint is used in axle driveshaft or in steering shaft applications, the maximum intermittent operating angle of the former application or the relatively continuous operating angle of the latter application throughout the entire axial stroke range, must be within the limit lines of the angular capability chart for a given joint design as described in *Appendix G*.

References

1. E. Cordiano, *Autobianchi Primula Transverse Power Plant*, SAE Paper 670002, 1967.

2. E. R. Wagner, P.E., *Driveline Splines and Axial Motion Mechanisms*, SAE Paper 740670, 1974.

American Axle v. Neapco - IPR2025-00091
PET_AAM_1012-0099

Section 3.1.5
Rubber Couplings

E. R. Wagner, P.E. — Saginaw Steering Gear Div., GMC

A rubber coupling is a mechanical device with an intermediate resilient elastomeric drive element or elements, which absorbs impact and shock forces, dampens drivetrain disturbances, and functions with universal joint characteristics by providing for angular misalignment. Rubber couplings of varying design have been used in both driveline and axle driveshaft applications in certain European passenger cars and in some industrial drives. When operated at an angle, these devices generally transmit motion with nonconstant velocity characteristics which introduce nonuniform forces and moments into the drive system. Natural rubber is usually used because of its desirable mechanical properties and damping characteristics.

With regard to advantages, these devices reduce shock loads, torsional vibration, and noise transmission. Loads on gear boxes, bearings, and other drive components are reduced. Depending on their particular design, they may allow some axial compliance, varying degrees of joint angle capability, and torsional resilience. They are maintenance free, require no lubrication except for the centering device when used, and are relatively unaffected by dirt and moisture. A major disadvantage of rubber couplings is that they become excessively large in swing diameter with increasing torque requirements. For adequate life they are generally limited to low torque applications and must operate at very low or 0 deg joint angles under continuous operating conditions. Certain couplings, however, can operate continuously at angles up to approximately 3 deg and intermittently at angles up to nearly 15 deg.

A commonly used rubber coupling has been the regular polygon shaped annular type shown in Fig. 1, in two constructions. The coupling consists of a regular polygon of rubber with metal inserts and usually has four, six or eight sides. After molding, the rubber elements are compressed to the assembled position by fitting a steel retaining band around the outside. This band is discarded after assembly of the coupling to the mating forked shafts in an alternating attaching arrangement of the driving and driven members. Maximum fatigue life and torque capacity is thus assured by the rubber being loaded in compression. The use of metal interleaves provides for increased torque capacity when required. For speeds in excess of vehicle axle driveshaft speeds, a centering device is required as shown in Fig. 2, in a typical driveline application.

Fig. 3 illustrates another basic type of rubber coupling in two constructions. Both the link and integral annular variations are assembled to mating forked shafts in an alternating attaching arrangement of driving and driven members. Because of the molded internal braids, the rubber can be loaded in tension to transmit the torque. A centering device, as shown in Fig. 4, is employed when the coupling is used in driveline applications.

Fig. 5 illustrates a Cardan joint type of rubber coupling used in some axle driveshaft applications where the rubber is molded to

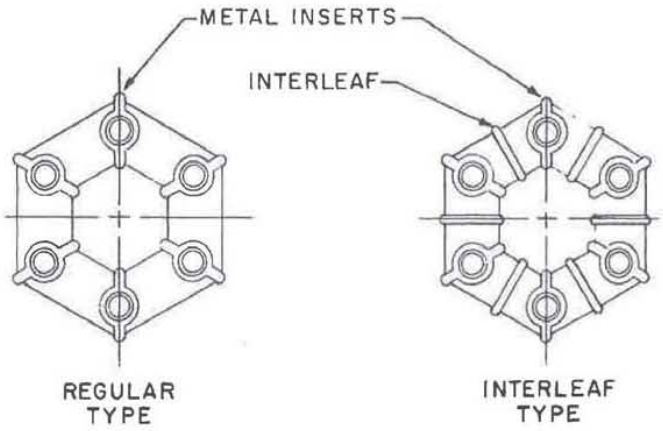


Fig. 1 — Regular polygon shaped annular type rubber coupling

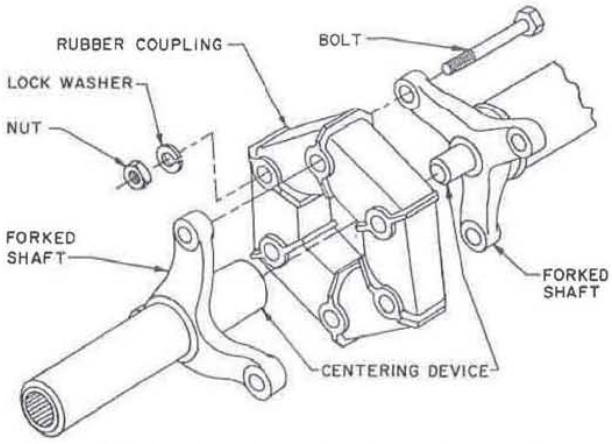


Fig. 2 — Regular polygon shaped annular type rubber coupling with centering device

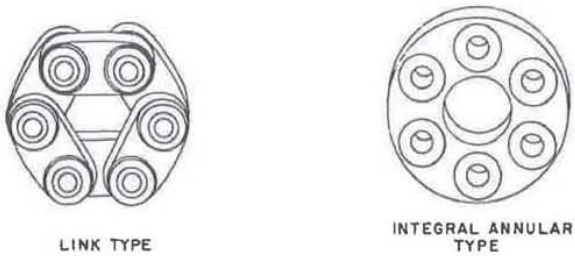


Fig. 3 — Rubber coupling with molded internal braids

American Axle v. Neapco - IPR2025-00091
PET_AAM_1012-0101

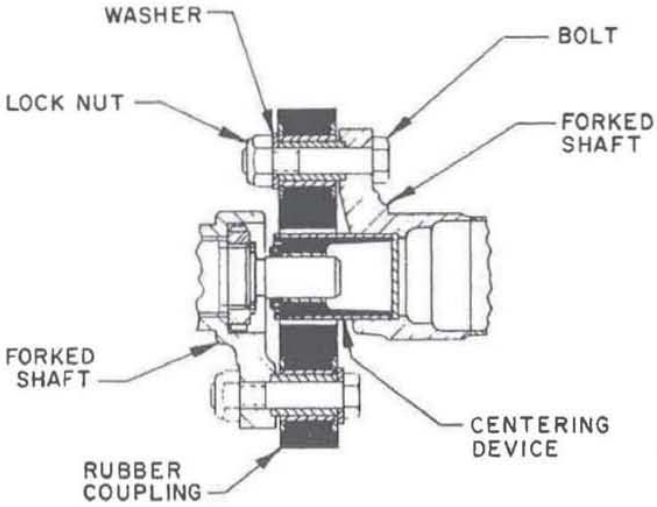


Fig. 4 — Round annular type rubber coupling with centering device

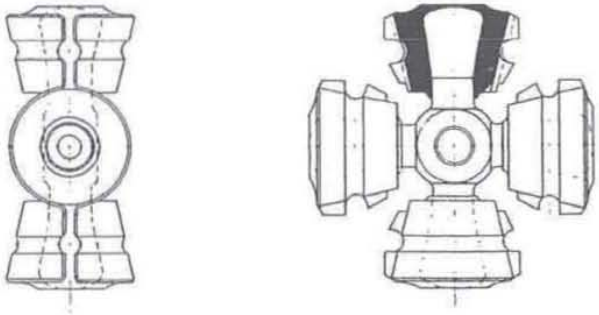


Fig. 5 — Cardan joint type rubber coupling in free state

the cross trunnions between split, conical-shaped steel stamped members. The coupling is attached to mating yoke members with U-bolts as shown in Fig. 6, which preloads the rubber in compression.

Fig. 7 shows a rubber coupling consisting of two, thin steel stamped and formed round plates which serve as a housing for four, molded-in-place rubber bushings. These plates are fastened together by roll forming. The bonding and preloading of the rubber in compression ensures maximum torque capacity and fatigue life. The thin rubber sections loaded in compression provide for a relatively high radial stiffness and thus allow the use of this coupling without a centering device in driveshaft applications. The coupling is attached to mating forked shafts in an alternating attaching arrangement of the driving and driven members.

Fig. 8 shows a rubber coupling used in some axle driveshaft applications. This design which provides for the rubber to be loaded principally in compresssion when torque is applied to the shaft coupling member, has equally spaced integral paddles positioned by rubber molding, in the cavities of the outer coupling member.

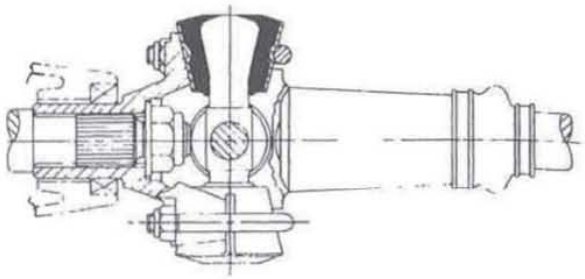


Fig. 6 — Cardan joint type rubber coupling in assembled position

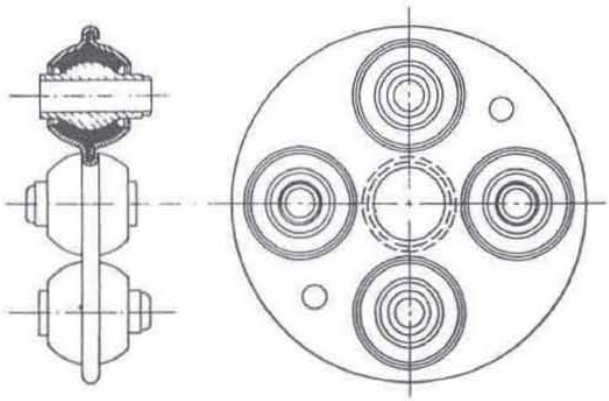


Fig. 7 — Rubber coupling with compression loaded rubber ball joints

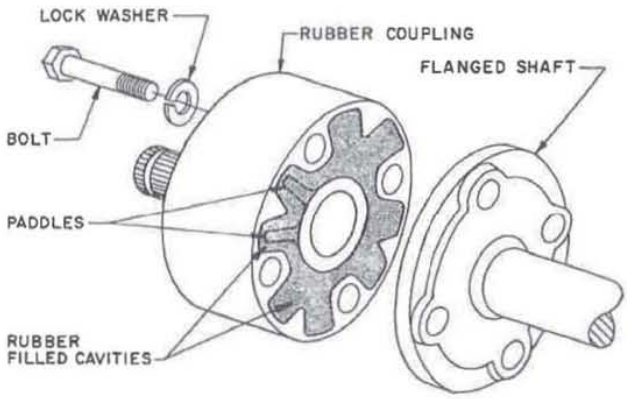


Fig. 8 — Rubber coupling with internally molded paddles

References

1. J. R. Gensheimer, "How to Design Flexible Couplings To Match Specific Drive Requirements," *Machine Design*, September 14, 1961, pp. 154-159.

2. "Rubber in Transmissions," *Automobile Engineer*, May, 1962.

3. W. Ker Wilson, "Practical Solution of Torsional Vibration Problems," Vol. II *Amplitude Calculations*, 3rd ed. Chapman and Hall, Ltd., London, 1963.

American Axle v. Neapco - IPR2025-00091
PET_AAM_1012-0102

4. W. Ker Wilson, "Practical Solution of Torsional Vibration Problems," Vol. IV, *Devices for Controlling Vibration*, 3rd ed. Chapman and Hall, Ltd., London, 1968.

5. *Elasticity in the Propulsion Members of Vehicles-Rubber in Transport Engineering*, Proceedings of a conference held at Imperial College of Science and Technology, London, 1970.

6. G. Bowen, "Rubber Couplings for Drivelines," *The Journal of Automotive Engineering*, January, 1971, pp. 3-8.

American Axle v. Neapco - IPR2025-00091
PET_AAM_1012-0103

Section 3.2–Constant Velocity Universal Joints
Section 3.2.1– Basic Requirements for Constant Velocity (CV) Universal Joints 99
Section 3.2.2– Double Cardan Universal Joint 103
Section 3.2.3– Double Cardan Universal Joint (Trunnion Pin Type) 119
Section 3.2.4– Double Cardan Universal Joint (Twin Ball and Centering Plate Type) 123
Section 3.2.5– Tracta Universal Joint 127
Section 3.2.6– Tripot Universal Joint (End Motion Type) 131
Section 3.2.7– Tripot Universal Joint (Fixed Center Type) 141
Section 3.2.8– Rzeppa Universal Joint 145
Section 3.2.9– Ball Spline Rzeppa Universal Joint 151
Section 3.2.10– Weiss Universal Joint (End Motion Type) 155
Section 3.2.11– Weiss Universal Joint (Fixed Center Type) 159
Section 3.2.12– Cross Groove Universal Joint 163
Section 3.2.13– Double Offset Universal Joint (End Motion Type) 167
Section 3.2.14– Double Offset Universal Joint (Fixed Center Type) 171

Universal Joints

American Axle v. Neapco - IPR2025-00091
PET_AAM_1012-0105

Section 3.2.1

Basic Requirements for Constant Velocity (CV) Universal Joints

E. R. Wagner, P.E. — Saginaw Steering Gear Div., GMC

Basic relationships can be established which show the mathematical conditions necessary for a universal joint to transmit constant velocity when operating at an angle. The following conditions required to achieve constant velocity must be satisfied by all universal joint constructions with but one known exception, the tripot joint, which will be described later:

1. The plane of contact between the driving and driven or input and output members, respectively, of a universal joint, must be held constant in space. (Note: In a nonconstant velocity joint, such as the well known Cardan joint, this plane of contact oscillates back and forth in space and is alternately perpendicular to the two yokes.)
2. The plane of contact must be perpendicular or normal to the plane determined by the rotational axes of the driving and driven members of the universal joint.
3. The plane of contact must form a relative angle to both driving and driven members which is equivalent to one half of the total joint angle. This is usually defined as *bisecting the obtuse angle formed by the driving and driven member rotational axes*.

Synonymous terms used for the *constant velocity plane* are, *bisecting angle plane* and *homokinetic plane*. Therefore, the *constant velocity plane* is the plane described by all contact points of a universal joint which produces an angular velocity ratio of unity between the output and input members. This plane bisects the obtuse angle formed by the input and output member rotational axes and is perpendicular to the plane containing these axes.

It should be further emphasized that a requirement for constant velocity is that all contact points between the driving and driven members must at all times lie in the bisecting angle plane for the entire design angular displacement range of the joint. Some joint constructions, however, produce constant velocity at a specific joint angle or over a limited angular range only, while at other angles they transmit approximate constant velocity. In order to fulfill the requirement for constant velocity, it is obvious that no point in the constant velocity plane can be rigidly connected to or be a fixed part of either the driving or driven members of the joint.

The basic principle of operation of a simplified constant velocity joint is shown in Fig. 1. Both shafts 2 and 3 have arms which are equally bent to angle ψ. When the input and output centerlines of the shafts are displaced at joint angle θ, the point of contact of 2 and 3, point B, lies in the plane of the paper and in the constant velocity or bisecting angle plane previously described. The velocity of B as a point in 3 coincides with that of B as a point in 2. The perpendiculars to the axes, BC and BD are equal. Because of symmetry, the point of contact B will lie in the bisecting angle plane for all other positions of rotation. The radius to the point of contact will be the same for both members and, therefore, the angular velocities of the two shafts will be equal at all times.

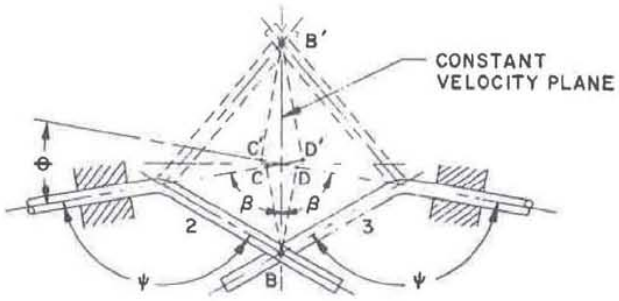


Fig. 1 — Simplified constant velocity universal joint

Ball type joints in various constructions have been the most common means used to achieve constant velocity utilizing the principle of the constant velocity or bisecting angle plane. In these ball type joints, this plane passes through the instantaneous center of the joint and bisects the driving and driven member rotational axes at any instant. The *instantaneous center* of a body is defined as that axis, through a point, about which the motion of the body at any instant is one of rotation only and no translatory motion need be combined with the rotation to produce the actual motion of the body. The intersecting rotational axes locate the joint geometric center and thus the instantaneous center of rotation of a ball type joint coincides with its geometric center, whenever the plane of contact is maintained in the bisecting angle plane.

In order to transmit constant velocity, a system or means must be incorporated in a ball type joint which requires that the balls serve as the intermediate drive member in the constant velocity plane. These balls, when located in cooperating grooves in the joint driving and driven members, must allow relative angular displacement between these members, and when properly guided, will maintain contact through the bisecting angle plane. When a ball type joint transmits constant velocity by utilizing the principle of this plane, all major joint elements rotate at constant velocity. The design problem in ball type CV joint constructions, therefore, is that of producing an arrangement which provides contact between driving and driven members always through the bisecting angle plane; and this can be achieved as follows:

1. By having ball grooves in the mating members whose centerlines intersect at one defined location. This location then positions the ball. (for example, the Weiss joint)
2. By having ball grooves that are inclined relative to one another in such a manner that the ball is positioned in one direction but is permitted to move in the other direction. By alternately inclining these grooves, the adjacent balls are allowed to move in essentially opposite directions; and

American Axle v. Neapco - IPR2025-00091
PET_AAM_1012-0107

when a cage is provided, the adjacent balls effectively hold each other in position. (for example, the cross groove joint)

3. By having ball grooves that position the ball in one direction only, but with a cage construction which is located between one or both members and positions the balls in the proper plane. (for example, the Rzeppa joint)
4. By having parallel ball grooves and providing some external locating element which could be a located cage or individual piloting means for each ball. (for example, the double offset joint)

Many ball type CV joints use some form of intersecting groove design. In this construction, the grooves cross each other in such a way that the intersection point always lies in the bisecting angle plane. It can be shown that any groove construction will achieve this result, provided the mating grooves are of the same geometric characteristics but of the opposite hand. The grooves may be curved, or straight, or any combination thereof, as long as they are not concentric. Reference is often made to the term *mirror image*.

The same mathematical relationship which produces contact through the bisecting angle plane will usually allow axial slip or end motion. Where the grooves intersect each other, axial movement will provide the same type of geometry as when operating through a joint angle. This geometry will make the drive balls move one half of the distance of the relative axial motion of the driving and driven members and will maintain contact through the grooves. Some ball type CV joints which are permitted to telescope, maintain the ball contact between the piloting device in one member. The other member is allowed to move axially which does provide considerably more sliding but still permits reasonably free axial movement.

If it were assumed that the grooves in the driving and driven members of a ball type CV joint were perfectly concentric, such as in a typical ball bearing, the balls could roll to their half angle position when the joint was operating at an angle. Since the grooves are not concentric and generally intersect each other, this true rolling condition cannot exist.

When a joint has been turned through a given joint angle, the ball itself must move into the bisecting angle plane in order for the joint to produce constant velocity. Theoretically, pure rolling occurs only around the center through which the joint angle takes place. Therefore, depending on the geometric characteristics of the grooves employed in a particular joint design, it follows that the distance outward or inward in a radial plane, or sideways on a tangential line, or a combination of both that the ball must move, is a function of the relative sliding which occurs.

The relative rolling movement of the ball is reasonably free of friction and can produce a substantially high capacity contact between the groove and ball. The relative sliding movement, however, has higher friction characteristics which increases the operating temperature. The groove contact subjected to this sliding load has relatively less capacity. It is generally true that the ratio of rolling to sliding motion in any joint is an important factor in defining permissible operating speeds and loads. The higher relative sliding motion characteristics place more limitations on the extremes of the operating conditions. Not only is the load carrying capacity of the joint somewhat reduced, but the higher temperatures produced by the frictional heat severely limit the operating speeds and loads.

In constant velocity joint constructions, it is also possible to use rolling elements other than balls as the intermediate drive member. These rolling elements which have been rollers, partial spheres, cones, or other geometric shapes, often can produce better groove contact with mating, driving, and driven members, and provide increased capacity.

They do, however, introduce an additional problem of properly orienting the axis of rotation of the rolling element in the bisecting angle plane. They often produce larger relative sliding components of motion than simpler balls which are free to rotate about any axis.

Constant velocity can also be produced by joint constructions which do not incorporate rolling elements as the intermediate drive member or members. The most common example of these designs is the double Cardan joint which consists essentially of two Cardan joints connected by a coupling yoke and having a suitable centering device for support and for dividing the total joint angle. The rotational axis of the coupling yoke lies in the plane of this joint angle. When the total joint angle is equally divided, the coupling yoke is symmetrically positioned with respect to, and its rotational axis is normal to, the bisecting angle plane. The coupling yoke provides the contact requirements to produce constant velocity. However, the coupling yoke and other components connected to it do not rotate uniformly within the joint. The double Cardan joint can be designed to produce constant velocity at one specific joint angle only, over a limited angular range or over its entire angular range.

Another joint with constant velocity characteristics is the Tracta joint, which consists of two fork yokes connected by two intermediate members. When properly supported and centered by external means, the intermediate members equally divide the total joint angle between the two fork yokes. Also, these two intermediate members are then always symmetrically positioned with respect to the bisecting angle plane in the plane of the joint angle, and constant velocity is transmitted. This function of dividing the joint angle is very similar to that of the coupling yoke of a double Cardan joint.

In the preceding discussion of the requirements for constant velocity, it was emphasized that the joint construction must be such that the driving and driven members always maintain contact through the bisecting angle plane. A ball type CV joint construction does exist, however, in which contact is always perpendicular to the rotational axis of either the driving or driven member. This joint is the tripot joint and consists essentially of three equally spaced balls located on one member and perpendicular to its rotational axis. These balls mate with three equally spaced axial bores in the other member. Therefore, when the joint is angulated, an offset must take place between the driving and driven member geometric centers, and when the joint is rotated, an orbiting motion occurs. Since the geometric centers of the two members do not coincide, the instantaneous center of rotation of the joint also does not coincide with either of these points but must also rotate in an orbital path about the joint center in order to produce constant velocity. This orbiting characteristic is not present in other ball type CV joints which utilize the principle of the bisecting angle plane since in those joints, the geometric center and instantaneous center of rotation always coincide.

American Axle v. Neapco - IPR2025-00091
PET_AAM_1012-0108

Various specific joint constructions have been used to satisfy the previously described requirements for constant velocity. These designs are described in detail in the following sections.

Reference

1. P. J. Mazziotti, *Dynamic Characteristics of Truck Driveline Systems*, Published in SAE SP-262, 1964.

American Axle v. Neapco - IPR2025-00091
PET_AAM_1012-0109

Section 3.2.2
Double Cardan Universal Joint

E. R. Wagner, P.E. — Saginaw Steering Gear Div., GMC

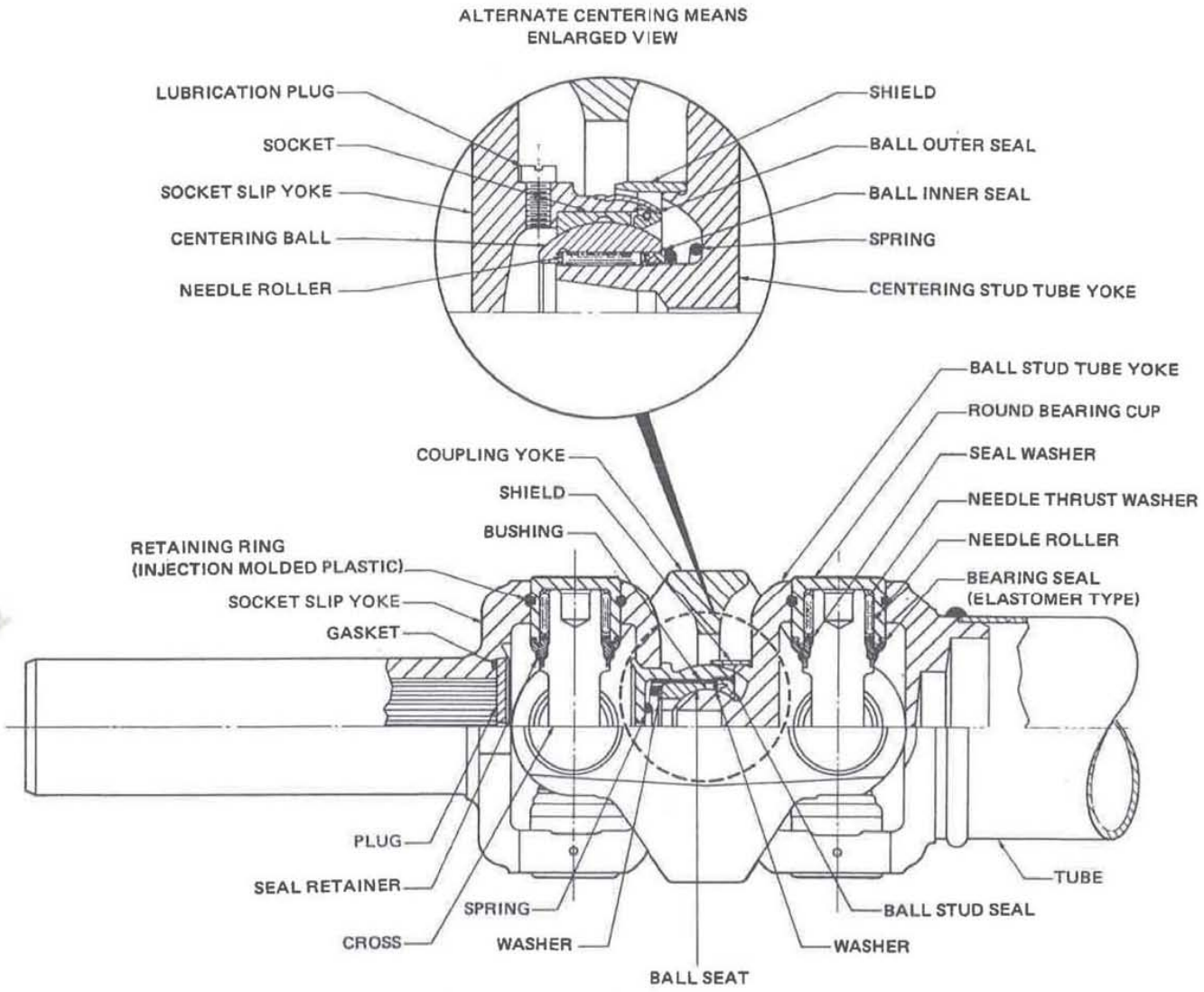


Fig. 1 — Double Cardan universal joint

Introduction

The patent literature shows that the concept of the double Cardan universal joint was developed as early as 1903 and that patents on various applicable features were issued through the mid 1970s. Its first known vehicle usage began in the late 1920s and early 1930s as the outboard joint in early American and French front wheel drive passenger cars. Since that time, it has found wide acceptance in automotive drivelines and other applications where increased joint angles have precluded the use of the Cardan joint.

The double Cardan universal joint shown in Fig. 1, in a typical design, is a near constant velocity universal joint, which consists of two Cardan universal joints, whose crosses are connected by a coupling yoke with internal supporting and centering means and has intersecting shaft axes. At the design joint angle and at zero, the instantaneous angular velocity ratio is unity while at other joint angles it is near unity.

American Axle v. Neapco - IPR2025-00091
PET_AAM_1012-0111

The ball and socket centering device divides nearly equally the total joint angle between the two joints. The double Cardan joint transmits constant velocity because the second joint compensates for the fluctuations in angular velocity created by the first joint. It does not have true constant velocity at all operating angles, but the error is so slight that it can generally be neglected, as will be shown.

In order to appreciate the advantages of the double Cardan joint, the limitations of the Cardan joint must first be understood.

The kinematics of the Cardan joint are discussed in detail in a previous section and will be repeated here only briefly. When operating at an angle, this joint does not produce a uniform transmission of angular velocity and torque since the output or driven yoke rotates at nonuniform angular velocity with respect to the input or driving yoke. Depending on the type of installation, the maximum continuous operating angle must be controlled so that this nonuniform motion will not set up exciting vibrations in the driveline system. The joint angle limitations are determined by these three basic parameters:

1. Torsional excitation produced by nonuniform transmission of velocty.
2. Inertia excitation produced by the oscillating torque loads resulting from the driveshaft inertia being accelerated and decelerated through nonuniform motion.
3. Secondary couple excitation caused by the transmission of torque when operating a Cardan joint at an angle. This tends to excite the end supports.

In comparison, the double Cardan joint has the following kinematic advantages:

1. Torsional excitation is effectively cancelled within the joint itself.
2. The large inertia of the driveshaft will rotate at effective uniform velocity when driven by a constant velocity joint. The coupling yoke of the double Cardan joint does not turn uniformly; however, this produces a comparatively small rotating inertia.
3. The secondary couple forces from the double Cardan joint are effectively reduced to static components only. This eliminates the exciting forces on the end supports and will be shown with an illustrative problem.

In addition to these kinematic characteristics and the ability to operate at higher joint angles than the Cardan joint, the double Cardan joint in driveline applications offers the following additional advantages:

1. Use of common bearing and cross components of the Cardan joint
2. Relatively low cost
3. Rugged construction
4. Relatively long life
5. Ability to operate at a relatively cool temperature
6. Relatively high axial thrust capability
7. Relatively higher continuous operating angle than other constant velocity joints

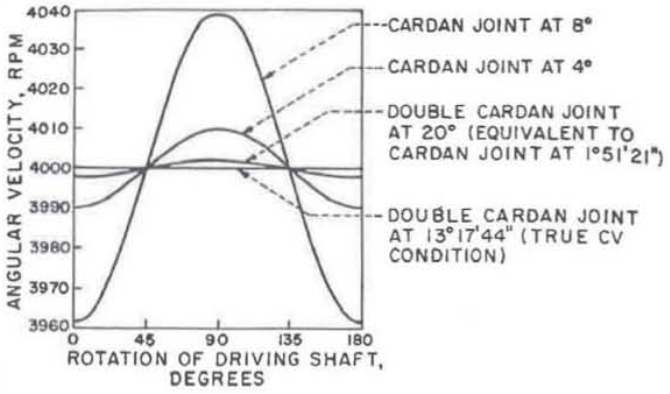


Fig. 2 — Output velocity variation of double Cardan joint versus Cardan joint

Kinematics

Velocity Variation and Torsional Excitation

Since the double Cardan joint does not transmit true constant velocity at all operating joint angles, the output velocity variation at a given joint angle will depend on how this angle is divided between the two halves of the joint. This is determined by the location of the centering device in the joint.

Fig. 2 shows a comparison of the output velocity variation of a double Cardan joint versus a Cardan joint. The constant input angular velocity of the joints is assumed to be 4000 rpm and output speeds are shown for various positions of rotation of the driving shaft.

In the case of a double Cardan joint designed to produce true constant velocity at a 13°17′44″ total joint angle, for example, the output speed is shown as a straight line when the joint operates at this angle. This is as it should be since the output follows the input exactly at this operating angle. Since there is no output velocity variation from this joint, the torsional excitation is also effectively cancelled within the joint itself.

If this same joint is operated at a 20 deg joint angle, the division of this angle between the two halves of the joint produces an output velocity variation and torsional excitation equivalent to a Cardan joint operating at a 1° 51′21″ joint angle. The output speed of this equivalent Cardan joint varies from $\omega \cos\theta$ to $\omega/\cos\theta$ twice per revolution. When $\omega = 4000$ rpm and $\theta = 1°\,51'21''$, these minimum and maximum output speeds are:

$$\omega \cos\theta = 4000 \times 0.999475 = 3997.9 \text{ rpm}$$

$$\frac{\omega}{\cos\theta} = \frac{4000}{0.999475} = 4002.1 \text{ rpm}$$

With these extreme velocity variations, the speed fluctuations can be expressed in percent as follows:

$$\text{Speed fluctuation} = \frac{(\omega_{max} - \omega_{min})}{\omega_{mean}} \times 100$$

$$= \frac{(4002.1 - 3997.9)}{4000} \times 100$$

American Axle v. Neapco - IPR2025-00091
PET_AAM_1012-0112

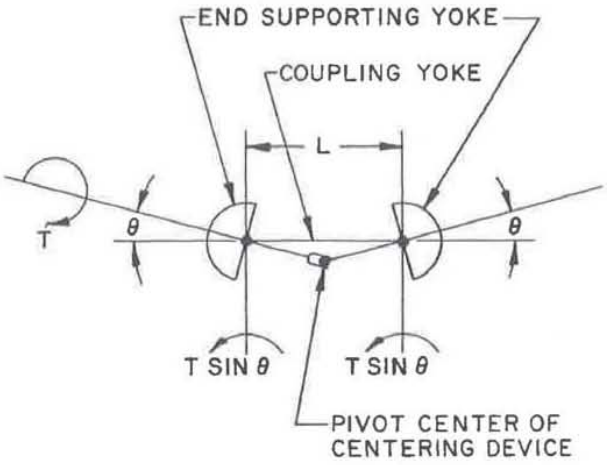


Fig. 3 — Schematic view of double Cardan joint

Speed fluctuation = 0.105%

When a Cardan joint operates at a 4 deg joint angle, its speed fluctuation is 0.488%, while at an 8 deg joint angle, it is 1.955%. Therefore, a double Cardan joint, even though it is not operating at or near its true constant velocity position, will give a significant reduction in velocity variation and torsional excitation. It should be noted that the 20 deg joint angle was chosen because its speed variation deviates enough from a straight line so that it can be seen clearly in Fig. 2. In practice, a double Cardan joint would operate only intermittently at such a high joint angle at driveshaft speeds.

Inertia Excitation

In a double Cardan joint, the coupling yoke rotates at nonuniform speed when the input angular velocity is constant. This coupling yoke or intermediate member, therefore, accelerates and decelerates twice per shaft revolution. Since the rotational inertia of the coupling yoke is accelerated and decelerated through nonuniform motion, oscillating torque loads are impressed on the driveline system. This is known as inertia excitation, and its magnitude depends on the size of the joint angle and the inertia of the coupling yoke.

For a typical joint used in a driveline for a large passenger car, the effective mass moment of inertia of the coupling yoke and its associated cross and bearing components was found by experimental means to be 0.0290 lb-in-s^2. The normal design operating joint angle is considered to be 10 deg; and therefore the angle of the input half of the joint is approximately 5 deg. At a rotational speed of 3000 rpm, the maximum value of the inertia torque can be computed as follows:

$$T = J\alpha$$

where:

J = Mass polar moment of inertia, lb-in-s^2

α = Angular acceleration, rad/s^2

The approximate value of the maximum angular acceleration can be determined with the following expression developed in the section on the *Cardan or Hooke Universal joint:*

$$\alpha_{max} = \theta^2\omega^2 = \theta^2 \left(\frac{2\pi N}{60} \right)^2$$

where:

θ = Joint angle, rad

ω = Angular velocity of driving yoke, rad/s

N = Rotational speed of driving yoke, rpm

Also, 1 rad = 57.296 deg

Hence:

$$\alpha_{max} = \left(\frac{5}{57.296}\right)^2 \times \left(\frac{2\pi \times 3000}{60}\right)^2$$

$$\alpha_{max} = 751.61 \text{ rad/s}^2$$

Thus:

$$T = J\alpha = 0.0290 \times 751.61$$

$$T = 21.80 \text{ lb-in}$$

Even though this inertia excitation cannot be eliminated from a double Cardan joint, its effect can be reduced if desired in multiple joint arrangements where the accelerations are placed out-of-phase with each other. Cancellation is also possible to a degree where a double Cardan joint is used in combination with a Cardan joint. Here again, proper phasing can cancel inertia effects with the torsional characteristics of the Cardan joint. The detailed procedure for analyzing these inertia effects is discussed in the section on the *Cardan or Hooke Universal joint*.

Secondary Couple Excitation

Since the double Cardan joint is basically two Cardan joints in series with a centering device, secondary couples react on their supporting bearings when torque is transmitted at a given joint angle. It will be shown with an illustrative problem that these couple forces on the supports are effectively reduced to static components only. The dynamic or exciting forces which cause disturbances are eliminated in a true constant velocity joint. In a near constant velocity joint, such as the double Cardan joint, they are almost zero.

The double Cardan joint includes a centering device about which it is self-supporting and self-aligning. This centering device must support the secondary couples on the coupling yoke resolved into forces around its length. Fig. 3 shows a schematic view of a double Cardan joint in the rotational position where the couples T sin θ react on the coupling yoke. The forces resulting from these couples must be supported by the centering device.

American Axle v. Neapco - IPR2025-00091
PET_AAM_1012-0113